Improvement of Indoor Air Quality Through The Development of Polymeric Microfibrous Material

by

Eric Amor Luna

A dissertation submitted to the Graduate Faculty of
Auburn University
in partial fulfillment of the
requirements for the Degree of
Doctor of Philosophy

Auburn, Alabama
December 18, 2009

Keywords: Microfibrous Materials, IAQ,
synthetic wet-lay material, absorption

Approved by

Bruce J. Tatarchuk, Chair, Professor of Chemical Engineering
Gopal A. Krishnagopalan, Professor of Chemical Engineering
Steve R. Duke, Associate Professor of Chemical Engineering
Sabit Adanur, Professor of Polymer and Fiber Engineering

Abstract

It was desired to create a healthier and more comfortable living environment for persons whom spend an increasingly amount of time indoors. Two main goals are necessary for the accomplishments of this objective: develop a base composite material using polymeric fibers and activated carbon; and analyze new and emerging standards for Indoor Air Quality (IAQ) to produce a robust and efficient Heating Ventilation and Air Conditioning (HVAC) filter.

The development of a polymeric composite material was based on current research using metal fibers in a sinter-locked network to entrap small sorbent particles. This composite, known as Microfibrous Materials, has been traditionally used as a substrate for catalysis and adsorption applications. This work builds upon the knowledge obtained in the area of adsorption. For one-time use applications it is necessary to move from a high value, metal medium to a more cost-effective, polymer medium. Standards for chemical contaminant levels with regards to IAQ do not currently exist for residential and automotive environments. The removal of Volatile Organic Chemicals (VOC) and Toxic Industrial Chemicals (TIC) via an HVAC filter is not currently addressed. Such chemical contaminants (all present in non-industrial or residential environments) have a negative impact on human health. The level of contamination in residential environments has been found to be at unacceptable levels resulting in detrimental health effects due to prolonged exposure.

Novel and emerging filtration technologies are being developed to perform particulate and chemical contaminant filtration. These technologies were evaluated, with respect to the

performance of Microfibrous Materials, to determine the most efficient HVAC filtration medium. The different media was evaluated according to their basis weight deviation, pressure drop, and single pass contacting efficiency.

A commercial HVAC filter must adhere to several standards. The novel media were subjected to flammability testing based upon ANSI/UL-900. This testing, along with empirical reaction modeling based upon the Shrinking Core Model, determined the best filter media for the next generation HVAC filter.

Acknowledgments

The financial support of Army contract W56HZV-05-C-0686 is greatly appreciated.

I extend my deep gratitude to my advisory committee for all of their hard work and charity toward me and my research. The expert advice and guidance of my advisor Dr. Bruce J. Tatarchuk along with the many frank conversations are greatly appreciated. The support and wisdom of my committee members, Dr. Gopal Krishnagopalan, Dr. Steve R. Duke, and Dr. Sabit Adanur are truly valued.

I would like to thank all the CM3 group members during my tenure on campus, especially Dr. Donald R. Cahela, Dr. Yong Lu, Dr. Mukund Karanjikar, Andrew P. Queen (M.Sc. ChE), and Dwight E. Cahela, MSgt. (Ret). Also, the expertise and help of Mr. Troy Barron of Intramicron, Inc. was invaluable. Without their guidance, wisdom, and support this work would not have been possible.

Finally I would like to thank all those who provided the support, encouragement and love that enabled me to accomplish a life long goal. I would like to extend a special acknowledgement to my family (my parents J. Felipe and Natalia Luna), friends (Dr. Jason Keiper, Dr. Andrew Pearson, Miss Stacy Kissel, and Mrs. Felisha Vestal), and my graduate companions (Dr. Tracey L. Mole and Dr. Siddarth Venkatesh) whom endured all the experiences and challenges of my graduate career.

Table of Contents

List of Tables

List of Figures

INTRODUCTION

The improvement of human health has always been of concern. Leading up to 2008, more attention has been focused on the detrimental health effects of poor air quality. The first step was to improve the outdoor air quality through federal regulations imposed by the Environmental Protection Agency. Now that the outdoor air quality has been improved, the quality of indoor air has become the focus of researchers. The industrial setting is federally regulated through the Occupational Health and Safety Administration (OSHA). OSHA has imposed strict regulations to protect the well being of laborers during their time at work. Unfortunately, no such regulations exist for the residential setting.

This gap in federal regulation has led to the goal of this dissertation: to improve indoor air quality (IAQ) for every resident with a Heating Ventilation and Air Conditioning (HVAC) system. The improvement of residential IAQ is important because IAQ is of paramount concern when we spend 90% of the day indoors where the air is controlled and could be filtered. Also, IAQ has been shown to either worsen existing medical conditions and/or cause new ones.

Improvement of residential IAQ could be done through many different methods. There are commercial units available to reduce the concentration of particulate in the residential setting. Although particulate is detrimental to health and IAQ, it is the chemical contaminants found in the residential setting that are the most concerning. For this reason, a filter which performs particulate and chemical contaminant removal is desired as the generation of HVAC filter to improve residential IAQ. This would be accomplished by replacing existing filters with a similar

filter (based upon appearance) that would do the same level of particulate filtration and also chemical filtration.

In order to accomplish this task, a new filter medium must be developed. This novel medium will be based upon current research done in the Center for Microfibrous Material Manufacturing. Microfibrous materials provide efficient sorbent usage and a favorable pressure drop regime. A new version utilizing polymer fibers would need to be developed because of the low cost for HVAC filters. Through extensive testing including physical characteristic metrics, pressure drop testing, gas life testing, and combustion testing the optimum medium will be determined. Theoretical reaction modeling will be used to better define the behavior of activated carbon particles in combustion testing. Through the empirical and theoretical data, the system will be defined in order to predict the medium make up for future generations or applications. The end result should be an optimized filtration medium, which can be easily tailored to various applications through modeling based upon extensive empirical results. This novel medium should also be robust and easy to manufacture, as well as be used in current HVAC filter manufacturing processes.

AN AMERICAN BASED VIEW OF INDOOR AIR QUALITY

With the advance of medical science and technology, the average life expectancy continues to increase. This, along with improved diagnosis capabilities, allows medical professionals to accurately identify causes of diseases and death. A recent increase in awareness about diseases and death from poor Indoor Air Quality (IAQ) has become the focus of global scientists and researches in order to identify pollution sources, acceptable pollutant levels, and techniques/technology to improve the quality of life. In the US, the Katrina tragedy has brought focus to several IAQ problems including mold toxicity and hazardous levels of formaldehyde in manufactured housing.

The unique collection of research and demographic data assembled here attempts to answer who are at risk, where the risk is, what is causing the risk, and how this risk is manifested in humans. The compilation of data and information from diverse sources provides an accurate American perspective to this global problem in order to accurately address these questions.

II.1 Demographics and Time Apportionment

People are averaging more time indoors and this increase in time spent indoors has elucidated several aspects of the indoors including IAQ. The problem emerging to the forefront is the detrimental effects of poor IAQ on human health. Understanding of

this problem begins with the determination of who is at an increased risk and where that fraction of the population is spending time. Figure II.1 illustrates the demographic breakdown of the United States with regard to those at an elevated pulmonary or health risk. This figure is derived from federal agency reports, published research, and special interest group communications (USCB, 2006; USDOL, 2004; ALA, 2006.1; HCUP, 2003; OSG, 2005). The data presented in these sources was evaluated and compared to obtain an arithmetic average for each population fraction addressed.

Figure II.1: Population Breakdown Concerning Required IAQ Protection

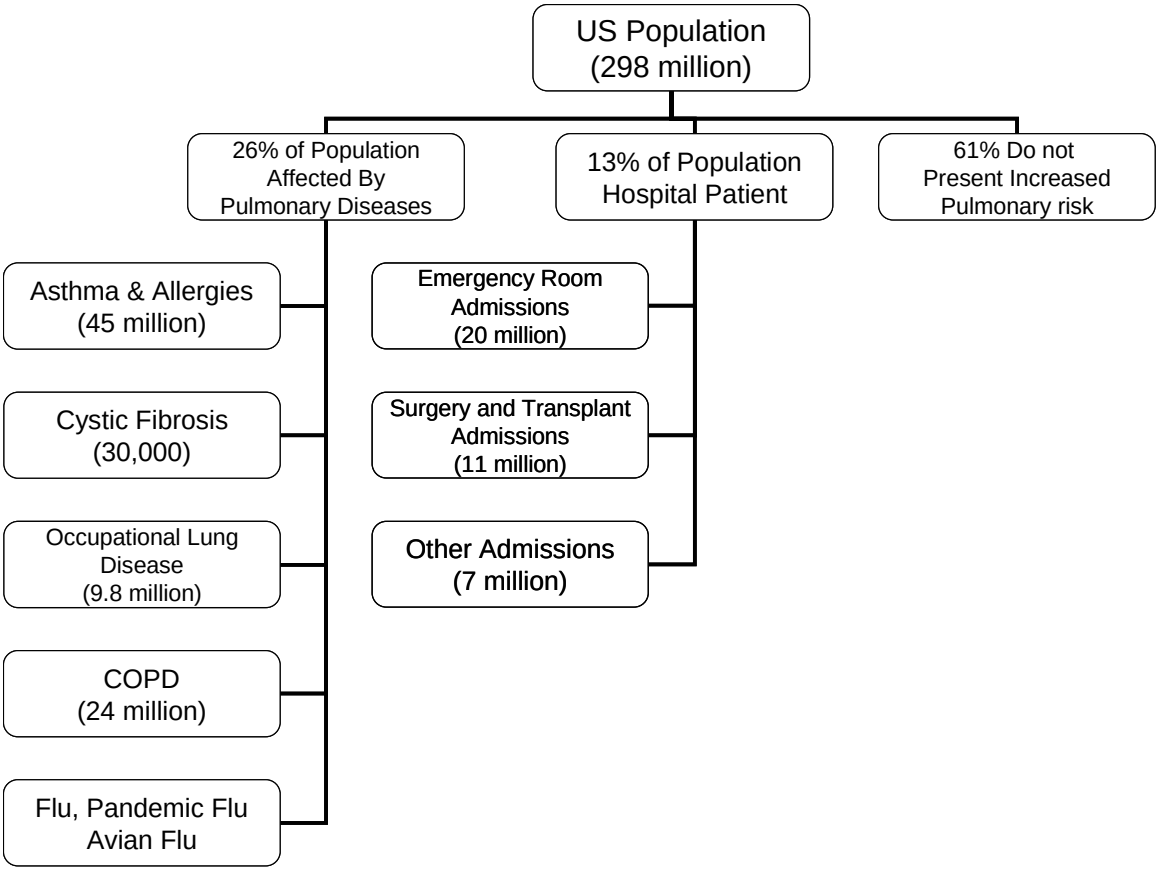

II.1.1 Population Demographics

The population of the United States as of October, 2006 was 298,768 thousand (USCB, 2006). This population is responsible for all of the manufacturing and selling of goods and services throughout the entire United States as 145,279 thousand people are employed (USDOL, 2004). When this population is finished working, they return home to an estimated 105,842 thousand housing units (including owned and rented) to rest, recover, and relax. The time spent at home and work is the bulk of time spent by the average American. With this knowledge, it is important to address where Americans are spending this time and what is the nature of that environment. The Sierra Club reports 49% of the population lives in areas where smog pollution makes the air unsafe to breathe (SC, 2003). The time spent at home and work is the bulk of time spent by the average American. With this knowledge, it is important to address where Americans are spending this time and what is the nature of that environment. These statistics, when combined with the time partitioned at home and at work, help obtain a complete understanding of possible detrimental health effects.

The American Lung Association (ALA) shines even more light on this problem by estimating that 152 million Americans live in counties with unhealthy levels of the two most prevalent contaminants, ozone and particulate matter (ALA, 2006.1). These are staggering statistics but are even more impressive when combined with the time partitioned at home and at work. According to the Sierra Club, tens of thousands of Americans die prematurely every year from air pollution (SC, 2003). A drastic end of the health concern scale, the effects of poor air quality can also be seen in what seem to be hackneyed visits to the doctor or hospital. During the summer time there are approximately 159,000 emergency room visits and 53,000 hospital

admissions, as reported by the Sierra Club, related to increased air pollution (SC, 2003). This is a significant number when noted that the government sponsored Healthcare Cost and Utilization Project (HCUP) reported that in 2003, 38 million Americans (15% of the population) were admitted to the hospital (HCUP, 2003). This shows that Americans are greatly affected by the quality of the ambient air not only outdoors, but more importantly indoors and in cars where Americans spend 69% of all their time.

II.1.2 Elevated Pulmonary Risk Population

From Figure II.1, the portion of the population at an elevated pulmonary risk is the 26% of Americans with pulmonary diseases. These diseases include allergies, asthma, Chronic Obstructive Pulmonary Disease (COPD), cystic fibrosis, and Occupational Lung Disease (OLD). Although these diseases may seem mundane, they can quickly become critical or fatal through exacerbation from air chemical contaminants.

Another portion of the population at an elevated risk is the portion in hospitals. Approximately 13% of the American population is, or spends time, in a hospital on a yearly average. Patients undergoing surgery or transplants are the portion of the population of even greater concern. Protection from foreign objects and contaminants is of utmost concern to successful treatment and health of all patients. Although a large portion of the American population (61%) does not presently exhibit an elevated pulmonary risk, more protection would be better for the overall health of this group.

II.1.3 Average Time Apportionment

The next step in defining the air quality problem is to understand how and where Americans spend time (shown in Figure II.2). This unique presentation of American based data has been compiled from a variety of resources (including governmental reports, social action committee reports, and peer review articles) (USDOL, 2004; SC, 2003; OSG, 2005; CTE, 2002; NUG, 2006; TIAA, 2005; Piechocki-Minguy et al., 2006; Laccardi et al., 2000; Sexton and Hayward, 1987; Jenkins et al., 1992).

Figure II.2: Breakdown of Time Spent by Americans

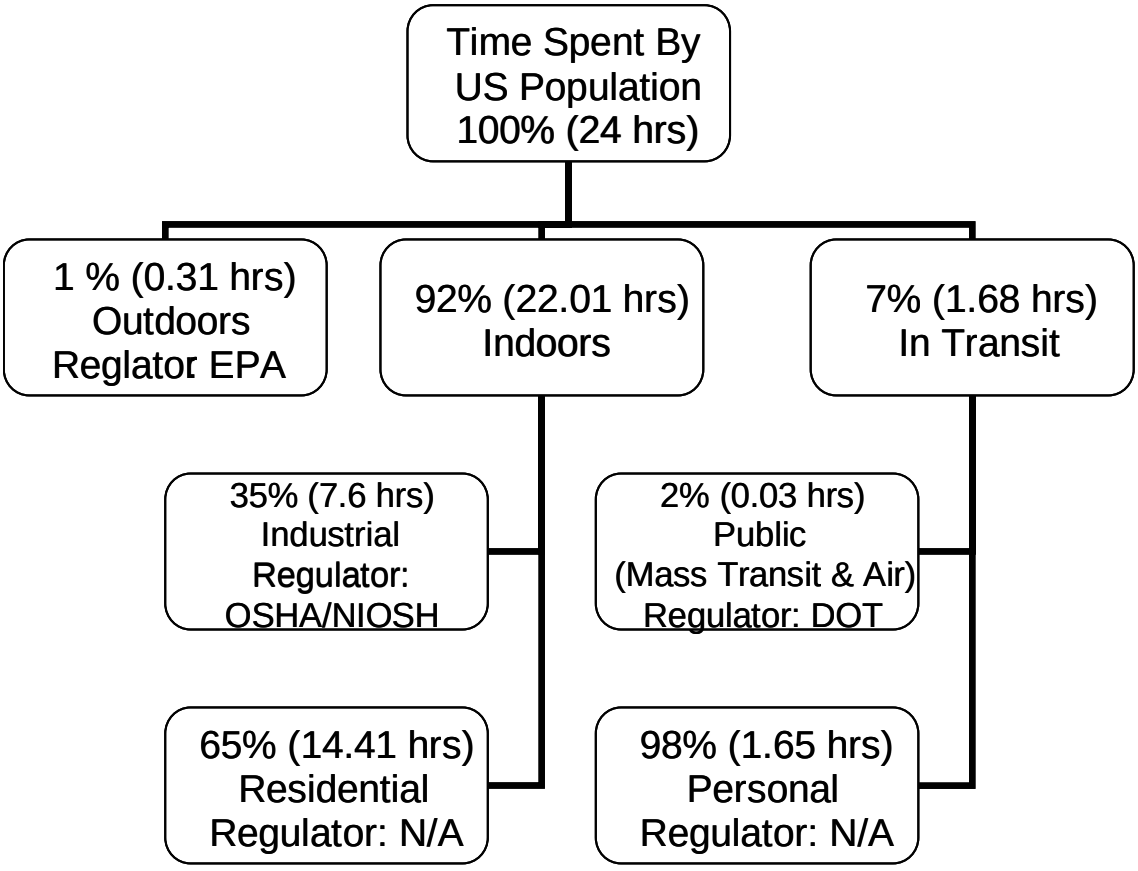

The Department of Labor presented the findings from a 2005 report concerning the average partitioning of time for average Americans (USDOL, 2004). This study shows that Americans spend a total average of 7.6 hours per day at work. This means that approximately 32% of an average day is spent at work. This also translates into 35% of the time spent indoors. All workers combined average 7.63 hours at work during an average weekday with 82.9% working during said workday. 32.9% of these same workers worked 5.82 hours on an average weekend.

The rest of the day must be divided up among personal care activities (such as sleep and hygiene) and other activities needed to complete the day. The Department of Labor reports that people spend approximately 22.01 hours a day indoors (including work, home, and indoor activities) (USDOL, 2004). This is supported by a report from the Surgeon General of the United States which states that Americans spend between 85% and 95% of their time indoors (OSG, 2005). This means that approximately 92% of the day is spent in an environment where the quality of air can be altered.

As can be seen in Figure II.2, Americans only spend 1% of their day outdoors. Outdoor air quality is monitored and regulated by the Environmental Protection Agency (EPA). The EPA regulates emissions from industry and issues public air quality alerts for many major cities. Another note of interest from Figure II.2 is that only outdoor air is closely regulated by a governing body. The industrial setting is monitored and regulated by the Occupational Safety and Health Administration (OSHA) and the National Institute for Safety and Health (NIOSH). Currently, regulations do not exist concerning air quality in work places, such as office

buildings. Mass transit is regulated by the Department of Transportation (DOT). Unfortunately the DOT does not regulate the air quality for mass transit riders.

In the areas of personal residences and personal transit there is no regulating body or standards regarding air quality. Personal residences and personal transit are where Americans spend the majority of their time. It is in this environment where Americans are at the most risk.

II.1.3a Time in Transit

Mobility and transportation are important to the success and happiness of Americans whose national culture is based upon independence and speed. The result is a nation which relies heavily upon personal transportation. American travel is estimated to be divided up accordingly: 91% is spent in private vehicles; 5% is spent in air travel; and 2% in mass transit. Personal transit is where the exposure to VOCs, carbon monoxide (CO), nitrogen oxides (NOx), sulfur oxides (SOx), and ozone is the greatest and most lethal. Drivers in one-third of U.S. cities spend over 40 hours per year (the equivalent of one work week) in non-moving traffic (CTE, 2002). This means that the driver is breathing air heavily contaminated with internal combustion engine exhaust. On-road vehicles have been shown as being responsible for 44% of all CO_2, 33% of all NOx, and 25% of all VOC emissions in the U.S. This means that the driver is not in a position to receive fresh flowing air, but rather air heavily contaminated with internal combustion engine exhaust. Unfortunately, commute time is not the only time spent in an automobile. The Green Life Group estimates that the average American will spend 101 minutes in their cars every day performing the miscellaneous tasks of errands (OSG, 2005). These activities have caused reliance upon personal automobiles and driving between destinations. Time in transit equates to

a greater risk of detrimental health effects due to prolonged exposure to poor air quality. The New Urbanism Group reports while the population only grew by 20% from 1982 to 2000, the time spent by Americans in traffic has increased 236% (NUG, 2006). Over the same time period, major cities have seen the combined daily rush hour increase from less than three hours to nearly six hours today.

The effects of this increase in traffic can be seen in detrimental health effects, but it can also be seen economically. The National Transportation Board (NTB) has predicted an increase of 5.6 billion hours in delays caused by congestion and a wasting of 7.3 billion gallons of fuel (NUG, 2006). At the current price of regular gasoline ($3.952/gallon) that amount of wasted fuel equates to $28.85 billion. The CTE reports an average rush-hour driver will waste 99 gallons of gasoline annually stuck in traffic (CTE, 2002). Annually, drivers wasted an estimated $1,160 per person in time and fuel. Not only is time spent in transit a health and economic problem, but it is also a social problem. According to Time Magazine, Americans will spend on average of 6 months during their lives waiting for light changes and over 5 years of their lives stuck in traffic (NUG, 2006). This shows the dire circumstance of time spent in traffic.

In major American cities, the alternative to personal vehicle usage is the utilization of a mass transit system including rail, light rail, and buses/motor coaches. The CTE estimated that 14 million Americans use public transportation every weekday and additionally 25 million Americans use it less frequently but still on a regular basis (CTE, 2002). The use of a mass transit system is a more efficient usage of time (on the average) and a more environmentally conscious choice of commute vehicle. The Sierra Club estimates that mass transit emits only 5% of the CO, < 8% of the VOC's, and 50% of CO_2 and NOx per mile compared to automobile use

(SC, 2003). Annually, this amounts to 70,000 tons less of VOC's and 27,000 tons less of NOx in the air. Estimates from the CTE predict if 1/5 of all Americans used public transportation daily, CO pollution would decrease by more than all the emissions from the entire chemical manufacturing industry and metal processing plants in the U.S., combined (CTE, 2002). Public transportation saves more than 855 million gallons of gasoline or 45 million barrels of oil a year or 5.2 billion kilowatt hours of electricity (which is less than 1% of all U.S. energy consumed) in 1999 – a level equivalent to the energy used to annually heat, cool, and operate 25% of all American homes, according to the CTE. Mass transit is more environmentally friendly but it does have associated time restrictions. A single U.S. subway line can carry up to 30,000 passengers in one hour (CTE, 2002).

Unfortunately when traveling, Americans overwhelming use automobiles. Fortunately, there is a growing trend to use mass transportation for travel purposes. The Travel Industry Association of America estimates 22% of Americans currently use mass transit for the travel needs including airplane, motor coach, ship, and train (TIAA, 2005)). This increase in mass transit usage also elucidates problems in the mass transit system. For example, there is growing concern with the quality of cabin air in aircraft. A growing number of online communities have been formed to alert and spread concern about the quality of cabin air (TIAA, 2005). These online communities present the personal accounts of travelers with respect to detrimental health affects and cabin air quality. Several travelers report feelings of light headedness, headaches, dizziness, and nausea due to "stale air," or air with elevated levels of CO_2. These communities are also reporting that a higher quality of cabin air achieved by reducing the amount of air that recycled throughout the cabin has produced a more comfortable travel experience. Aircraft

manufacturers, such as Boeing, dispute these testimonials with scientific findings which show that air craft cabin air contains levels of contaminants far below acceptable levels for each contaminant (TIAA, 2005). Boeing reports that findings from various research groups show that air cabin levels of CO (1.4 ppm), CO_2 (600-1,500 ppm), Ozone (0.02 ppm), NO_2 (very low), SO_2 (very low), and VOC's (1.8-3.2 ppm) are very low. With such drastic differences between what passengers and aircraft manufacturers are reporting, the difference must be in how airlines are operating the cabin air system. With 50% cabin air recycle, it is very conceivable that low levels of contaminants can quickly become high levels of contaminants if the filtration system is not serviced regularly or used per the manufacturers directions. Such a risk must be addressed or Americans at elevated risks of detrimental health effects due to high levels of contaminants will be further harmed.

II.1.3b Time Spent Indoors

Americans spend a total average of 7.63 hours at work during an average weekday with 82.9% working during said workday (USDOL, 2004). 32.9% of these same workers worked 5.82 hours on an average weekend. This means that approximately 32% of an average day is spent at work. Thus, the rest of the day is divided up among personal care activities (such as sleep and hygiene) and other activities needed to complete the day, yielding approximately 22.01 hours a day indoors. This is supported by a report from the Surgeon General of the United States (OSG, 2005) which states that Americans spend between 85% and 95% of their time indoors. This means that approximately 92% of the day is spent in an environment where the quality of air is important.

Figure II.2 shows the time spent indoors is divided by 35% at work and 65% at home. The bulk of time spent indoors during an average 24 hour period is spent at home where IAQ contamination could be a maximum. From data gathered to asses the impact of IAQ on health, it was found that urbanites spend between 79% and 96% of their day indoors; of the total day 58% to 67% is spent in a residential setting (Sexton and Hayward, 1987). Sexton and Hayward hypothesize that the important factor in IAQ and health is the time weighted average exposure. This was shown by studying the impact of selected pollutants on IAQ. These pollutants were selected because of their propensity to be found in various settings monitored (residential and industrial). From the data gathered, Sexton shows that urbanites spend between 79% and 96% of their day indoors; of the total day 58% to 67% is spent in a residential setting. Sexton hypothesizes that the important factor in IAQ and health is the time weighted average exposure. This measurement is important because it is weighted according to indoor concentrations comprising the bulk of exposure for the average person. Knowing the breakdown of time spent indoors, these contaminants (formaldehyde, NO_2, radon, PM, micro-organisms, and CO) can be adequately averaged out to yield the true long term exposure of a person. These contaminants are often found in higher concentrations indoors (including residential and workplace settings) than outdoors. Through this knowledge, Sexton was able to build a model to describe the source and flow of contaminants in flux throughout outdoor and indoor air. The notes of importance from this work are the time apportionment of individuals and the knowledge of time weighted exposure averages yielding a more accurate exposure model versus instantaneous exposure levels.

Having this average available, it can be seen that the indoor environment plays an important role in the overall exposure of humans to contaminants. Liccardi et al. present findings on two increasing causes of allergies in indoor environments as well as selected prevention strategies (Liccardi et al., 2006). Pets and cockroaches were found to cause an increased likelihood of respiratory allergic diseases due to their corresponding allergens. Liccardi also proposes that changes in lifestyles and indoor environments are emphasizing these contaminants. These changes include energy saving construction of homes, upholstery and furniture, HVAC systems, an increasing practice of keeping furred pets indoors, and sedentary lifestyles. The major changes causing the most effect are increased time spent indoors, deterioration of the ambient air in urban and suburban areas, new building materials and their associated chemicals, and the presence of many chemicals in the home. Liccardi suggests many preventative measures to remove allergens and contaminants including cleaning and washing of contaminated surfaces (carpet, clothes, and upholstery), natural ventilation, and the use of high-efficiency particulate arresting (HEPA) filters. Maintaining a clean environment with fresh air is key to maintaining a healthy home.

With a general idea of what could be found in a residential setting, the other main component of time spent is time spent at the workplace. With this in mind, the possible exposure levels found in the workplace should be identified. Riveros-Rosas et al. (1997) measured the personal exposure in Mexico City air with respect to elemental metals. Riveros divided the subjects into two groups; Group A were required by their employment to spend the majority of their time outdoors and Group B were required to spend the majority of their time indoors. Through subject surveys, it was found that Group A spent 68 ± 8.5% indoors and Group B spent

89.3 ± 6.7% indoors. This shows that even outdoor laborers spend the majority of their day indoors, and the bulk of that time is spent inside of a residence. Riveros also determined that urbanites spend over 80% of their time indoors. Riveros was also concerned with the amount of contamination and level of exposure to that contamination.

Table II.1: Personal Exposure Averages for Selected Metals Adapted from (Riveros-Rosas et al., 1997)

Metal	Exposure Level (ng/m^3)	Ambient Air Quality Standard (ng/m^3 - US EPA)	Occupational Exposure Limit (OSHA 8-hr TWA)
Lead	435 ± 220	500 (annual mean)	50,000
Zinc	361 ± 253	---	5,000,000
Vanadium	23 ± 12	---	1,000,000
Chromium	8.4 ± 5.6	---	1,000,000
Copper	34 ± 37	---	1,000,000

Table II.1 encapsulates selected data from Riveros showing the level of contamination from metals in the Mexico City Metropolitan Area. Although the average exposure levels are well below the mandated occupational exposure levels, the levels are alarming when considered on an annual basis. For a person to be exposed to such levels for an entire year would be very dangerous and possibly fatal. The US EPA only has standards for levels of lead. The occupational exposure levels set by the US OSHA are for 8hr time weight averages. These standards are not appropriate for long term exposure levels.

II.1.3c Seasonal Fluctuations in Time Apportionment

A study measuring personal exposure to nitrogen oxides determined the average time breakdown for the individuals monitored (Piechocki-Minguy et al., 2006). It was found that time spent at home during the winter occupied 62% during the work week and 88% during the

weekend, and during the summer occupied 64% during the work week and 84% during the weekend. Time spent in other indoor places during the winter occupied 32% during the work week and 5% during the weekend, and during the summer occupied 29% during the work week and 4% during the weekend. This translates into a range of 88% to 94% of time spent indoors for those surveyed. Even with the seasonal variability of time spent indoors, the time spent indoors at home is 90%, on average. The California Air Resources Board (CARB) published the findings of a statewide study (from fall 1987 through summer 1988) to determine the activity patterns of Californians over the age of 11 (CARB, 2005).

Jenkins et al. (1992) used this study to create an accurate assessment of the exposure to indoor contaminants. According to average results, Californians spend their time in the following manner: 6% outdoors, 7% in transit, and 87% indoors. Of the 87% of time spent indoors, 62% is spent at home and 25% is spent indoors away from home. The time spent indoors away from home is divided among work and daily activities such as dining out and visits to office buildings. The population was found to visit restaurants (34.5% of the population) more than office building (25.5% of the population), but the time spent in office buildings (275 minutes) is greater than the time spent in restaurants (81 minutes). Another facet of the survey is a breakdown of the time spent doing various activities. The breakdown shows 35% of the day is spent sleeping and 13% of the day is spent at work. The time spent indoors comprises a large portion of the day due to human habits and necessities such as sleeping, eating, and hygiene.

II.2 Common Air Chemical Contaminants

Since the earliest HVAC, the control of the indoor environment has become an integral part of everyday life. Poor air quality can be responsible for a myriad of detrimental health implications, such as respiratory disease, irritation, cancer, and even premature death (CARB, 2005). These health problems can be caused by common air chemical contaminants such as Environmental Tobacco Smoke (ETS) and pet dander or from toxic chemicals such as Polycyclic Aromatic Hydrocarbons (PAHs), Volatile Organic Compounds (VOCs), and radon. Since the inception of HVAC systems, particulate removal has been of the utmost concern. Innovations in HVAC filter media and filter manufacturing have provided great strides in the removal of fine particulate from indoor air. HEPA and Ultra Low Penetration Air (ULPA) filter media can provide air free of 99.97% of 0.3 μm in size and 99.999% of 0.12 μm in size (respectively). Although the amount of particulate in the air is reduced, chemical contaminants causing adverse health effects have not been addressed.

II.2.1 Outdoor Chemical Contaminants

IAQ is a function of outdoor air contaminants as well as indoor air contaminants. Before energy efficient building materials, the main contributions to poor IAQ were contaminants and particulates entering from the outdoor air. Outdoor air contamination is dependent upon location; where large cities are a “worst case” scenario and rural areas are the “best case” scenario. Tran et al. (2000) focused on the monitoring and quantification of Volatile Aromatic Hydrocarbons (VAHs - benzene, toluene, ethyl-benzene, o-, p-, and p-xylene) as well as oxalic

acid, malonic acid, succinic acid, and adipic acid in the air during various times of the day in and around the University of Las Vegas. Selected results from Tran are encapsulated in Table II.2.

Table II.2: VAH Concentration Measurements Obtained from (Tran et al., 2000)

Volatile Aromatic Hydrocarbon	Measured Concentration (ppbV)	
	Highest Concentration Measured	Lowest Concentration Measured
Benzene	2.3	0
Toluene	5.1	0
Ethyl-Benzene	0.5	0
m- & p- Xylene	2.0	0
o-Xylene	4.6	0

Tran et al. correlates these VAH levels with an increased level of ozone and CO. VAHs will convert into ozone and CO through naturally occurring photochemical destruction. Taking this conversion into account along with exhaust from internal combustion engines and evaporative fuel loss, the levels of ozone and CO were found to be higher later in the day. This poses a greater health risk factor for these VAHs as opposed to others due to the increased toxicity of the decomposition products over the reagents themselves.

Pankow et al. (2003) measured the concentrations (in ppbV) and co-occurrence of 88 VOCs in ambient air of 13 locations (ranging from and urban to semi-rural setting) in the United States. From the data, Pankow et al. found a co-occurrence (or the possibility of finding one compound class with a second) between the gasoline additive related class of compounds and the monocyclic aromatic hydrocarbons, namely the BTEX group (benzene, toluene, ethyl-benzene, and xylene) and MTBE. A poor correlation was found with CFCs, 2-butanone, possible biogenic compounds and all other compounds. Another result of note is that benzene, toluene, and MTBE

were found to exhibit seasonal behavior with maximums occurring during the winter and minimums in the summer (shown in Figure II.3). Seasonal fluctuation is important because it mimics the time when Americans spend more time than average indoors.

Figure II.3: Ambient Air Contaminant Concentrations in Roseville, CA Obtained from (Pankow et al., 2003)

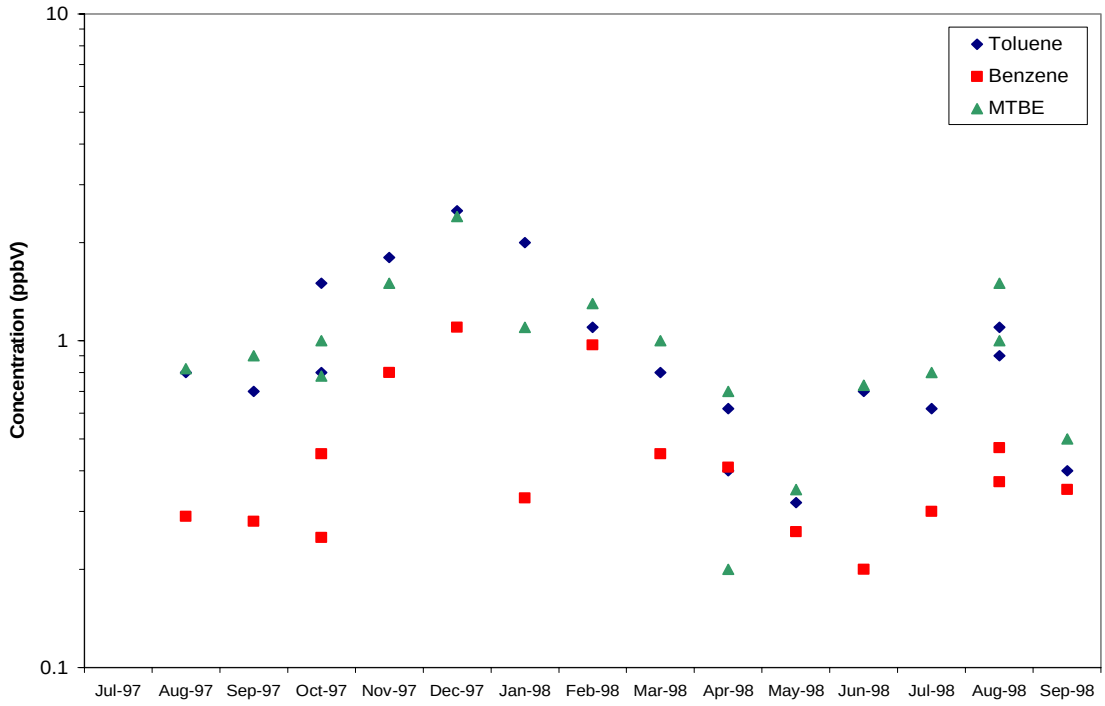

II.2.2 Indoor Chemical Contaminants

The main contaminants in all homes are VOCs and particulate matter (PM). In order to illustrate this, ten homes in southeast Chicago were monitored for one year to determine the levels of VOCs, PAHs, and various elements (Van Winkle and Scheff, 2001). A large assay of VOCs and PAHs were detected with the predominant VOCs being methylene chloride, m- and p-xylene, and 1,1,1-trichloroethane. The most common PAHs detected were naphthalene and

fluorene. Lead was ubiquitously detected in the ten homes monitored. Selected results from Van Winkle and Scheff are encapsulated in Table II.3. The results show high levels of methylene chloride, 1,1,1-trichloroethane, and xylenes. These compounds are known to be toxic and are suspected carcinogens.

Table II.3: Summary of Contaminant Concentrations Obtained from (Van Winkle and Scheff, 2001)

Compound	Indoor (ng/m^3)			Outdoor Median (ng/m^3)
	Mean	Minimum	Maximum	
Methylene Chloride	140,000	760	1,190,000	486
Toluene	15,300	2,370	29,400	2,693
m,p-xylene	34,900	5,720	56,000	1,715
o-xylene	11,200	1,130	186,000	695
1,1,1-trichloroethane	24,900	980	293,000	1,037
Naphthalene	851	Nd	5000	Nd
Fluorene	59.0	Nd	600	6.4
Calcium	796	Nd	2,710	4,100
Sodium	391	Nd	2,130	570
Iron	359	Nd	1,460	1,600
Lead	19	1.5	88	32

The levels of VOCs in apartment buildings were measured and modeled to identify the typical level of indoor contamination (Jo et al., 2009). On site measurements and surveys were used to collect data regarding air quality in newly built apartment homes in the Republic of Korea. The results show that many of the VOCs measured (formaldehyde, toluene, xylene, and TVOC) all seemed to increase in concentration with an increase in temperature, but only formaldehyde showed a direct relationship with temperature. It was also shown that chemical contaminants exhibited a direct relationship with humidity. Formaldehyde and toluene showed linearly proportional results; while TVOC's, xylene, benzene, and styrene reached a maximum

concentration at approximately 50% humidity. The other interesting result is the possibility of a direct relationship of all contaminants (except for formaldehyde) with apartment size. This illustrates an additive effect of having more pollutant causing materials in a home yielding increasingly higher VOC concentrations. The study also show a decline in contaminant concentration over the first year (~50%); but formaldehyde concentrations did not decline as rapidly as other contaminants.

A similar study was done in Europe and showed similar trends (Rehwagen et al., 2003). Through data collected it was shown that VOC levels generally fluctuate throughout the course of a year with a maximum in January and a minimum in August (shown in Figure II.4)

Figure II.4: Seasonal Fluctuation Pattern for a 30 VOC Sum Obtained from (Rehwagen et al., 2003)

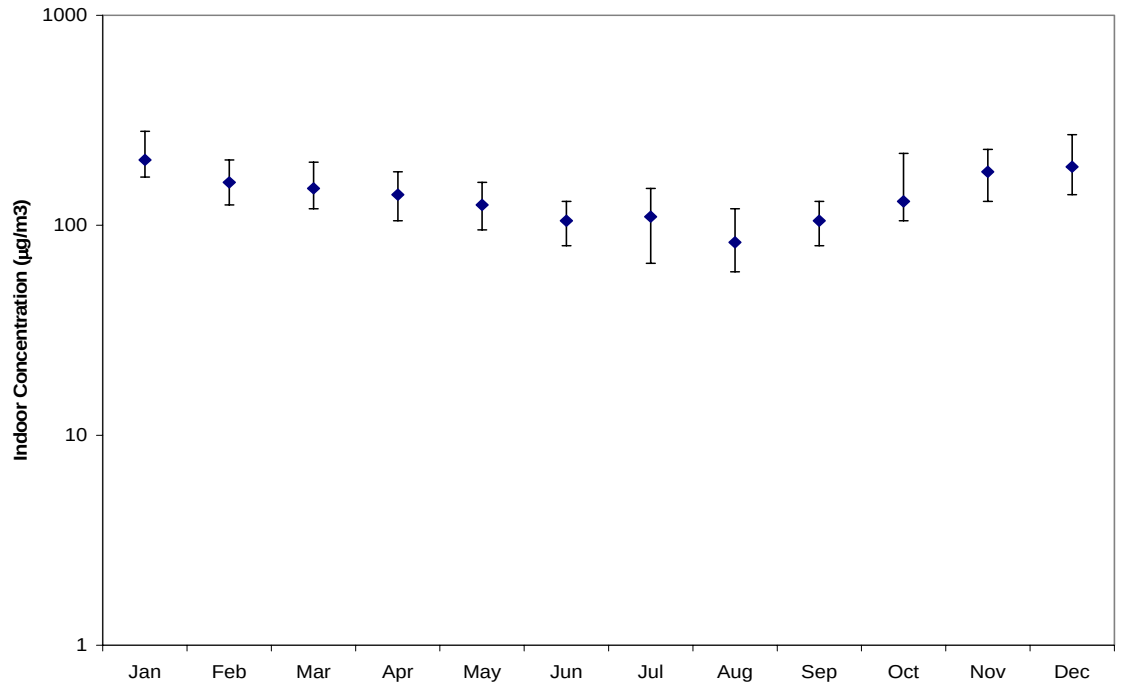

The maximum in January could be attributed to the weather and increased time spent indoors. Activities such as cooking, repeated cleaning, and building hearth fires all increase VOC

contamination. Due to the cold weather forcing those studied to stay indoors, and the increase of VOC generating activities (i.e. holiday cooking and hearth fires) would likely lead to a maximum. The minimum in August is due to the opposite effect caused by warm weather. This seasonal cycle mirrors the cycle found in Figure II.3. Rehwagen et al. also noted the levels of 30 different VOC, which were divided into five groups (alkanes, cycloalkanes, aromatics, halogenated hydrocarbons, and terpenes) for reporting purposes (selected results are encapsulated in Table II.4).

Table II.4: Statistical Values of VOC Concentrations Obtained from (Rehwagen et al., 2003)

Compound	Indoor Concentrations ($\mu g/m^3$)		Outdoor Concentrations ($\mu g/m^3$)	
	Mean	Maximum	Mean	Maximum
Decane	10.01	807.54	0.53	9.36
Undecane	10.19	581.89	0.55	14.71
Toluene	31.81	813.74	4.28	39.73
α-Pinene	24.77	392.71	1.40	43.46
Limonene	36.69	1277.66	0.57	16.98
30 VOC Sum	199.69	4597.11	20.85	159.39
Alkanes Sum	51.52	2133.68	5.00	72.84
Cycloalkanes Sum	12.42	319.74	2.15	18.00
Aromatic Sum	58.79	3250.25	10.62	64.43
Halogenated Hydrocarbon Sum	6.33	554.62	0.56	6.35
Terpenes Sum	69.61	1361.23	2.51	63.48

The 30 VOC sum is comprised of approximately 25% alkanes, 7% cycloalkanes, 30% aromatics, 3% halogenated hydrocarbons, and 35% terpenes. The maximum 30 VOC sum for indoor air is an order of magnitude greater than the outdoor air measurement. Almost all of the compounds

were measured in greater concentrations indoors versus outdoors. Taking into account Americans spend 14.41 hours of the day in this environment, the health risk is clearly elevated.

II.2.3 Sources of Chemical Contaminants

The concentrations of VOCs in newly built houses with respect to ventilation rates were measured in Minnesota (Bartekova et al., 2005). This work attempted to isolate typical levels of overall contamination, contamination evolving from elements in the house, and the effect of ventilation operation on contamination levels. TVOC levels were found to be high (2.3 milligrams per cubic meter) during the first month after completion. After six months and the use of the ventilation system, the TVOC level dropped significantly to 0.455 milligrams per cubic meter. The bulk of the VOC emissions in the houses were attributed to the materials used in construction, such as oriented strand board (OSB) and wall paint. The OSB samples all eluted the same compounds of nonane, α-pinene, and aromatics (including benzene and toluene), all suspected carcinogens.

Not only is the determination of individual VOC's in IAQ important, but the identification of sources is also important. Wilke et al. (2004) measured the emission of VOC's and Semi-Volatile Organic Compounds (SVOC's) from floor covering structures. Emission test chambers were employed to measure the emission rates of VOC's from individual components and complete flooring structures (concrete, primer, screed, adhesive, PVC, carpet, and linoleum). The samples were held no less than 28 days in the test chamber under 23ºC, 50% RH and an air flow rate of 1.25 cubic meter per square meter – hour. Wilke concludes that the individual components emit a significant amount of VOC's and SVOC's, but can not be used to determine

the emission of the complete flooring structure. In all cases, the emission rate of the complete flooring structure was found to be less than the sum of the emission rates for the individual parts. It was also found that PVC and linoleum flooring suppressed the emission rate of the individual flooring components underneath. Another alarming result was discovered when all of the flooring components tested emitted an amount of unknown compounds which increased the possible health risks associated with VOC emission. One encouraging note is that TVOC and TSVOC levels decrease along time. From these results, it can be seen how easily common sources of IAQ contamination can be overlooked.

Osawa and Hayashi (2009) present results from a Japanese nationwide survey of indoor air quality. The concentrations of various VOCs were measured in new built homes over a five year period. The home owners were also administered surveys to ascertain any detrimental physical effects of the living in the newly built home. Japan has suggested guidelines for contaminant concentrations. These guidelines include contaminants such as formaldehyde (0.08 ppm), toluene (0.07 ppm), xylene (0.20 ppm), ethyl-benzene (0.88 ppm), styrene (0.05), and acetaldehyde (0.03 ppm). These guidelines may seem stringent, but the results from the five year study show that only formaldehyde and toluene were measured at levels above the suggested guidelines (maximum of 0.10 ppm and 0.08 ppm, respectively). Although all contaminants showed a marked decrease in concentration within the first year, the initial concentration is of concern due to the proximity of the contaminants to the suggested guidelines.

Singer et al. (2004) simulated an indoor residence to determine the sorption of VOC's into the room constituents. The study monitored a 50 cubic meter room with painted wallboard, carpet with cushion pad, and furnishings including draperies. A pulse of gas-phase VOC's was

introduced in the room and measured during an adsorption and desorption period. It was found that benzene, MTBE, isoprene, and 2-butanone were not absorbed into the room materials. Conversely, C_8-C_{10} aromatics, terpenes, and pyridine along with many other VOC's were absorbed into the room materials. Figure II.5 shows selected results from Singer illustrating the effect of sorption into the room on the gas phase concentrations of contaminants at two residence times.

Figure II.5: Fraction of Contaminants in the Gas Phase Adapted from (Singer et al., 2004)

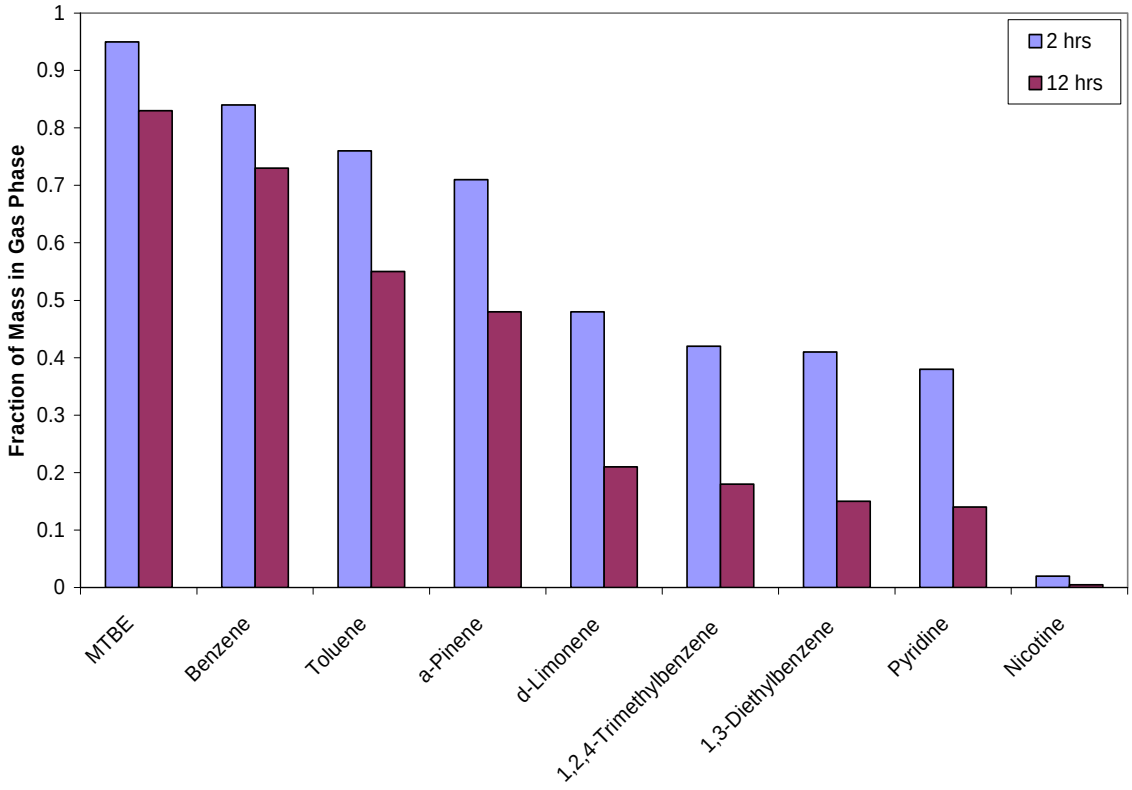

This work shows that not only do materials in the home produce VOC's, but they can also absorb and desorb VOC's degrading the quality of residential IAQ.

Even if an HVAC system were to be equipped with sophisticated filtration and operated at high duty cycles, the problem of unhealthy contaminants would not be remedied. Parti-Pellinen et al. (2000) studied the relationships between ventilation and air filtration systems on IAQ in a Finnish day care. The levels of nitrogen oxides (NO, NO_2) and particulate matter (PM_{10}) were monitored during various periods of activity and outdoor air infiltration of the center. It was found that during levels of high activity (both indoors and outdoors) the PM_{10} was found to be as high as 25% of the outdoor PM_{10} level. Also during times of high pollution outside of the school, the level of nitrogen oxide penetration inside the school was found to be very high (NO level of 34.8 micrograms per cubic meter and NO_2 level of 21.3 micrograms per cubic meter). This illustrates that even when a filtration system is being operated at design levels current methods of filtration are inadequate. Focusing solely on particulate filtration does not account for the toxic chemical contaminants. This requires a new focus on removal of contaminants as well as particulate while operating within current HVAC design constraints.

This problem does not only apply for this type of building; this problem has been observed in several types of buildings and places worldwide. Nilsson et al. (2004) studied the effects of residential humidity on the presence of microorganisms and VOC's in Swedish residences. This study revealed that damp homes have a greater presence of molds and bacteria than the control homes. The damp residences were found to have 23 different types of mold where the control homes only contained 18 types, with the mold homes having 9 types of mold not found in the control homes. The identification of *Aspergillus*, *Cladosporium*, and *Penicillum* revealed a number of VOC's known to be produced by these species (medium to long chain

alkanes, ketones, and alcohols) as well as a number of traditional VOC's irritating to the skin and eyes.

This type of IAQ contamination is more prevalent than ever due to improved home insulation and removal of outside air infiltration. Another reason for biological growth contamination is a natural disaster such as the recent tragedy of Hurricane Katrina in the Southern United States. Shoemaker (2006) studied the effects of mold and the health of patients in St. Bernard Parish in Louisiana from February 9, 2006 until February 12, 2006. Shoemaker is attempting to identify the correlation between prolonged exposure to toxigenic molds (such as spirochetes, dinoflagellates, and cyanobacteria) and water-damaged buildings (which can contain fungi, endotoxin forming bacteria, and actinomycetes). Shoemaker defines the term mold illness as a complex, multi-symptom, multi-system illness that follows exposure to buildings with water damage or intrusion. Through interviews with 206 patients, Shoemaker yielded a hypothesis that 24% of all exposed to water damaged buildings would become ill regardless of age, race, and gender. This shows contamination can come from various sources normally unseen by the average home owner including common house hold molds and mildew. Molds will grow in conditions where relative humidity is above 60%. As long as this humidity condition is satisfied, the ability of common indoor molds (such as *Penicillium*, *Cladosporium*, *Stachybotrys*, and *Aspergillius*) to grow is unimpeded. Another factor leading to the widespread growth of such molds is the HVAC system. The HVAC system is the perfect distribution tool for mold spores throughout an entire building. Having a cool temperature, the right humidity, and a lack of light helps to develop and distribute mold spores easily. Having good control of humidity is one way

of controlling mold, but providing an efficient and effective filtration method to protect the HVAC system is the key to preventing the spread of mold spores.

Shinohara et al. (2009) monitored a third floor suite and measured not only the concentrations, but also the emission rates of VOCs. The VOCs measured included formaldehyde, toluene, and acetone. The study focused on measuring formaldehyde and toluene concentrations and identifying the sources of these contaminants. It was found that formaldehyde eluted mainly from the furniture (125 $\mu g/m^2$-h), and toluene from the ceiling and carpet (80.0 $\mu g/m^2$-h and 72.3 $\mu g/m^2$-h, respectively). The suite also had a relatively high air exchange rate of 1.84/h; which was used to help calculate the contaminant flux. The carpet, ceiling, and walls were noted as the highest emitting sources in the suite (other notable sources include the doors, closet, and flooring). This shows that not only do newly constructed buildings contribute to chemical contamination, but also the materials contained within the building.

Knowing the appropriate ventilation rates to control VOC concentrations is vital to understanding how HVAC systems can protect residents from poor IAQ. The ventilation rates and the concentrations of 54 different VOCs in manufactured and site-built houses in the Southeast United States were measured to identify this possibility (Hodgson et al., 2000). The most common compounds found in both manufactured and site-built houses are α-pinene, ethylene glycol, hexanal, acetic acid, and formaldehyde (selected data is encapsulated in Table II.5).

Table II.5: Common Contaminant Concentrations Obtained from (Hodgson et al., 2000)

Compound	Manufactured House (ppb)		Site Built House (ppb)	
	Mean	Range	Mean	Range
α-Pinene	16.3	5.4 – 35.3	28.1	12.2 – 60.0
Ethylene glycol	17.9	<9.2 – 43.8	83.0	20.7 – 491
Formaldehyde	34	21 – 47	36	14 – 58
Hexanal	16.1	7.9 – 25.9	26.3	14.1 – 51.3
Acetic Acid	117	24.9 - 275	53.9	36.0 – 91.8

Using this as a baseline, the effect of ventilation rate on VOC emission rate can be seen. The ventilation rate was lowered from 0.32 air changes per hour in the first week to 0.14 air change per hour in the second week (both below the minimum ASHRAE standard for air change rate of 0.35 h^{-1} for these houses). Ventilation rate, or air change rate, is the volumetric flow rate of the air per hour divided by the volume of the space (or in this case the entire house) being ventilated. The majority of compounds did not exhibit any change in their emission rates between the two ventilation rates, but a few did exhibit a change (Table II.6 contains selected results).

Table II.6: Effect of Ventilation Rate Change for Selected Contaminants Obtained from (Hodgson et al., 2000)

Compound	Emission Rate (μg/m^2-h)	
	Week 1 (0.32/h)	Week 2 (0.14/h)
Acetic Acid	246	157
Tridecane	50.4	37.2
Tetradecane	43.1	30.0
TMPD-DIB	69.6	47.6
α-Pinene	56.1	45.8
Hexanal	42.1	34.0
Nonanal	12.6	7.0
Toluene	7.8	8.5
2-Butanone	6.8	6.7
Formaldehyde	29	27
Acetaldehyde	16	15

As can be seen, a change in ventilation rate is a tool that can be used to improve air quality. In this instance, the lowering of air change rate improved air quality but this does not hold true for every case. Unfortunately, it is not a definitive solution for all poor air quality cases. Since the air exchange rate in all buildings can not be manipulated enough to make a major difference in the level of chemical contaminants another solution must be identified.

II.2.4 Current and Proposed IAQ Contamination Regulations

Not only is removal of toxic chemicals important to improving health and IAQ, but also the determination of the permissible level of pollutants. This is a task that the appropriate professional societies and governmental agencies must undertake and enforce to improve the quality of life and health for all people. The State of California Air Resources Board (CARB, 2005) has taken the lead in researching and proposing exposure limits for IAQ pollutants. In a 2005 report submitted to the California State Legislature, CARB presented volumes of research and literature to support revolutionary changes and limits for the improvement of residential IAQ. Figure II.6 compares the standards set for outdoor air by CARB and the United Stated Environmental Protection Agency (US EPA) to CARB recommended indoor standards. As can be seen in Figure II.6, there are no limits recommended for PAH's or chlorinated HC's but there is a recommended limit of <27 ppm for formaldehyde. The only recommendation that CARB can make at the moment with the available research is to limit or avoid exposure to a minimum in order to reduce the risk of cancer.

Figure II.6: CARB Recommendations for Residential IAQ Replicated from (CARB, 2005)

Pollutant	Measurement Period	Outdoor Air Quality Standards		ARB Recommended Maximum Indoor Levels
		ARB	U. S. EPA	
Formaldehyde (HCHO)	24-hour 8-hour	---	---	Lowest level feasible to reduce cancer < 27 ppb to avoid acute irritant effects
Carbon Monoxide (CO)	8 hours	9 ppm	9 ppm	9 ppm
	1 hour	20 ppm	35 ppm	20 ppm
Nitrogen Dioxide (NO_2)	24 hours	---	---	0.08 ppm avoid repeated high exposures
	1 hour	0.25 ppm	---	0.25 ppm
Particles – (PM10)*	24 hours	50 $\mu g/m^3$	150 $\mu g/m^3$	50 $\mu g/m^3$
Particles – (PM2.5)*	24 hours	---	65 $\mu g/m^3$	65 $\mu g/m^3$
Polycyclic Aromatic Hydrocarbons (PAHs)	---	---	---	Lowest levels feasible to avoid cancer risk. Avoid or minimize exposure.
Chlorinated Hydrocarbons, e.g., chloroform Trichloroethylene *p*-dichlorobenzene methylene chloride perchloroethylene methyl chloroform	---	---	---	Lowest levels feasible to avoid cancer risk. Avoid or minimize personal exposures.

Another entity that is leading the way in awareness is the State of Washington Department of Health (WSDOH, 1999). Although the department has not set any residential standards, it has done extensive research into the most common pollutants and has begun to disseminate information about health effects, sources of these pollutants, and control methods. Unfortunately the information provided is very limited in scope. The pollutants chosen are formaldehyde, asbestos, radon, ETS, combustion by-products, household chemicals, pesticides, microorganisms, allergens, and mold. This list may seem to cover all of the possible IAQ pollutants but it does not shed enough attention in the area of VOC's and PAH's where toxicity is high. The only VOC specifically addressed is formaldehyde, and the guidelines that are proposed are workplace guidelines set by ACGIH, OSHA, and NIOSH (ACGIH proposes a

maximum exposure limit of 0.3 ppm; OSHA specifies 0.75 ppm TWA-8hr, 0.5 ppm action level, and 2 ppm 15 minute exposure limit; NIOSH specifies 0.016 ppm TWA-8hr and 0.1 ppm 15 minute exposure limit). The lack of firm recommendations is compensated by the raising of awareness about IAQ and health.

The US EPA (1995) has also published a similar document describing residential IAQ, sources and methods of control for various pollutants, and how to identify problem buildings. In this publication, the EPA presents a similar list of pollutants as the Washington State Department of Health with the addition of lead and asbestos. The EPA also places a great emphasis on appropriate design and usage of a mechanical ventilation system and air cleaning. The EPA (1990) places so much emphasis on air cleaning that a document was published rating all of the residential air cleaning devices available in 1990. A wide range of air cleaners were evaluated including electronic air cleaners, panel filters, activated carbon, portable units, and ion generators. The EPA clearly makes the disclaimer that it is not an air cleaner certifying agency, thus does not make a clear determination of which type of device is best for removing IAQ pollutants. The EPA did find that for all filtration devices a heavy dependency on placement in the room, air flow rate through the device, the mass of particles/type of gaseous compound, and how the device degraded (or efficiency of filtration with increased amount captured) over time. For particulate filtration, portable units were found to perform adequately (depending on model) but were influenced by a number of factors. The in-duct HVAC system filter systems were all based upon their ASHRAE rating and their performance was well documented and known. For gaseous contaminants, the in-duct HVAC filter systems had little to no data to support any filtration capability. Specialized systems tested utilizing activated carbon or other

sorbent/reactive systems were ineffective against a broad spectrum of contaminants. The portable units also proved ineffective against removing chemical contaminants. Unfortunately, the lack of firm and strict standards and guidelines illustrates the lack of knowledge about IAQ. What can be derived from these emerging standards is a push toward novel filtration mechanisms to remove not only PM but also chemical contaminants such as VOC's. In order to truly understand this need, the effect of poor IAQ on health must be defined.

II.3 Effect of Poor Air Quality on Human Health

The recent volume increase of research performed on air quality is evidence that corporations, governments, and scientific communities are concerned with the current state of air quality and human health. True understanding of the importance of good air quality is achieved by researching the detrimental health effects of poor air quality.

The percentage of health evaluations concerning air quality conducted by the National Institute for Occupational Safety and Health (NIOSH) at the Center for Disease Control and Prevention (CDC) over the past 25 years has increased from 0.5% to 52% of all evaluations. This shows an increased concern and awareness of the effect of IAQ on the quality of life (OSG, 2005). This new research focus is well placed due the annual death of 349,000 Americans from lung disease (resulting from all possible sources) (ALA, 2006.1). This death rate is increasing while death rates for heart disease and cancer have been on the decline.

Such an interest in air quality research and findings of poor indoor air quality point to the need for a greater level of protection not only for all American but especially for those with

existing or developing lung diseases. Figure II.1 illustrates this demographic breakdown concerning those at an elevated risk of pulmonary damage or infection due to poor air quality.

II.3.1 Pre-Disposed Conditions Exacerbated by Poor Air Quality

Following is a selection of health conditions which are sensitive to poor air quality, especially indoor air quality. This is only a selection of the most common health conditions and represent the largest population percentage at risk from poor air quality.

II.3.1a Asthma and Allergies

Asthma is a chronic condition in which the muscles tighten around the airways resulting in difficult breathing, wheezing or coughing and inflammation or swelling of airway lining (PSR, 1997). This disease is characterized by an excessive sensitivity of the lungs to various stimuli such as viral infections, particles in the air, and irritating gases (ALA, 2005.1; ALA, 2005.2). Allergies are defined as any disease of the immune system which causes an overreaction to substances known as allergens (AAFA, 2005). Allergies are classified according to their specific allergen, target of the body, and chronology. The allergies of particular interest are termed indoor and outdoor allergies. These allergies, known as perennial allergic rhinitis, are caused when allergens such as mold, pet dander, and indoor air pollutants are inhaled resulting in allergic reactions. This can be prevented by simply controlling the air quality and removing the allergen sources, maintaining a clean environment, and air filtration.

Asthma is not only a disease that affects adults. Asthma can become a life threatening disease early in childhood. The Surgeon General has reported that IAQ is affecting the health of

children since millions of homes and 1 in 5 schools in America have IAQ problems, which trigger a myriad of allergies and asthma attacks (OSG, 2005). Exposure to poor IAQ has a more pronounced effect on children due to the lack of bodily development. According to the Surgeon General, the time from 1990 to 2005 experienced a rise in asthma in young children of 160% resulting in one out of every thirteen children having asthma.

An attempt to identify a relationship between asthma and certain criteria pollutants was done with a specified list of pollutants (Koren, 1995). The list of pollutants included ozone, SO_2, NO_2, and particulate matter less than 10 micrometer in diameter (PM_{10}) by which to test asthmatics for bronchial response. The results from clinical testing revealed no clear tie between the selected pollutants and asthmatic response as compared to the response from a non-asthmatic person. But the results did show that asthmatics are more sensitive to the pollutants studied than healthy patients. The main result of note is that regardless of the patient's condition, all were susceptible to reaction.

A health survey was conducted to determine the relationship between asthma and newly painted surface emissions (Wieslander et al., 1997). Monitoring the air quality of selected homes, it was identified that the presence of formaldehyde eluted from wood chip composites, paint, and polyurethane foams. Homes with a combination of the formaldehyde contributions could lead to breathing problems such as bronchial hyper-responsiveness (BHR), asthma, and nocturnal breathlessness with very little contamination. Strong correlations were identified between newly painted surfaces (both residential and industrial) and asthma as well as nocturnal breathlessness, wheezing. In general, exposures to VOCs exhibit a direct relationship to asthma

and BHR. Wieslander et al. recommend that asthma management may by improved by taking notice of IAQ and minimizing exposure to and concentration of VOCs.

II.3.1b Cystic Fibrosis

Cystic fibrosis (CF) is a genetic disease causing the body to produce abnormally thick and sticky mucus that clogs the lungs and leads to fatal lung infections affecting 30,000 adults and children in the U.S. (CFF, 2005). According to the Cystic Fibrosis Foundation, approximately 1000 new cases of CF are diagnosed each year commonly affiliated with chronic cough and an increased likelihood for upper respiratory infection. Approximately 90% of all CF cases involve the lungs and an increased pulmonary sensitivity to air contaminants (AARC, 2002). Environmental control is often part of the prescribed treatment plan for chronic care and can become such a high priority that the location of a home and the environment surrounding the home are critical. In such cases CF is no longer a disease that can integrate into daily life but must be planned around.

II.3.1c Chronic Obstructive Pulmonary Disease

Chronic obstructive pulmonary disease (COPD) is defined as the combination of chronic bronchitis and emphysema, both characterized by obstruction of airflow interfering with normal breathing (ALA, 2006.2). It was estimated that in 2003 that COPD was found in 24 million Americans with an original estimate of 10.7 million, showing an under diagnosis of the disease. COPD was reported as the fourth leading cause of death in 2002 claiming the lives of 120,000 Americans. COPD has many risk factors including air pollution and smoking (including second-

hand). In occupational exposure cases, a study estimated that 19.2% of all COPD cases were attributed to work and among those with COPD who never smoke 31.1% were from occupational exposure.

II.3.1d Occupational Lung Disease

Occupational exposure is becoming a leading cause of lung disease. Occupational Lung Disease (OLD) is defined as a broad category of diseases which can be non-occupationally specific but work aggravated or occupationally specific disease (ALA, 2006.1; ALA, 2005.3). Such diseases could be adult-onset asthma, COPD, lung cancer, asbestosis, coal worker's pneumoconiosis (black lung), byssinosis (brown lung), and farmer's lung. Adult onset asthma (the most common form of occupational lung disease) is estimated to account for 15% to 25% of all new adult onset asthma cases in the U.S. caused from occupation exposure to contaminants. The most lethal disease, black lung, brown lung, and asbestosis/mesothelioma can be directly caused by exposures found in the workplace. Long-term exposure to irritating or toxic agents in an occupational setting is the main cause of occupational lung disease. While occupational lung diseases are often not curable they are always preventable by taking the appropriate precautions regarding ventilation, personal protective equipment, and collective protective equipment.

II.3.2 Diseases Caused from Exposure to Poor Air Quality

Over the course of a lifetime, the average human will intake more than half of their air from inside the home (Sundell, 2004). Sundell presents evidence showing IAQ as being responsible for increased occurrences in disease and death. The diseases linked to IAQ range

from the common cold and allergies to serious airway infections and even cancer. A pre-emptive way to determine the effect of poor IAQ on health is to determine the concentration of pollutants in the human system.

A way to determine the ingestion of pollutants, other than biomarkers and resultant diseases, is gas-chromatography mass-spectrometry which was utilized by Phillips et al. (1999) in the evaluation of variation in VOC's found in the breath of humans. From the testing results, a total of 3481 VOC's were measured in the breath of 50 subjects with only 27 of those common to all subjects. On average, 200 VOC's were measured in each subject's breath. The common compounds include isoprene (alveolar gradient of 60.34), benzene (gradient of 4.77), naphthalene (gradient of 4.07), and long chain alkanes (tetradecane measured an alveolar gradient of 0.23). One compound common to 98% of all the subjects and common in the IAQ research is α-pinene. The study also measured the concentration of VOC's in the air and in alveolar expiration. This difference, or alveolar gradient, is the measure by which Phillips determined the concentration of contaminants in the subjects. The assumption is that the VOC's are ingested or inspired and then expelled from the body through hepatic (liver) and renal (kidney) functions but excess contaminants are expired. Phillips hypothesizes that this measure illustrates how inspired VOC's can be measured and used to determine IAQ and possible contaminants. This is an interesting tool to diagnose and investigate possible sources of illnesses if IAQ is a suspected culprit.

II.3.2a Industrial Setting

Sick Building Syndrome and Legionnaire's Disease are two diseases caused by poor IAQ that have recently received media attention. Environmental and human characteristics in a non-problem building were measured to determine the cause of symptoms related to Sick Building Syndrome (SBS) (Hodgson et al., 1991). A correlation was made determining the causes for SBS symptoms by measuring the environment around the test subjects and monitoring their physical responses to the changing environment. Positive individual correlations were found between noise and air flow rate, chest tightness and particulate matter and VOCs. It was also noted that as VOC concentration increased, a positive relationship was formed with relative humidity and temperature. CO_2 concentration and lack of mental concentration and chest tightness also exhibited a positive relationship. Hodgson suggests that SBS is specifically caused by environmental causes as shown by the correlations observed, namely VOCs. Hodgson also suggests that the ventilation standards set by the American Society of Heating, Refrigerating, and Air-conditioning Engineers (ASHRAE 62-89: 15 cfm/person) are enough to dilute and purge a building from human produced pollutants but not human and non-human produced pollutants combined (approximately 85% of pollution found was not produced by humans).

In a similar office environment, the detrimental effects of poor IAQ on productivity and performance were measured (Wyon, 2004). Productivity rates were found to decrease by 6% (in the laboratory setting) to 9% (in the actual offices). Wyon was not able to isolate the mechanism or specific cause for the discomfort but was able to find a relationship of increased discomfort with increased air chemical contamination. Wyon varied ventilation rates in selected experiments and found in every case increased ventilation rates (more fresh air and less recycled

air) decreased discomfort. Discomfort and lack of productivity are preliminary signs of poor air quality impacting human health. The next piece of the puzzle is to define the level of contamination required to observe detrimental health effects in the denizens of buildings.

Evaluation of the human response to chemicals through odor, irritation, and non-sensory factors (external influences) was done to help guide the setting of Occupational Exposure Limits (OELs) (Smeets and Dalton, 2005). Chemicals were divided into three groups: potent irritants, intermediate irritants, and weak irritants which are also potent odorants. Using this division, it was shown that potent irritants cause irritation at low concentration (10 ppb) but are detected through odor at higher concentrations (500 ppb) while weak irritants with odor compounds exhibit the exact opposite phenomenon (1000 ppb for irritation and 1 ppb for odor perception). Intermediate irritants exhibit odor detection first with irritation occurring at relatively similar concentrations (0.2 ppb for odor perception and 0.9 ppb for irritation). Those repeatedly exposed to certain chemicals have been shown to have higher odor and irritation thresholds compared to persons not exposed to those chemicals. The conclusion was that the connection between odor, facial nerve reaction, and symptom recognition existed but was too complicated to identify a singular relationship.

Photocopy centers in Singapore were monitored to evaluate the health impacts of occupationally generated VOCs (Lee et al., 2006). The cancer risk factor for selected compounds was calculated from the data gathered and compared to a reference dose (levels for each compound are encapsulated in Table II.7). The reference dose is the estimate of the amount of personal exposure one can have without harmful effects over a lifespan.

Table II.7: BTEXS, Corresponding Concentrations, and Risk Factors Obtained from (Lee et al., 2006)

Selected Compounds	Reference Dose	Mean VOC Concentration ($\mu g/m^3$)		Health Risk Assessment	
	mg/kg-day	Maximum	Minimum	Maximum	Minimum
Benzene	8.57×10^{-3}	964.6 [1]	0.9	2.5×10^{-3} *	8.5×10^{-5} *
				25.10 +	0.86 +
Toluene	1.14×10^{-1}	8173.6 [2]	289.8	0.73 +	0.14 +
Ethylbenzene	2.86×10^{-1}	100.1 [2]	5.2	0.04 +	0.01 +
Xylenes	2.86×10^{-2}	224.6 [2]	24.8	0.71 +	0.18 +
Styrene	2.86×10^{-1}	73.6 [2]	1.7	0.02 +	0.01 +

[1] – Measured in a photocopier center while burning incense
[2] – Measured in a photocopier center during maintenance
* – Cancer Risk (Benzene is the only compound with an EPA cancer slope factor)
+ – Hazard Quotient (the ratio of estimated exposure to reference dose)

The measured level of toluene is high, and the cancer risk and hazard quotient for benzene are also high because benzene is a known carcinogen and is detrimental to human health at high exposure levels. Other results of note are the relatively low level and hazard quotient for both ethylbenzene and styrene. One of the conclusions from the results was the discovery that the VOCs measured were not only produced by the copy machines but also other unidentified sources. Sources could possibly be from furnishings, human sources, or even the outside air infiltrating the copier centers. The end result was that all centers surpassed the lifetime cancer risk of $1x10^{-6}$ (this risk level is the benchmark of safe operation). This illustrates that even in a relatively benign environment (such as a copier center), poor air quality can lead to the high possibility of detrimental health effects.

II.3.2b Residential Setting

Not only is exposure possible at the workplace, but also at the home. SBS has also been found in apartment homes in Hong Kong (Wong et al., 2009). This study covered 748 households in Hong Kong with a survey about their indoor air quality and health. Nasal

discomfort was the leading SBS symptom followed by noise (noise is considered an indoor environmental quality disruption). It was also noted that those who experienced SBS symptoms rated their indoor environmental quality as poor, while those who experienced no symptoms rated their indoor environmental quality as fair to good. This study shows that poor indoor environmental quality is not only a product of chemical contaminants, but also factors that cause discomfort and that IAQ is a specific subset of indoor environmental quality that must be further studied.

Xu and Weisel (2005) show the amount of VOC uptake during a typical shower through their work monitoring the inhalation of chloroform and haloketones. The study used a typical shower stall with two curtains (one to separate the stall from the bathroom and one to split the shower in half to reduce the air exchange rate in the shower). The shower head was set to produce a mist in order to facilitate volatization of the haloketones. From the data collected, Xu and Weisel developed a residence time model to determine the time the compounds spend in the human circulatory system. Table II.8 shows the results for selected compounds and residence times.

Table II.8: Haloketone Concentrations and Residence Times Adapted from (Xu and Weisel, 2005)

Selected Compounds	Water Concentration (μg/L)	Air Concentration ($\mu g/m^3$)	Bodily Residence Time (min)
Chloroform	18.0 ± 0.6	181 ± 18.2	13.1
1,1-dichloropropanone	27.0 ± 3.5	47.7 ± 5.1	6.25
1,1,1-trichloropropanone	28.1 ± 3.3	40.6 ± 5.6	5.96

The results show higher concentrations in the air as compared to what is in the water, leading credence to the idea that a shower head mist does help easily volatilize contaminants into the air. An interesting result is how the compounds absorbed differently in the body with the haloketones absorbing 85-90% of the ingested concentration and chloroform between 40-80% of the ingested concentration. On the other hand, chloroform has a much higher residence time in the body as compared to the other two compounds. Although the residence time may seem short, this shows that once contamination reaches the body, it can stay inside the body creating a worse health hazard than exposure alone. Even if the residence times are short, the ingesting of chemical contaminants should be avoided because detrimental effects do not require a long residence time to take effect.

Nazaroff and Weschler (2004) attempt to define the exposure scenarios possible around primary and secondary contaminants derived from cleaning chemicals and air fresheners. Their work builds upon current research to quantitatively define, or at least qualitatively, the influences and factors contributing to pollution from these chemicals and their interaction with other factors (sorption into building materials or constituents, reactions, and fluid dynamics). It is proposed that these chemicals transfer from their intended use by volatilization (wood floor cleaning spray eluting formaldehyde), droplet formation (aerosol delivery systems), powder suspension (carpet freshener yielding particulate matter), unapproved mixing (mixing bleach and ammonia to form chloramines), and chemical reactions (terpenes with ozone yield hydroxide radicals). Cases were presented in which these modes of action have caused hazardous situations. The mixing of products containing hypochlorite and ammonia will produce chloramines and ammonia gas. With the addition of detergent to this case, the result elevates from an acute illness to a life-

threatening toxic pneumonitis. The mixing of bleach containing products with acidic products evolves chlorine gas. These scenarios would be hazardous, if not fatal, to anyone near the mix with such results as hemorrhaging of alveoli and extended terms of hospitalization. A more common application would be carpet cleaners. Several cases involving carpet cleaners ranged form mild asthma and respiratory irritation to anaphylactic shock with respiratory failure. Selected compounds with their reference exposure levels and their possible sources are contained in Table II.9. Knowing that such compounds are a risk at low concentrations, it can be seen how the use of common cleaning chemicals can results in toxic levels of contaminants.

Table II.9: Selected Contaminants, Risk Levels, and Possible Sources Obtained from (Nazaroff and Weschler, 2004)

Selected Compounds	No Significant Risk Level (μg/day)	Risk Exposure Level ($\mu g/m^3$)	Sources
Benzene	7	60	Liquid detergent, steel wool pads, furniture wax, building materials
Toluene	7000	300	Disinfecting bathroom cleaners, polishes, paste wax, detergent, carpet and carpet materials, furnishings, textiles, building materials
Formaldehyde	40	3	Wood floor cleaner, liquid floor detergent, gypsum wallboard
Carbon Tetrachloride	5	40	Cleaners and polishes
Dichloromethane	200	400	Cleaners and polishes
Trichloroethylene	80	600	Cleaners, polishes, and chlorine scouring powder, textiles, rubbers
1,4-Dioxane	30	3000	Cleaners and polishes

Mold is becoming increasingly present in residences as homes are becoming more energy efficient. Thus the effects of mold and mold byproducts on the human body should be identified (Bush et al., 2006). It is known that exposure to mold causes the following detrimental health

effects: harmful bodily responses, toxic effects of mold byproducts, and bodily infection. This work focuses specifically on the areas of mold affecting allergies/asthma, allergic bronchopulmonary aspergillosis and sinusitis, infection, toxic effects of mold exposure, and exposure irritation. Bush concludes that mold will produce antigens in the respiratory system (asthma), allergic bronchopulmonary and sinusitis, infection on the skin and inside the body, and toxicity from mold and byproducts would cause symptoms similar to mucosal membrane irritation.

Although adults may experience more exposure to contaminants, a study was performed monitoring the effects of indoor painting and smoking on airways symptoms during the first year of life of children (Diez et al., 2000). Of the subjects, 67% lived in homes which were renovated during embryonic gestation. The results showed a positive correlation between new home improvements and an increase in upper respiratory infections in 6 week old babies. Although the German standard for styrene in indoor air is 30 micrograms per cubic meter, the level measured in this study was less than one-tenth of that level. Yet, irritation and infection are common at this level. This illustrates the inadequacy in regulations and lack of understanding of safe exposure limits.

II.3.2c Outdoor Setting

The cause of cancer is known to be a complex relationship between several different factors. Boeglin et al. (2006) attempted to specifically study the relationship between VOCs in the environment and the incidence of cancer by analyzing several Indiana counties. A does-response model was selected to monitor the relationship of exposure and cancer. The study was

also focused on the following cancer sites in order to fully utilize the data available from the Indiana State Department of Health: oral cavity and pharynx, digestive and respiratory systems, skin, breast, female and male genitals, urinary, brain and nervous systems, endocrine, lymphoma, leukemia, and multiple myeloma. Linear and quadratic models correlated well with each other and yielded positive relationships between lymphoma and total contaminant emissions, leukemia and chlorinated contaminants, and oral cancer to total environmental contamination. Toxic release emissions with thyroid, brain, skin, melanoma, nervous and endocrine systems have positive relationships. It was concluded that the models provide credible, positive relationships for toxic compounds (specifically non-chlorinated contaminants) and the instances of brain, thyroid, skin, and nervous and endocrine system cancer. In this case, the contamination from outdoor air was studied, but this contamination could also be found indoors.

The effect of air pollution particulate matter on lung capacity (namely oxidative stress, cytotoxicity, and epithelial lung cell inflammation was monitored in the city of Dunkerque, France (Garçon et al., 2006). Air samples taken from the city downtown were analyzed for particulate matter size distribution and chemical contaminants and respective concentrations (selected results can be found in Table II.10). The particulate matter gathered was found to have a particle size distribution of 92.15% less than 2.5 micrometers.

Table II.10: Selected Contaminants and Health Effects Obtained from (Garçon et al., 2006)

Selected Contaminant	Compound Class	Concentration	Main Health Effect
Iron	Inorganic	7.84 [1]	Irritant
Aluminum	Inorganic	5.83 [1]	Irritant
Lead	Inorganic	0.80 [1]	Irritant
Manganese	Inorganic	0.352 [1]	Irritant
Benzene	VOC	--- [2]	Carcinogen
Styrene	VOC	--- [2]	Carcinogen
Toluene	VOC	--- [2]	Carcinogen
Naphthalene	VOC	--- [2]	Carcinogen
Pyrene	PAH	4.03 [3]	Carcinogen
Phenanthrene	PAH	9.94 [3]	Carcinogen

[1] – Concentration in weight percent (% w/w)
[2] – Concentration not measured
[3] – Concentration in micrograms/gram

The Lethal Concentrations at 10% (LC_{10}) and 50% (LC_{50}) were determined for the particulate matter collected by exposing live epithelial cells in culture to the particulate matter collected from the city air. It was determined that the LC_{10} and LC_{50} for this particulate matter were 18.84 micrograms per milliliter and 75.36 micrograms per milliliter, respectively. Through this work, Garçon was able to show that the particulate matter was cytotoxic to epithelial cells. This cytotoxicity was dependent upon concentration of particulate matter and time exposure but all tests revealed some level of cytotoxicity. The particulate matter was also studied to identify inflammatory capability on these same cells and the results were positive for oxidative stress and inflammation in the live epithelial cells. This shows that chemical contamination exposure can be coupled with other contaminants, such as particulate matter.

The effect of particulate free gas phase of cigarette smoke on respiratory function (lung epithelial cells) was also determined (Pouli et al., 2003). To further refine the detrimental effects of cigarette smoke, VOC concentration of the smoke was also removed. The gas phase was found to contain compounds such as acetaldehyde (405.3 micrograms per cigarette), isoprene

(270 micrograms per cigarette), acetone (191.8 micrograms per cigarette), toluene (44.6 micrograms per cigarette), furan (37.3 micrograms per cigarette), acrylonitrile (35.4 micrograms per cigarette), methacrolein (14.8 micrograms per cigarette), and ethyl-benzene (3.1 micrograms per cigarette). The results showed that the NO contained in the gas phase contributed to cell damage but also was found to inhibit tissue injury. This contradictory behavior could be explained from the lack of VOC content. Without VOCs, the NO can not react to form more cytotoxic compounds. CO did not exhibit a cytotoxic effect on the cells. This result lends credence to the idea that CO is only detrimental to health because of its ability to bind strongly to hemoglobin and elute nitric oxide. Free NO creates free radicals and toxic oxidizers in the body. Such radicals and by products are known to be carcinogens and catalysts for cancer growth.

It can be seen how pollution can be detrimental to adult and adolescent health, but Farrow and Farrow (1999) hypothesize exposure to elevated levels of nitrogen oxides can trigger a corporal response of incontinence in infants. One of the interesting facts about NO, is that it has been shown that elevated levels of NO do not affect lung capacity in asthmatics and non asthmatics. Also, NO_2 research has revealed that it can not diffuse through the lung lining but can react in the lower alveoli and the reaction byproducts can then move through the alveoli. NO2 also reacts with hemoglobin forming methemoglobin resulting in detrimental effects to oxygen capacity. These effects include Methemoglobinaemia; a condition in which 10% or more of the hemoglobin has been oxidized to methemoglobin. Occupational exposure limits for nitrogen oxides range from 3 ppm (UK 8 hour TWA) to 1 ppm (US NIOSH 15 minute TWA) to 0.106 ppm (EEC hourly mean). But since nitrogen oxides do not diffuse into the body through the lungs, other sources need to be identified. Farrow and Farrow believe that the body intakes

nitrates from nitrate rich vegetables (potatoes, cabbage, and spinach) and in contaminated water. Approximately 97% of a person's daily nitrate intake (estimated 75 milligrams) comes from vegetable and 3% comes from contaminated sources, such as water. If this intake is reduced to nitrite through bacterial digestion, bodily function (especially in infants) is affected by the incursion of diarrhea. This leads to the need for increased awareness of general pollutants, but also uncommon methods of infiltration for pollutants into the body.

In the spirit of attempting to further define the causes of general diagnoses, Staessen et al. (2001) evaluated the feasibility of using biomarkers to identify ingested environmental pollutants by monitoring renal function, sexual development, and cytogenic measurements in adolescents. Staessen et al. identified a specific test area which included two suburban areas near a lead smelter and waster incinerators and a rural control area. Pollutant exposure was measured as follows: blood concentrations of lead and cadmium were taken and specific urinary metabolites measured for VOC's and PAH's. It was found that concentrations of lead, cadmium, and metabolites of VOC's were found in greater levels in the suburban children (from either one or both suburbs depending on the contaminants) versus the control area. Also, those adolescents with glomerular or tubular renal dysfunction were also identified with elevated levels of lead in the blood (a positive relationship for this biomarker). Finally, those adolescents near the waste incinerators were found to have sexual maturity earlier and the adolescent males had smaller testicular volume (a positive relationship for this biomarker). Staessen et al. conclude that present standards for environmental standards are insufficient and would not be able to prevent biological effects.

II.4 Summary

The data presented point to the imminent need for improved IAQ, especially in the residence where most people from adults to infants spend the majority of their day.

The 26% of Americans at an elevated pulmonary risk are the population segment of most concern, when taking into account that an average of 14.41 hours per day is spent indoors (at home or work). Although the time spent in transit (7% of the day) yields the highest instantaneous exposure level to chemical contaminants (mainly internal combustion engine exhaust), indoor air contaminant exposure would yield greater risks due to the time weighted average exposure being much greater. Another factor in the elevated risk from poor IAQ is the myriad of contaminants detected. These contaminants, found in both the residential and industrial settings, range from VOCs (formaldehyde, toluene, α-pinene, and benzene) to PAHs (naphthalene, pyrene, and phenanthrene) to particulate matter and heavy metal compounds. Such contaminants are known, or suspected, carcinogens, cytotoxins, or pulmonary irritants causing corporal reactions from mild coughs to fatal lung failure.

Although awareness and the ability to monitor IAQ are increasing, the drive for regulations is not moving at the same rate. The EPA has set guidelines and regulations for outdoor air with regards to point sources and large contamination contributors. OSHA and NIOSH have set standards for industrial settings with regards to the most toxic chemicals. There are currently no federal regulations, standards, or guidelines for residential IAQ. The number of states calling for improved IAQ or proposing regulations is few with California and Washington at the forefront (CARB, 2005; WSDOH, 1999). Although these state regulations exist, they are not complete and do not cover a wide range of contaminants. The need for new standards and an

engineered solution has never been greater due to this increase in contamination and awareness. Chemical contaminants are eluted from many sources including common cleaners, building materials, and furnishings. These contaminant sources show that improvement can not only come from a singular solution, but from the synergistic combination of using several different solutions. These solutions could be a change in ventilation rates, low VOC building materials, and novel filtration mechanisms. The first step is to have standards and regulations to drive development of these solutions. Finally, the solutions should not only be effective, but also practical and economical for all people to use.

CURRENT AND FUTURE HVAC MATERIALS AND REQUIREMENTS

III.1 HVAC Introduction

Heating-Ventilation and Air Conditioning (HVAC) systems are responsible for environmental control of both industrial and residential settings. These systems not only provide the appropriate temperature and comfort for the occupants of the building, but also provide much needed fresh air. For this reason, one of the important facets of an HVAC system is the filtering mechanism. The purification of building air is important for the health and sustainability of the inhabitants as well as the maintenance of the HVAC system. Hence, the removal of contaminants from the system is a priority. Currently, the majority of HVAC filtering is done by mechanical filtration. Within mechanical filtration, non-woven glass fiber filters predominate among sales in the United States. These filters are designed to only perform particulate filtration and yield very low pressure drop across the filter.

As of January 2009, there have been a number of studies related to Indoor Air Quality (IAQ) both in the work place and residential settings but no federal regulations. The focus of these studies has been two-fold: to determine contaminants in the air; and to understand constituents in the environment contributing to the contaminants.

This increased awareness has created the need for a new class of filter material performing particulate and chemical contaminant filtration. Many novel filters have been developed to perform such tasks. Jo and Yang (2009) describe a filter composed of granular

carbon and a photocatalytic system to remove aromatic compounds from indoor air. Such filters are expensive and not practical for most home owners to use on a continuous basis.

III.1.1 Current HVAC Filter Design

Current HVAC filter designs are dictated by the design of HVAC units. Traditionally, filters are only used to remove particulate contaminants from the air stream to protect the parts inside the HVAC unit instead of protecting residents. This sole function dictated the design of filters to be about function and simplicity. Hence, current filters are only required to afford particulate filtration and yield low pressure drop values rather than protecting residents and improving IAQ. The first step in improving IAQ is to understand the nature and use of what is currently available. The nature of current HVAC filter material is low cost and high volume; thus providing a natural fit for the non-woven industry. The material is placed in a filter that is under stringent pressure drop and high flow rate requirements. The cyclic flow that is passed through the filter is partially recycled, with varying amounts of fresh air entering the system depending on the setting.

III.1.1a Size Specifications

A simple glance of market shelves reveals a myriad of filter sizes and shapes for residential HVAC units. Although stores such as Lowes, Home Depot and Ace Hardware contain a wide range of filters, there are several sizes which are the most ubiquitous for residential HVAC units. A survey of retail suppliers of filters and several local HVAC installers provided the basis of the list of most common filters shown in Table III.1. It is important to note

that this is a table of filter configurations having depths of one inch; the only depth available in popular consumer stores. The other distinction of these sizes is the inclusion of both flat panel and pleated filters.

Table III.1: Common Residential HVAC Filter Sizes

Nominal Height (inch)	Nominal Width (inch)	Nominal Un-Pleated Face Area (in^2)	Typical Nominal Pleated Face Area (in^2) [1]
20	30	600	1342
20	25	500	1118
20	20	400	894
16	25	400	894
14	24	336	751
16	20	320	715
12	24	288	644
14	20	280	626

[1] For a one inch deep pleat and a pleat factor of 2.2

As there are certain filter sizes that are more popular in use, it is possible to use these sizes to understand which HVAC units are most commonly installed. A further survey of HVAC installers provided the following "averages": From approximately 200 HVAC unit installations per year, small unit installations averaged 1.5 to 2.5 tons of cooling and large units averaged 3 to 4 tons of cooling. All installers contacted used the same rule of thumb for installing filters - the designed filter area (in square inches) is double the unit flow rate (in cubic feet per minute or CFM). The State of Alabama has a requirement that the minimum design filter area (in square inches) is 40% of the air flow rate (in CFM) (SAHACC, 2008). The standard conversion for volume flow rate per ton of cooling is 400 CFM/ton of cooling capacity. This translates into average small units requiring 1200 to 2000 square inches of filter area and average large units requiring 2400 to 3200 square inches of filter area.

With an understanding of what is commonly available and what is commonly required, it can be determined which size of flat panel filters are needed to fulfill the requirements and local rules of thumb for filter design. The data for this comparison is contained in Table III.2.

Table III.2: Common HVAC Unit and Filter Requirements

Air Cooling Capacity (ton)	Volume Flow Rate (CFM)	Designed Filter Area (in^2)	
		AL Sate Requirement	Local Rule of Thumb
0.5	200	80	400
1.0	400	160	800
1.5	600	240	1200
2.0	800	320	1600
2.5	1000	400	2000
3.0	1200	480	2400
3.5	1400	560	2800
4.0	1600	640	3200
4.5	1800	720	3600
5.0	2000	800	4000

This table shows that for the typical small residential HVAC unit installations, a combination of the commonly available filters is needed. For example, for a 1.5 ton unit requiring 1200 square inches of filter area, two 20x30x1 un-pleated filters or one pleated 20x30x1 filter would be needed to satisfy this requirement. Table III.2 illustrates the need for something more efficient when compared to a flat panel filter material. This need can be illustrated by the wide offering of pleated filters available at retail outlets as compared to the flat panel filters. In most stores, there are at least three pleated filters offered for every flat panel filter for a given size.

Another manifestation of this need for more filter area in HVAC unit design is the installation of multiple air return points. Builders and contractors, in an effort to satisfy their design rules and ensure the HVAC unit operates properly, design the system based on flat panel filter face area as opposed to a pleated filter face area. To satisfy their requirements for filter

area, the installation of multiple returns is required. Although this benefits the construction companies, it can also be advantageous to residents by allowing them more filtration capability by simply installing a pleated filter as opposed to a flat panel filter. With the substitution of a pleated filter, the resident is able to install a filter with a higher filter rating or Minimum Efficiency Reporting Value (MERV) (ASHRAE, 1999). MERV rating is defined as a performance value that is derived from particle size removal efficiency in three different particle size ranges (0.30 – 1.0, 1.0 – 3.0, and 3.0 – 10.0 micrometers). A second component of MERV rating is the minimum final resistance or the resulting pressure drop across the filter once it has been contaminated with a known amount of particulate material. This restriction can be likened to a redundancy check regarding the filter performance. If the filter is removing a certain amount of particulate according to particle size range, then this should equal the amount removed according to mass. This amount by mass can be correlated to final pressure drop of the filter.

III.1.1b Pressure Drop Specifications

For filter manufacturers, the pressure drop of the filter media is the most important parameter. If the filter does not meet specified pressure drop requirements, damage can be done to the HVAC system. Since it is the most important parameter for performance, in the present dissertation pressure drop will be measured and compared across the different filter materials. Pressure drop will also be used as the first selection criteria when developing a novel HVAC filter material. Pressure drop testing will be done under a wide range of local face velocities, but 121 centimeters per second and 75 centimeters per second will be the two velocities of concern.

These two local face velocities are for one inch deep pleat and two inch deep pleat filters, respectively. Filter manufacturers desire a maximum pressure drop of 0.15 inches of H_2O at 121 centimeters per second and 0.2 inches of H_2O at 75 centimeters per second. These pressure drop specifications are set to protect the air handler and heat transfer coils in common HVAC units. If the pressure drop is too great across the filter, over time, the air handler will fail due to overload and the coils will not be able to efficiently transfer heat to and from the air stream.

For the next generation HVAC filter, the filter depth of choice is two inches. This depth is preferred because it is currently the only filter depth with commercial filters performing chemical contaminant removal. There is currently no one inch deep filter available on the commercial market which performs both particulate and chemical contaminant removal. The commercial HVAC market does have a few filter options which claim to perform chemical contaminant and particulate removal. Since there are already filtration structures available in this market, the two inch deep filter is where the comparison of materials for the next generation HVAC filter will begin.

III.1.2 Future HVAC Filter Design Requirements

The next generation HVAC filter will be required to perform particulate filtration, chemical contaminant removal, yield low pressure drop, and mimic currently available HVAC filters. This will require the next generation filtration structure to mimic some of the attributes of current filtration structures (i.e., pressure drop, thickness, basis weight, and particle size removal efficiency). The new attributes that the next generation filtration structure will have to define are chemical contaminant capacity, manufacturability, and cost. It is important to understand what is

currently available, in terms of performance, and use that baseline to determine what will be needed in future filtration structures. Thus rigorous testing of various filtration structures to determine their performance will be required along with the development of a novel filtration type to satisfy the next generation requirements.

The material must adhere to the necessary pressure drop requirement, and also meet several secondary requirements. Aesthetics are the second most important material constraint. The material must be processed and used without shedding of any sorbent particles while still retaining a dark black color signifying the presence of sorbent in the material. Shedding of particles is detrimental to both the filter manufacturing machinery and the installed HVAC system. Performance is the least important material constraint due to a lack of firm recommendations from professional organizations and governmental regulations available as of January 2008. The main considerations for developing the appropriate material for these filters are finding the total sheet basis weight yielding the required pressure drop, and determining the appropriate basis weights for the individual recipe constituents yielding the same as well as material aesthetics.

III.1.2a Size and Pressure Drop Specifications

The size specifications for the future generations of residential HVAC filters will remain the same. Although HVAC unit manufacturers are in the early stages of producing additional units to increase filtration capability for standard units, there have been no drastic changes to the standard HVAC unit itself. This alludes to a slow changing HVAC manufacturing body which will eventually change, but not as of January 2008. Hence, the first iteration of the next

generation of residential HVAC filters will need to conform to the current filter sizes and specifications (i.e., the sizes shown in Table III.1) for a facile introduction into the market. Future generations can be modified or contain modification equipment, allowing for new sizes and configurations to current HVAC systems.

Another physical specification for the filtration structure is thickness and basis weight. Current particulate filtration structures call for a material which will perform efficiently while having as little material as possible. This translates into a material which has a small thickness, high density (high basis weight), and overall less cost (because there is as little material as possible). The next generation filter will have to adhere to some of the specifications but expand and redefine others. Thickness is one specification in which the next generation will have to comply with current expectations. Thickness plays a direct role in how easily the filtration structure will flow through the filter manufacturing process. If the material is too thick, it will not pleat easily and could impact processing time per lot of HVAC filters. Thus a thin material is preferred for the next generation HVAC filtration structure. In the areas of cost and basis weight, the next generation filtration structure will expand what is currently expected. Basis weight, the measure of mass per unit area, is currently desired to be high while yielding as little material as possible in the final HVAC filter. Less material in the final filter translates directly into lower cost for the filter manufacturer. The next generation filtration structure will increase the cost of the filter in exchange for the added performance benefit. This added performance will also arise from an increased basis weight material. Although both basis weight and cost are increasing for the next generation, the two are not necessarily mutually inclusive. The cost should increase more because of components which provide chemical contaminant capacity as

opposed to the overall increase in material basis weight. Hence the next generation HVAC filtration structure should remain as thin as current materials, but have a higher basis weight to provide adequate performance and manufacturability.

A general consumer may not be able to replace their current HVAC system to improve filtration capability, but they are able to change the filter. This means that any new filter must adhere to the pressure drop specifications currently set for 2 inch deep HVAC filters (0.2 inches of H_2O at 75 centimeters per second air velocity at the filter face). These rather strict specifications are currently required; but to allow for a higher performing next generation HVAC filter these specifications must allow for a higher pressure drop. A higher pressure drop specification will allow for more particulate and chemical filtration capability resulting in a longer filter lifetime and better protection for the residents.

III.1.2b Gas Life Specifications

Current HVAC filters have a life span of 90 days due to particulate matter clogging the filter and causing it to perform outside of the pressure drop requirements. There are currently no standards in existence for the gas life requirements for a filter which performs chemical and particulate removal in a residential HVAC. For the same reasons as the size requirements for the next generation, the gas life requirement should be the same as the requirement for current particulate filters (90 days). This will facilitate introduction of the next generation filter into the market, and mimic the current filter life spans. Achieving this requirement will involve balancing sorbent loading, pressure drop, and overall filter cost.

The 90 day timeframe must also be considered in light of actual filtration requirements. The following assumptions must be made to develop a filter which can last 90 days: that the HVAC unit will not run continuously over a 24 hour period but rather only 20% – 30% of the 24 hour period; the chemical contaminant level entering the HVAC unit will not be a constant stream and will typically be below 10 ppm; the average level of chemical contaminants in the air stream will decrease over time as the next generation HVAC filter is used. Taking these assumptions into account, the next generation HVAC filtration structure must withstand 25,000 – 39,000 minutes of continuous challenge testing to satisfy a 90 day requirement. Another requirement for this 90 day period is the number of chemical contaminants that the next generation residential HVAC filter will have to remove. There is a myriad of chemical contaminants detected in the residential setting. Successful filtration schemes must address this mixture of contaminants in order to adequately improve residential IAQ.

III.1.3 Current Chemical Absorptive HVAC Media

To begin identifying the appropriate filtration structure of matter, it is important to understand what is currently available. After a survey of currently available products, four products were chosen for further study and evaluation. These filtration structures are shown in Figure III.1.

Figure III.1: Selected Filtration Structures: A) Gray Matter V 1.8, B) OdorGuard, C) Lewcott

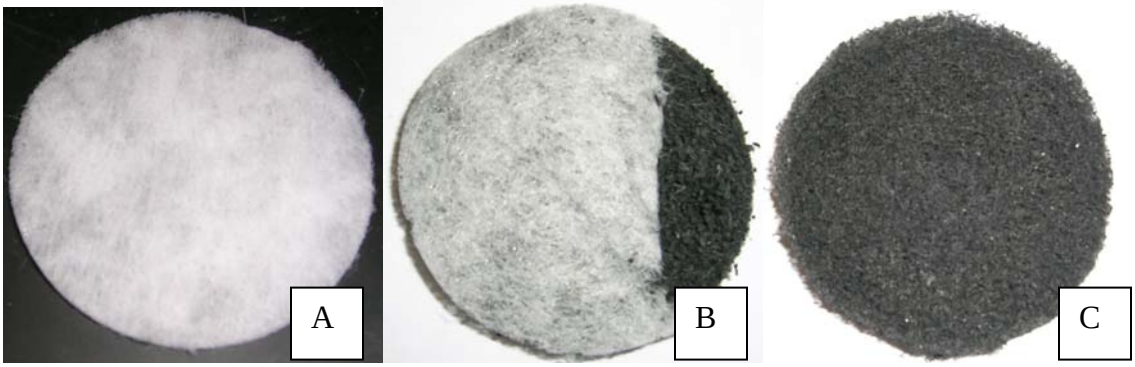

BEC Technologies, Inc. produces a gas phase filtration line of products termed Gray Matter shown in Figure III.1-A. Gray Matter is a non-woven structure which contains chemical contaminant absorbing carbon molecules. This filtration structure is made by thermally bonding continuous polyolefin fibers and coating the structure with the absorbing molecules. Gray Matter is currently available in two versions; the original version (black) differs from version 1.8 (off-white) only in color. Both structures are similar in construction, composition, total basis weight, and both are specified to perform odor and chemical contaminant removal. This filtration structure is fairly uniform upon visual inspection, with only a few sections of light basis weight material.

D-Mark, Inc. produces a filtration structure containing activated carbon particles and polymer fibers formed into a thick mat known as OdorGuard shown in Figure III.1-B. This is an air laid structure with activated carbon particles included into the air lay process. This produces a three dimensional dispersion of carbon through out the white and black polymer fibers. The one unattractive characteristic of such an air laid dispersion is the lack of even carbon dispersion through the entire structure. Another undesirable quality of such a structure is clear layering throughout the entire z-axis direction of the material. This leads to an increased chance of

shedding particles and fibers. This material can be laminated with a polyester pre-filter to improve the particulate filtration capability of the structure. OdorGuard comes in several versions, varying in basis weight of carbon particles. The two samples currently available are OdorGuard 15 and OdorGuard 45.

Lewcott Corporation produces the thick, black, polymeric non-woven labeled Lewcott filter material shown in Figure III.1-C. This structure is a non-woven which could utilize either the spunbonding or the air laid process, but was not confirmed by the manufacturer. These two processes are candidates because of the physical characteristics observed in the Lewcott material. The fibers are oriented in a circular pattern throughout the material indicating spunbonding. The structure is also very thick which would indicate several spunbound layers adhered together or air laying. The material also sheds fibers which would indicate chopped fibers, a necessity of the air lay process. This structure of matter is specified as containing carbon within the polymeric fiber to perform odor and chemical contaminant removal. This could be accomplished using either process.

III.2 Microfibrous Material Introduction

Microfibrous materials were first created in the late 1980's. The first version of this class of composites is characterized by the use of nickel fibers. Tatarchuk *et al.* patented a composite material that is composed of an interwoven matrix of carbon fibers interlocked among a network of fused metal fibers (Tatarchuk et al., 1992.1; Tatarchuk, 1992.2; Tatarchuk et al., 1992.3; Tatarchuk et al., 2004; Meffert, 1998; Marrion et al., 1994; Harris et al., 2001; Cahela and Tatarchuk, 2001). This class of composites was created by using a cellulosic binder along with

the fibers in a uniform, liquid dispersion processed through the wet lay (or paper making) process.

Although the metal fibers lend various desirable qualities to the media, it was preferable to incorporate low cost raw materials. For one-time use filtration units, it is necessary for the cost of materials to be economical and competitive with what is currently available in the market. Polymer fibers are the ideal raw material for these applications and can be used to tailor the final material for a specific application. Recent advances in polymer chemistry and manufacturing have led to several new products and technologies available for this application.

III.2.1 Wet Lay Technology Background

Wet lay technology has changed since the early 1900's but the key process parameters have remained relatively unchanged. There are two main facets of concern to the wet end of the paper making process: the wet lay technology itself and the wet end chemistry. The wet end technology has changed over the years and there are a few popular choices among available equipment. On the other hand, wet end chemistry is a relatively new development in the paper making process and there are a wide variety of products and choices available.

Wet lay technology refers to the equipment which converts stock material into a wet mat. This part of the paper machine is known as the wet end. There are many different kinds of wet lay technology, but the popular choices include Fourdrinier, twin-wire, inclined wire, and rotary drum forming sections. The two types of forming sections utilized in the development of polymeric microfibrous material were the Fourdrinier and inclined wire. The Fourdrinier is important because it is the most widely used and most traditional piece of wet end technology in

use today. The inclined wire (or delta former) was also selected because it is known as the most effective type of wet end technology in forming a uniform mat for light and ultra-light basis weight wet laid synthetics (wet-lay mats comprised of synthetic fibers such as glass or polymer).

Fourdrinier formers are the core machine at the heart of the pulp and paper industry. This type of machine is characterized by continuous operation, a separate wet and dry section, and a Fourdrinier head box. The Fourdrinier head box creates even pressure across an opening (called the slice); and it is this even pressure which creates an even distribution of stock flow across the slice yielding even sheet formation across the width of the machine. The sheet is formed in the wet section of the machine consisting of the head box, wire, and vacuum. As the stock flows out of the head box onto the wire, vacuum slats pull excess water out of the sheet as it passes. As the sheet passes onto the dry section of the machine, the wet end typically removes approximately 80% of the water in the sheet. In the dry section, the remaining amount of water is driven off by heat. The wet section of the Fourdrinier is also a tightly closed water loop recycling water from the stock, white water, and pit water into a continuous cycle of water. This tight water loop is important concerning the retention/accumulation of wet end additives, fiber material, and particulate. Metal based microfibrous material currently uses a modified 12 inch wide Fourdrinier machine for production of continuous rolls.

III.2.2 Metal Fiber Composite Background

The original composite was created by using a cellulosic binder, along with fibers, in a uniform liquid dispersion. This dispersion is then fed into the wet-lay process and a non-woven matrix is produced. This matrix is further processed to yield a network of bound particles

surrounded by fused fibers. Figure III.2 shows a scanning electron micrograph of a typical metal microfibrous material sample.

Figure III.2: SEM of Metal Microfibrous Material (500x Magnification: Reference line is 20 micrometers)

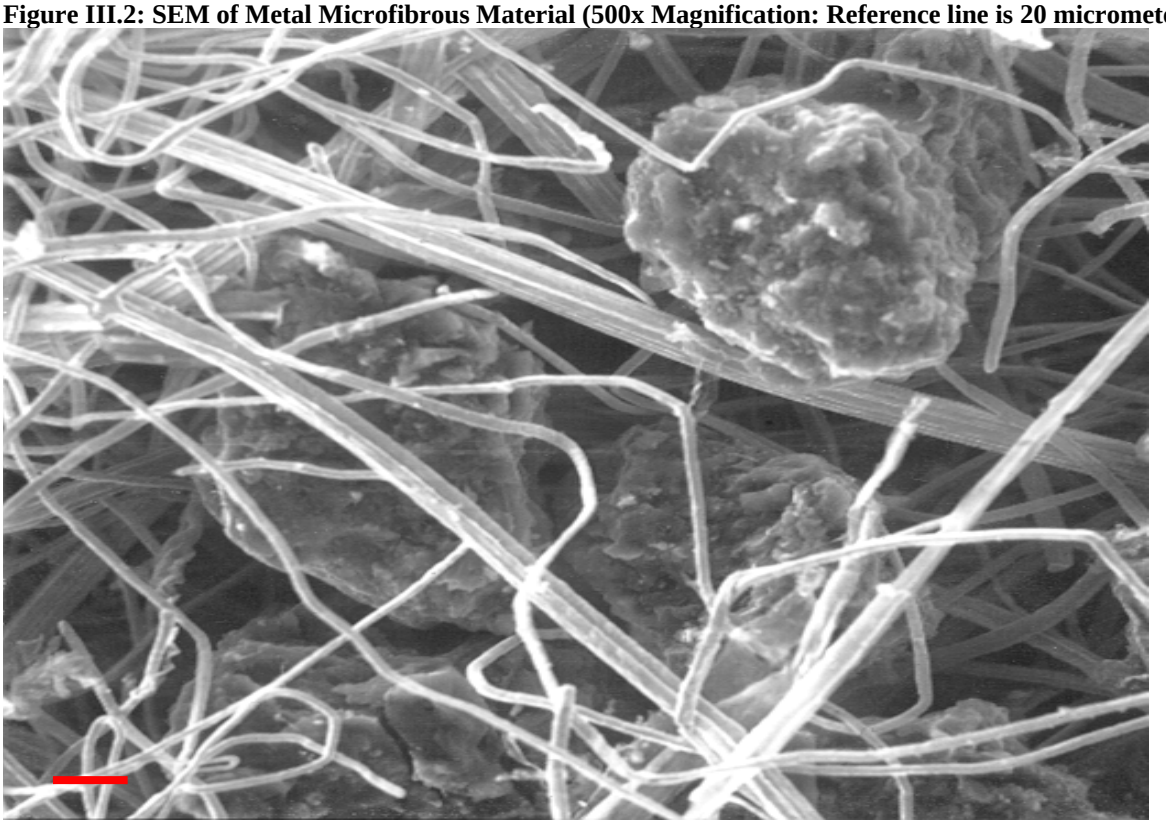

The original application for metal based microfibrous material was from the field of high surface area electrodes. This application facilitated the use of metal fibers such as nickel and stainless steel. As with high surface area electrodes, it was found that the metal fiber matrix would also lend high surface area availability to heterogeneous gas phase filtration applications. This is accomplished by the fiber network providing a stable separation for sorbent particles.

The fiber matrix is a characteristic created by the specialized wet lay process used to manufacture microfibrous materials. The wet lay process creates a random orientation of fibers in all three directions of the non-woven mat. Through this orientation of fibers and the sintering

process, the fiber matrix is formed around the entrapped particulate. Through entrapment, the particles are separated in a highly void bed and the fiber matrix creates low Reynolds Number micro-channel flows. This flow pattern enhances the contact between the contaminant flow and the sorbent particles.

The recipe for this filter application is a compilation of two different metal fiber diameters, cellulose fiber, and sorbent particulate. On a weight percent basis, the composition is 24.75% large diameter fiber, 8.25% small diameter fiber, 11.05% cellulose, and 55.95% catalyst or sorbent particle. The mix of fibers helps to improve retention during formation in both the machine direction and in the z-axis direction of the material. The cellulose adds green strength to the sheet before sintering as well as improving retention during formation. The sorbent particulate selected was dependent upon the final application but included catalyst supports (alumina, zeolite, and zirconia) and common adsorbent particles (i.e. activated carbon and carbon derivatives).

III.2.3 Heterogeneous Absorption Applications

Microfibrous material can be tailored to many applications, but it exhibits marked performance enhancement in the area of heterogeneous gas phase filtration. In particular, the removal of chemical contaminants to less than trace levels is an application well suited to the strengths of microfibrous material. An example of this type of filtration application is the development of a gas mask canister for full-face respirators. Another variation of this application well-suited for the use of microfibrous material is collective protection filtration. Collective protection filtration refers to the use of a large capacity filtration device to provide

contaminant free air to an entire building. Both of these applications rely on the concept of using microfibrous material as a polishing filter. In this configuration, the layer of microfibrous material removes the low level of effluent contaminants exiting the packed bed. This is advantageous for microfibrous material because it has little capacity which is used very efficiently.

Since the inception of Microfibrous Materials, it was believed that the fiber matrix enhanced the performance of the medium through static mixing. To have static mixing, turbulence must be present and turbulence is only produced when the Reynolds Number is above 4000. In micro-channel flows, such as the ones in microfibrous beds, the Reynolds number is three orders of magnitude below the turbulent level. In order to exploit and identify this performance enhancement, breakthrough testing and the resultant data are used to compare a packed bed with a microfibrous bed. To accurately show the performance of each bed, the amount of sorbent in each bed should be equal. The first difference that is observed is the difference in loading of each bed. This is a fundamental difference between the two bed structures. A packed bed typically has a volume loading on the order of 60% and a voidage of 40% where a microfibrous layer will have a volume loading on the order of 20% and a voidage of 80%. This two fold difference in voidage could be an advantage simply because the contaminant flow would have a longer residence time in the microfibrous bed over the packed bed. It is believed that the fiber mesh is the attribute lending the performance enhancement to the microfibrous bed. To isolate the effect of the fiber mesh, it is necessary to test the effect of separating sorbent particles. This is done by employing a dilute packed bed. A dilute packed

bed would still have the same amount of sorbent and flow characteristics as the packed bed but it would also have the volume of the microfibrous bed (hence the particle separation).

Knowing the bed parameters and the capacity for a given compound of each bed, the theoretical and actual capacity can be calculated. Having calculated the usable capacity and the total capacity, the utilization efficiency for each bed can be shown. The efficiency of the microfibrous bed ranges between 87% and 78% while the dilute packed bed showed 67% efficiency and the regular packed bed exhibited 55%. From this calculation, the microfibrous bed has approximately twice the efficiency of the standard packed bed (85% to 45%). The dilute packed bed has 25% more efficiency than the standard packed bed, but 30% less efficiency than the 4 micron microfibrous bed.

In order to truly understand the behavior of each bed and quantify the performance, it is necessary to compare the instantaneous adsorption rates.

Equation III.1: Bed Depth Service Time Equation

$$\frac{C}{C_0} = \frac{1}{1+\left(e^{k_{ads}C_0\tau}-1\right)e^{k_{ads}C_0(L/v_0-t)}}$$

The Bed Depth Service Time equation (Equation III.3) must be used to obtain this data. The Bed Depth Service Time (BDST) equation was developed by Adams and Bohart in 1920. This equation details the behavior of a gas or liquid adsorption onto a solid. This equation relates the key variables of any adsorption system: voidage, depth, challenge into, and capacity of the bed. Taking the original equation and obtaining an exact solution for the three beds, the breakthrough performance can modeled and compared against empirical data or empirical data can be analyzed

to obtain various system parameters. The latter is the main concern in this study. In this form of the equation, the variables are C(z,t)-concentration (mg/m^3), C_0-challenge concentration (mg/m^3), t-time (min.), τ-saturation capacity of bed (min.), k-adsorption rate constant (1/min), ν_0-face velocity (cm/min), and L-length of bed (cm).

The BDST equation must be expressed in another form to obtain the necessary data for this study. By rearranging the BDST equation and solving for time, Equation III.2 is derived.

Equation III.2: BDST Equation Solved for Time

$$t = \tau - \frac{\ln\left(\frac{C_0}{C} - 1\right)}{k_{ads} C_0}$$

This form can be used to solve for the gas life of a bed using literature or empirical values for adsorption rate constant and capacity. For this study, the derivative with respect to time will yield the instantaneous adsorption rate.

Equation III.3: Time Derivative of BDST Equation

$$k' = \left(\frac{dt}{d\left[\ln\left(\frac{C_0}{C} - 1 \right) \right]} \right)^{-1}$$

Having this derivative form of the BDST, the instantaneous adsorption rate can be calculated using the empirical breakthrough data. The instantaneous adsorption rate data can now be

plotted along a time versus C/C_0 axes to see the performance of the different bed configurations versus each other.

Figure III.3: Instantaneous Adsorption Rates for Different Bed Configurations

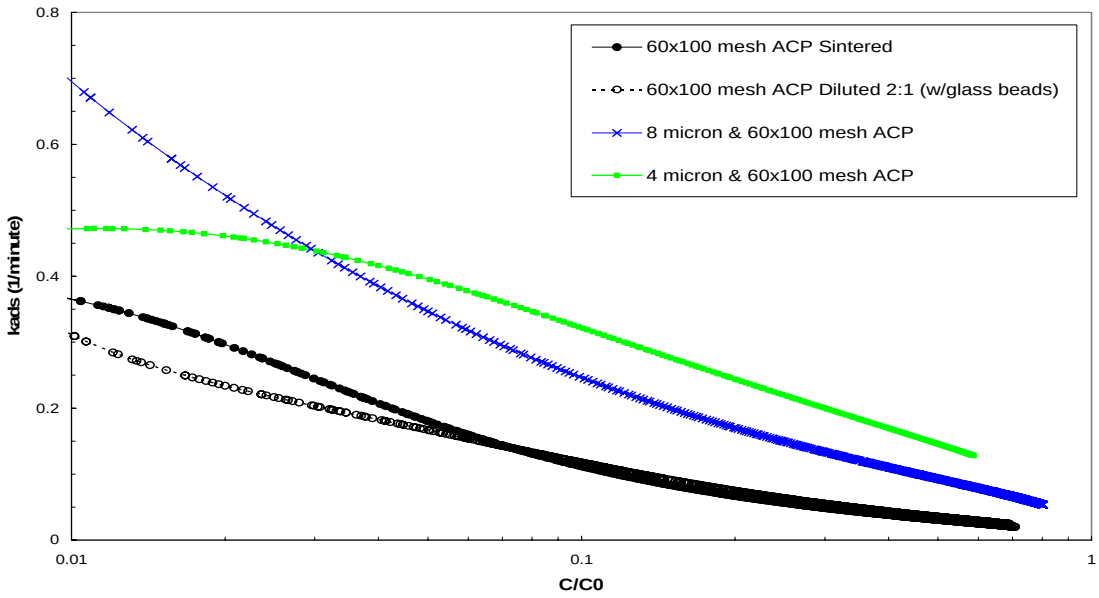

Figure III.3 shows the performance along the gas life of each bed. By analyzing this plot we can see that all of the curves have negative slopes, which agrees with the physical phenomenon of an adsorption system. As the system is in use, the number of available active sites is reduced; hence the activity (or adsorption rate) is reduced. The other interesting facet of this figure is the location of the microfibrous beds in comparison to the packed bed curves. Along the entire life of the bed, the microfibrous beds show a 2 to 4 fold increase in activity over both packed bed configurations (Bird et al., 1960, Yoon and Nelson, 1984, Bohart and Adams, 1920).

The rate of adsorption is governed by two factors: the rate of arrival of molecules to the surface, and the fraction of said molecules which undergo adsorption. Since the beds contain the same amount and type of sorbent, the distinguishing factor would be the rate at which molecules

encounter the sorbent particles. From Figure III.3, we can see that this rate is much higher for the microfibrous beds opposed to either of the packed beds. This validates that not the separation of sorbent particles, but rather the fiber mesh separating the particles provides a contacting enhancement from the enhanced adsorption rates observed in the microfibrous beds.

III.2.4 Sorbent Selection

Previous research shows that activated carbon is the sorbent of choice for VOC removal. Activated carbon is the preferred sorbent because of the ability to strongly adsorb a broad spectrum of chemicals including VOC's. Similar to catalyst supports (i.e. alumina and zeolite), activated carbon can be impregnated with other compounds or metals to improve adsorption of specific chemicals. Another benefit of using activated carbon is the large body of research and literature characterizing the behavior and capacity of activated carbon for a variety of chemicals and applications.

III.3 Polymeric Microfibrous Material

The need for a novel Heating Ventilation and Air Conditioning (HVAC) filter is apparent from recent Indoor Air Quality (IAQ) research. Current HVAC filters are not capable of performing both particulate and chemical contaminant filtration. For this reason, a novel filtration structure must be developed and tested to provide improved IAQ. Attempting to satisfy this need, a material utilizing three common aspects (polymers, activated carbon, and the wet-lay process) in a novel way was developed. Polymeric microfibrous material is a novel filtration structure comprised of bi-component polymer fibers and sorbent particles produced via the wet-

lay process. This unique combination yields a highly efficient and effective filtration medium to address changing HVAC needs.

Several goals were identified at the onset of development including a pressure drop target, gas life target, and physical structure requirements to produce a successful HVAC filter. Although metal fibers lend various desirable qualities to the media, it was desired to substitute the metal for a low cost raw material. For one-time use filtration units, it is necessary to balance performance with the cost of materials. Polymer fibers are the ideal raw material for these applications and can be selected for a specific application due to recent advances made in polymer processing technology.

The combination of the wet-lay process, synthetic fibers, and adsorbent particles to form a unique filtration structure is the outstanding characteristic of polymeric microfibrous material. The wet-lay process facilitates the random distribution of fibers throughout the entire filtration structure. The synthetic fibers create a robust filtration structure which can easily move through the filter manufacturing process while yielding a low cost raw material. The sorbent particles are chosen to provide the lowest pressure drop, highest filtration capacity, while not creating a high priced filtration structure. The filtration structure is based upon previous research using metallic microfibrous material for collective protection applications. The sorbent selection is based upon this research to provide chemical contaminant free air for entire buildings. This research was used to develop a material which would efficiently filter chemical contaminants from indoor air.

In the case of a novel HVAC material the key questions come under the umbrella of determining the total sheet basis weight. For example, the use of cellulose fiber is a critical factor to be considered because of the strict pressure drop requirements. If cellulose is not used

green strength will have to be provided by the entanglement of the polymer fibers. If this is the case, the dimensions of the polymer fiber become important to green strength and stock suspension dispersion. The particulate to total fiber ratio was fixed to obtain a dark-hued material satisfying one of the aesthetic criteria and lending the most performance (or capacity) to the material possible. Having addressed the issue of asthetics, other technical challenges remained including the use of cellulose. It was important to see the effect of cellulose on pressure drop. This was accomplished by making sheets of a single total sheet basis weight and varying the amount of cellulose in the recipe and recording the pressure drop of each sheet at a face velocity of 121 centimeters per second. The data was then analyzed to determine the relationship of cellulose to pressure drop for a given basis weight.

Figure III.4: Pressure Drop Versus Cellulose Loading of Polymeric Microfibrous Material

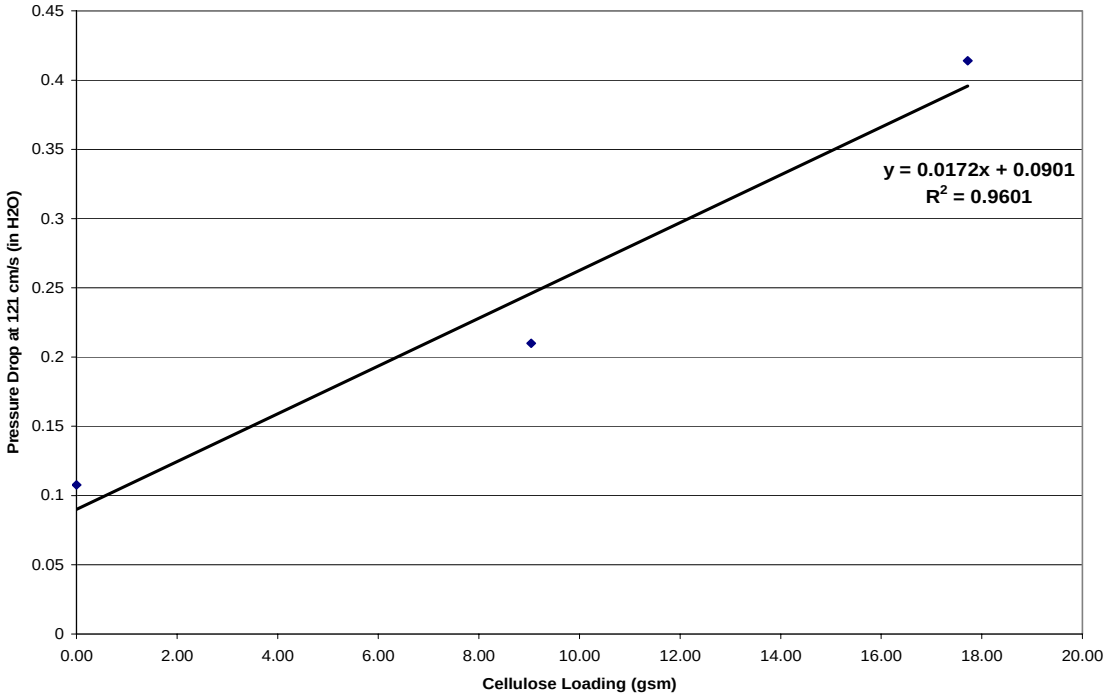

Through this relationship, it was found that the cellulose would have to be completely removed because at this basis weight the pressure drop contribution from the cellulose dominates the entire structure. The other decision that needed to be made concerning fiber was the dimensions of the polymer fiber. A mixture of fiber diameters was used (19 and 13 micrometers) while the cut length is the same (0.25 inch). The mixture of fiber diameters is used to achieve certain characteristics necessary for high filtration efficiency. The addition of a minor amount of small diameter fibers allows for higher particulate retention due to the construction of smaller fiber cages. But by adding only a minor amount of smaller diameter fiber, the pressure drop penalty is not as large as creating a microfibrous composite entirely of small diameter fibers. By comparing the pressure drop attributed by each fiber diameter, it was decided that only larger diameter fiber should be used to minimize the pressure drop through the material. Having made the decision concerning fibers and particulate, the next step was to determine what total basis weight would yield the necessary pressure drop. By using a recipe of a particulate to fiber ratio of 4:1 (by mass) and a bi-component polymer fiber of 19 micrometers in diameter and 0.25 inch in length, a range of total sheet basis weights were made and tested for pressure drop. Using this data set, a trend line was used to predict the appropriate basis weight for the necessary pressure drop and face velocity. Several of these sheets were made in the laboratory, but the remainder was made at South East Non-Wovens Inc. (SENW). The last half of recipe modification was done in our laboratories in conjunction with trial runs on the wet-lay lines at SENW.

III.3.1 Polymer Fiber Selection

Recent advances in polymer chemistry and manufacturing have led to several new products and technologies. These advances have been coming from industrial and academic-based research and development collaborations rather than solely academic-based research making the developed products readily available. This is seen directly by the amount of new composites utilizing these new technologies and products. The new technology and product of interest to this research is the bi-component fiber.

Today, even a trip to a local market or convenience store will afford the opportunity to purchase polymer fibers. For example, Poly-Fill polyester fibers can be purchased in a bag as batting material. These fibers were first used in this research to form a polymer fiber based sheet. Although none of the samples were satisfactory, much was learned in producing polymer fiber sheets. These fibers are approximately 50 micrometers in diameter, 5 centimeters long, and have a wavy crimp with a frequency of approximately 0.2 centimeters. This fiber length is too long for wet lay applications, resulting in entanglement and uneven dispersion in the stock suspension. The Poly-Fill fibers also exhibit a hydrophobic nature. Having experience with length and fiber finish, it became necessary to subsequently find a new kind of fiber that would meet the needs of the wet-lay process and microfibrous material. Common fibers available to the general public are coated with a hydrophobic finish to reduce static and increase lubricity. This finish is not conducive to wet-lay procedures so a new finish had to be identified. The other piece of knowledge gained from the Poly-Fill fibers was in the area of bonding. A few heating and bonding tests were done to establish the behavior of the polymer fibers in various heating conditions (oven and heated press) and environments (air, nitrogen, and helium). Polyester

degrades in the presence of moisture, oxygen and heat, elements present in the preliminary bonding tests and in the wet-lay process.

The necessity to switch from a staple fiber (i.e. Poly-Fill) to a specialty fiber became clear after the preliminary bonding tests. Previous literature concerning the metal fiber based microfibrous material was consulted. The theory behind sintering metal fibers needed to be transferred to polymer fibers. When sintering metal fibers, the outer atom layers have enough kinetic energy to melt together with surface atoms from another fiber resulting in the two fibers fusing together at the interstitial point. This is not totally possible with a staple polymer fiber. During typical wet lay bonding conditions, if polymer chains on the surface of a fiber have enough kinetic energy to fuse with the surface chains of another fiber the entire fiber has the same amount of kinetic energy and not enough core stability resulting in a molten pool instead of two fibers fused at an interstitial point. The key was to have a surface layer that would fuse to another surface layer while having a solid core throughout the entire bonding process. This led to the use of bi-component fibers. Bi-component fibers are characterized by the use of two different polymer types to construct a fiber. Bi-component fibers are constructed in many configurations; i.e. concentric sheath/core, pie slices, and islands in the sea. The ideal configuration for this application is the concentric sheath/core bi-component fiber. This fiber is made by a specialized extruder die pack where one polymer type is extruded in the core of the die while the sheath polymer is wrapped around the core as the entire fiber is extruded and the combination is then drawn to the desired diameter. This type of specialty fiber expands the fundamental idea behind sintering metal fiber composites to a larger scale versus surface atoms.

The dimensions of the fiber were the last parameter to be determined. This was done by mirroring the selections made for the metal microfibrous material. Fiber dimension was not initially investigated because of the available data and work done using the metal fiber composite. This allowed for the facilitation of work in other areas such as recipe development and formation development. Metal microfibrous material utilizes fibers in the range of 2 – 20 micrometers in diameter with a length of 0.25 inches in length. This information was used as the starting point in the polymer fiber selection process.

The next step was to begin finding specialty polymer fibers that would be in the diameter and length range desired. A fiber diameter in the range of 2 – 20 micrometers was needed to create the appropriate flow structure in the composite material while a length of 6 millimeters was desired to facilitate the wet-lay process. A search of polymer fiber producing companies yielded companies providing products meeting the desired specifications: Invista, ES Fibervisions, and Fiber Innovation Technology (FIT). Invista (formerly known as Kosa) offers a variety of bi-component fibers made especially for the wet-lay process. FIT is a research company that specializes in working with their customers to develop products. ES Fibervisions is a large multi-national corporation that produces many different fibers for a myriad of applications.

The Invista concentric sheath/core bi-component fiber is characterized by a sheath of specialized Liner Low Density Poly-Ethylene (LLDPE) on a core of any polymer with a higher melting point. This is advantageous because the final product can be tailored to a specific application. Invista is able to offer a wide choice of polymers, and the spunstock of fiber is extensive enough to fulfill production needs. If a product does not exist or happens to be

discontinued or changed, Invista has the ability to use a small pilot line to produce a fiber from various spunstock.

The Invista process of making fibers begins with a polymer stock; either chips or the necessary resin to produce the polymer needed. The chips (or resin) enter an extruder and are extruded out the specialized die pack, previously described. As the sheath and core are extruded in the same die pack, they are pulled into a bundle and fed through an intricate roller system to draw the fibers down to a certain denier and also receive the necessary amount of finish. The semi-drawn fibers, also known as tow fibers, are moved to another line for fiber finishing. Fiber finishing includes the final denier, amount of finish, and fiber characteristics such as crimp and cut length.

III.3.2 Wet End Chemistry Observations

Wet end chemistry consists of using chemicals or additives engineered specifically designed to enhance paper characteristics. Wet end chemistry is divided into three main areas: retention aids, formations aids, and wet/dry strength additives. The bulk of all additives are water-dispersible polymer based solutions. These polymers can be either long chain or short chain and charged (anionic or cationic) or neutral. The most popular polymers currently used are polyacrylamides (PAM), polyvinyl alcohol (PVA), and polyethyleneimine (PEI).

Along the process of scale up, new ideas and technologies were evaluated as the polymer media recipe evolved. The most beneficial addition to the recipe was that of dispersion aids and flocculants. The arena of wet end chemistry is a new facet of research within the Center for Microfibrous Materials Manufacturing research group. Metal fiber dispersions facilitated the

introduction to wet end chemistry through viscosity modification. Emerging and more sophisticated methods of fiber dispersion were used in the development of the polymer composite.

Regarding polymeric microfibrous material, the main concerns (in order of importance) are formation, retention, and wet strength. Formation is the most important factor due to the inherent difficulty of wet-laying synthetic fibers with particulate. The density difference between the fibers and the other stock components causes an imbalance in the formation with respect to dispersion of polymeric fibers across the width of the wet lay mat. An additive which can provide even dispersion in the stock and help formation is desirable.

Retention is the second most important factor because of the entrapped particulates. In traditional paper making, the entrapped particulates are additives such as rosin and alum which are inexpensive commodities but can become costly if lost at large rates. Polymeric microfibrous material is composed of large particulates such as carbon and alumina which can be expensive as a raw material. If these materials are lost in any amounts during formation, this will add to the expense of the material and could lead to process degradation (also leading to increased processing costs). Thus it is important to provide an additive which will help entrap the particles in the wet mat before bonding can provide the mechanical entrapment.

The third area of importance is wet strength. In cellulose based mats, physical entanglement along with the hydrogen bonding between fibers is enough to provide wet strength for the wet mat before drying. In the case of polymeric fibers, the hydrogen bonding between fibers does not exist or yield any force to hold the fibers together before bonding. In this case, a

wet end additive is needed to provide wet strength allowing the green (or unbonded) mat to travel through machine transfers and the rest of the wet-lay process.

Dispersion aids are a class of chemicals used to facilitate the dispersion and suspension of materials in an aqueous based system. Invista specialty fibers are coated with a finish to lubricate during the drawing process and facilitate their use in wet-lay applications. The finish used by Invista is Milease-T. Milease-T is a textile finishing agent, produced by the textile division of Clariant, used primarily with polyester fibers. It lends anti-static properties, increased moisture absorbency, and soil-release characteristics. Milease-T worked well with activated carbon, cellulose, and polymer fiber suspensions, but was less effective with other particulates. The dispersant began to show inactivity with suspensions of alumina and ultimately showed no activity with activated carbon impregnated with ASZM-TEDA. ASZM-TEDA is a commercially available activated carbon impregnated with copper, silver, zinc, molybdenum, and triethylene diamine. If this can be directly entrapped in polymeric fibers, the process time for production of a CBRN sorbent material would be faster and cheaper. One of the drawbacks to using an already impregnated material is the unknown effect of the process on the loading of the various impregnates. For example, TEDA is a deliquescent chemical with only a few degrees of difference between its melting and boiling temperatures (158ºC M.T. and 174ºC B.T.). When pre-impregnated ASZM-TEDA was added to a typical stock-slurry suspension, the even dispersion of material was quickly broken and the fibers floated to the surface of the suspension. I believe this was mainly a resultant of the TEDA counteracting the pH (pH = 5.0) and the dispersion effect of the Milease-T because TEDA is such a water-soluble material. As the TEDA dissolves into the water, the Milease-T is stripped from the fiber surface and attracted

to the TEDA. Thus the result is the naturally hydrophobic polymer fibers float to the surface. Although ASZM-TEDA impregnated carbon would not be used for HVAC applications, it shows that a more robust dispersant should be selected to avoid any future processing complications (i.e. process water changes or fiber finish changes).

The next wet-end additive trialed was Cruwik-SYN produced by Crucible Chemical Company. Cruwik-SYN is a finishing agent for general purpose padding or exhaust applications in the textile industry. When used in a typical stock-slurry suspension for a polisher, the dispersion of the suspension was far better than that of Milease-T. When using ASZM-TEDA the dispersion was not affected, this made Cruwik-SYN the optimum choice as the dispersant for polymer fibers. As a secondary test for this dispersant, it was applied to a more challenging dispersion scenario.

During this time, a problem in the dispersion of stainless steel fibers was observed. The current approach used in the dispersion of metal fibers (mainly nickel) is through high shear and high viscosity. Hydroxy Ethyl Cellulose (HEC) is used to increase suspension viscosity while a high shear mixer is used to mechanically separate the fiber bundles. In the dispersion of stainless steel fibers, this process did not reduce the amount of dispersion time but added extra steps to the dispersion process. Cruwik-SYN was used in varying amounts along with a small scale high shear mixer to evaluate the effectiveness of the dispersant on metal fibers in un-modified process water. The result was a reduction in the dispersing time from one hour to 5 – 15 minutes (depending on the amount of metal fiber). Less fiber damage was observed versus the original dispersion process.

Fiber flocculants are normally used to help formation. In the case of polymeric microfibrous material, flocculants are used to help carbon retention by adding a charge to the polymer fibers which attracts the charge on the particulate to be entrapped. In this capacity, the flocculants act as retention aids. The amount of this charge is not known, and no equipment (i.e. electrophoresis or non-contacting voltmeter) was readily available quantify the effect of the flocculants used in the recipe developed. Flocculants (divided into anionic and cationic additions) can be used in two ways: small amounts of a flocculant produce charge addition to the stock suspension constituents; large amounts of a flocculant will increase the viscosity greatly (which aids in formation) while also adding charge to the stock suspension constituents. After testing a variety of flocculants from various companies, it is concluded that the charge of the flocculant (anionic or cationic) did not matter, nor did the capacity in which it was used. The formation and retention benefited from any use of the flocculant. It was decided that the best use of flocculants is in large amounts to modify the viscosity of the thick stock. This was decided because it is the easiest way to meter the appropriate amount of flocculant since viscosity can be easily measured in a process environment as opposed to measuring the amount of charge accurately.

III.3.3 Wet End Technology Selection

Delta Formers are an alternative piece of wet end technology to Fourdrinier machines. This type of sheet former is characterized by a well-mixed head box (or stock pond) of stock suspension through which a wire is passed and a section of vacuum system helps to “pick up” stock from the pond forming the sheet. The Delta former is similar to the Fourdrinier in that it

has a separate wet end and dry end, but that is the only similarity. Where the Fourdrinier controls the flow rate of stock onto the wire through the slice, the Delta former controls the flow of stock on the wire through a pond regulator and/or the wire speed. The pond regulator is a device which is placed into the pond, creating a narrower opening (like the slice for a Fourdrinier head box). The pond regulator helps to prevent an uneven dispersion of stock material in the pond and preventing buoyant materials from floating to the surface of the pond (creating uneven sheet formation). The speed of the wire also dictates formation by either picking up more stock (slow wire speed) or less stock (fast wire speed). The wet end has a closed water loop, much like the Fourdrinier wet end. The Delta former is typically used in the formation of ultra-light weight non-wovens (5 – 80 grams per square meter) and sheets with little to no wet strength. The Delta former is also unique in that the type of dry end used is independent of the machine. This allows for a machine to be tailored to a specific product or line of products. This technology is essential in the formation of polymeric microfibrous material because of the large density difference between the stock components, the low consistency of the stock, and the need for an even dispersion during formation.

III.3.4 Dry End Technology Selection

It was not entirely anticipated how polymer fibers would behave in a sintering process. It is known that when a polymer (in any form) is heated to its melting temperature, it completely either melts and flows, or degrades. For this reason, a number of heating processes were used to bond samples from all the sheets made (Poly-Fill fibers, ES Fibervisions fibers, and Invista fibers).

Fiber-Fill is a pure PET fiber used for batting material. Pure PET is known to have a melting temperature in the range of 469°F - 482°F. Although PET is a thermoplastic polymer, it does degrade in the presence of air and moisture. For this reason, the Fiber-Fill sheets were bonded using different methods. The first method used was to place a sample of the sheet on a metal foil support and placed in a heated, hydraulic press. Any metal foil would have been sufficient, but aluminum was used due to availability.

A heated hydraulic press was used (Carver Heated Press – Model C) to compress and evenly heat the Fiber-Fill sheets. The press was operated at 475ºF and compressed to a pressure of 10 pounds per square inch. A dried sample was layered between two aluminum foil supports to prevent adhesion to the press platens. The results were mixed and varied but yielded important findings. All of the samples adhered to one or both of the foil layers and were impossible to remove without destroying the sample. The samples did not show any signs of degradation but the manner in which the fibers adhered to almost any contact surface did illustrate the need for a bicomponent fiber. The result of importance was the lack of degradation in all of the bonded samples. It was expected that with the moisture found in the air (RH ~30%) and the heat from the platens, the PET would degrade. This degradation was not observed indicating that it would require a more localized source of moisture (from within the sheet) to create the necessary environment. The final result of note is the subsequent lack of sheet strength after bonding. All of the samples tested were brittle after bonding and crumbled easily; signs of degradation. Although the PET did not degrade in an expected manner, this reduction of elasticity and strength proved that the bonding atmosphere was not conducive to producing a robust material.

The sintering furnace (BTU International – Model 2000 TCA) was not used to bond polymeric sheets due to the large volume of controlled environment needed, as well as the inaccurate control at the temperature level needed for polymer bonding. The sintering furnace was attractive for two main reasons. First was the controlled environment aspect of the furnace. Since PET degraded in the presence of air and moisture (mainly in the presence of oxygen), it was desired to have a controlled bonding environment. The other attractive quality of the sintering process is the reduction of the cellulose fibers. This is accomplished by creating a reducing environment in which the cellulose fibers are reduced to carbon and carbon compounds. This requires the appropriate ambient environment and the high temperature (800ºC – 1000ºC) which cannot be used with synthetic polymeric material.

Through hot air drying is a technique in which a stream of air is passed through a heating element (either gas or electric) and then passed down through a non-woven sheet. This provides a constant source of heat transferred into the sheet while also providing a method of constant moisture removal. This method of drying and bonding is attractive because it is can be operated efficiently (~70%), inexpensive to operate, and easy to control.

After manufacture, the composite enters a through hot air process to dry and bind the entire matrix using the lower melting sheath of the bi-component fiber. As the sheet dries and components of the sheet reach ambient temperature, the sheath begins to melt and flow along the core of the fiber to the interstitial points at fiber to fiber and fiber to carbon junctions. Semi-spherical shapes are formed along the core when the sheath can not easily flow to an interstitial point (see Figure III.5). This takes place according to physical laws that govern the minimization of free energy along a fluid surface (P Chem, 2006).

Figure III.5: SEM of Polymeric Microfibrous Material (100x Magnification: Reference line is 100 micrometers)

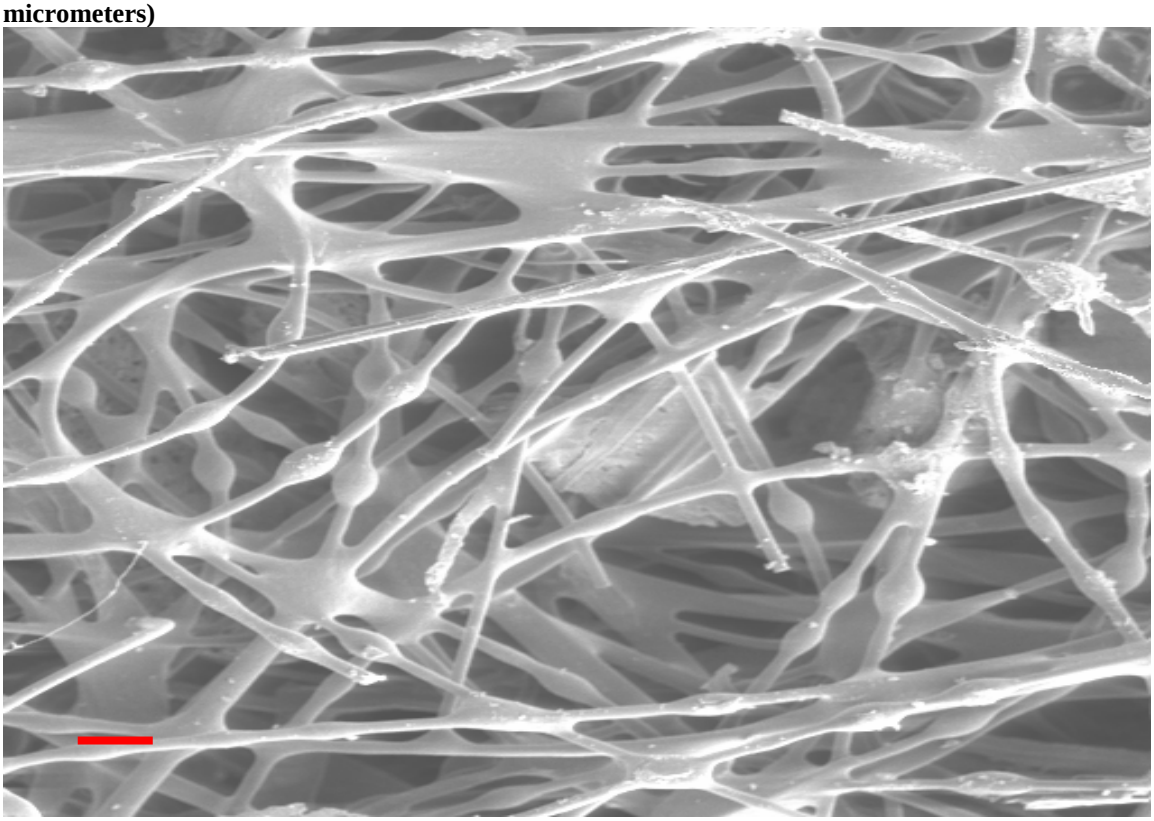

III.4 Scale Up Studies

Due to the large knowledge base in the science of papermaking, the scale up procedure for wet-lay applications is well documented. Thus, the scale up of polymeric microfibrous material was straight forward with a few engineering challenges. These challenges provided the opportunity to implement innovative engineering solutions.

III.4.1 Hand Sheet Studies

TAPPI standard hand sheet formers are the basis of formation research and development. This former consists of a metal column to hold the stock suspension and a wire mesh at the bottom through which the stock is drained by gravitational forces. Fibers and the rest of the stock materials are dispersed thoroughly using a hand held mixer (known as a dasher) in the column. This type of sheet former is necessary to evaluate basis weight, sheet formation parameters, and other fundamental paper characteristics before scaling up to a continuous machine. Sheet formers can be found in the TAPPI standard six inch diameter mold, one square foot mold, and even up to a one square meter mold. The differences in size allow for testing of different paper qualities. In development of polymeric microfibrous material, the six inch diameter and one square foot molds were both used to create samples for testing and scale up purposes.

Having successfully made sheets on a six inch basis, it was necessary to scale the recipe up. The next step up from a six inch disc is a one square foot sheet. The challenges faced in this stage of scale up were typical of the wet-lay process. Fiber dispersion and head box consistency were the two major obstacles that were encountered in this stage. Fiber dispersion in the six inch sheet mold is done using a dasher and hand mixing. For this reason a dasher was constructed to thoroughly disperse the fibers in the MK automated one square foot sheet mold head box. A dasher is a viable option at this scale because in further scale up it can be replaced with a number of currently available industrial mechanical mixers. With a one square foot sheet, the amount of fiber material needed to form the sheet is five times as much as a six inch sheet because of the five fold increase in the wire area. The major difference comes in that the head box for the one

square foot sheet is much larger than that of the six inch sheet. The six inch sheet has a finite amount of water that can be added, and therefore has a small range of consistencies that could be achieved. With the one square foot sheets, the head box allows for a wider range of consistencies. Consistency is the weight of dry material in the stock suspension with respect to the total weight of stock suspension. In general the lower the consistency the better the formation becomes, but there is a limit to how dilute the head box can be and still form a satisfactory sheet. If the consistency is too high (>1.0%) then there is not enough dilution to allow the fiber bundles to fully separate under conventional agitation. If the consistency is too low (<0.01%) then there is too much dilution and the sorbent particles will settle to the wire before the fibers creating uneven formation. Through the tests done using the polisher recipe, it was found that the optimum consistency for the particular sheet mold is 0.1%.

III.4.2 Pilot Machine Studies

Having developed a suitable recipe for HAVC filtration, it was necessary to transfer that recipe from hand sheet molds to a paper machine for continuous production. The twelve inch wide specialized Fourdrinier Machine owned by Intramicron, located on the campus of Auburn University, is currently the platform used for the production of metal based microfibrous material. This machine works well in the manufacture of metal based media, but does not currently work well for the production of polymeric microfibrous material. For this reason, SENW was approached as a research partner of Auburn University to help in the scale up studies for polymeric microfibrous material. SENW is a small research and development company located in Clover, South Carolina. SENW own several pieces of pilot size machinery for various

non-woven techniques. In the area of wet-lay equipment, SENW is capable of making sheets on a six inch sheet mold, one square foot sheet mold, one square meter automated sheet mold, a 21 inch wide inclined wire machine, and a 63 inch wide inclined wire machine.

Figure III.6: 21 inch Inclined Wire Non-Woven Machine

The next step in scale up was a 21 inch continuous paper machine (Figure III.6). The machine is 21 inches at full deckle and utilizes a white-water re-circulation system. The feedstock can be pumped (via Air Operated Diaphragm pumps) to the machine using one or more of three continuously stirred stock tanks. These tanks feed into a head tank that yields constant pressure flow of furnish into the head box. Furnish is fed into a delta former type head box. The delta former can be modified with the addition of a pond regulator to yield the appropriate amount of fiber pick up on the wire or lightning mixers can be added to provide

constant agitation. The wire is a 3D type weave from Albany International. The non-woven mat is transferred twice; both transfers are done onto a belt at a lower position than the previous. The first transfer is onto a belt where additives or special binders can be sprayed onto the wet mat and more vacuum can be applied to the material. The second transfer is into a Grieve through-air gas oven. The settings on the belt speed and oven temperature can both be manipulated to yield the desired amount of bonding. The material is loosely wound up at the end of the oven belt and can be placed on a separate winder for a tighter wind or for slitting. The machine speed is between 0 and 30 feet per minute.

A 63 inch wide inclined wire continuous paper machine was the next step in scale up research (Figure III.7). This machine utilizes the same feedstock setup as the 21 inch machine but differs in two ways: no transfers and no mixing in the head box. The forming wire is continuous all the way through bonding in a gas-fired through-hot-air oven. Also, there are no mixers in the head box (at the time of use). Winding can only be done after the oven, the current winder produces a tightly wound roll. The belt speed can be between 0 and 50 feet per minute.

Figure III.7: 63 inch Inclined Wire Non-Woven Machine

The major problem concerned the stock suspension in the stock tanks. Due to a large amount of material required for the stock tanks, it was suggested that stock be left to mix overnight and the material would be run on the machine the next morning. The stock suspension was mixed using the same wet end chemistry as in the 21 inch machine stock tanks. This chemistry included using a flocculant as an additive to add charge only. The agitation in the tank stopped overnight and the carbon began to absorb the flocculant; so much so that the carbon particles clumped together and separated from the polymer fibers. Two actions were taken to remedy the problem in the wet end chemistry: use the flocculant to modify the viscosity and use prepared stock as soon as possible. The addition of flocculant as a viscosity modifier ensured that the carbon would absorb flocculant but it would not clump to itself because the overwhelming amount of charge addition would keep the particles separate. By preparing stock

immediately before starting up the paper machine would also ensure the same, but would also produce a consistent stock suspension in the event the stirring mechanism failed.

The machine was able to operate enough to produce several 100 feet sections of media in the desired basis weight range. The pressure drop was below the specification by 25% (approximately 0.15 inches of H_2O). The use of this machine gave a glimpse into the possible material that could be made using the right equipment and recipe. The next step is finding a machine capable of producing polymeric microfibrous HVAC material on a large scale.

III.4.3 Full Scale Manufacturing Challenges

To truly appreciate the benefit of a non-woven process such as the wet lay process, a material must be made in large volumes. The typical machine speeds at this scale will drive the overall cost of a product down. It is with this in mind that the following steps were taken to scale up the manufacture of polymeric microfibrous material from a hand sheet mold onto pilot and large scale machines.

For further development of the HVAC material, a larger and faster machine must be employed to make the material cost effective. A 108 inch wide inclined wire wet-lay line has been identified as a possible next step in this scale up study. Possible negative aspects of this machine include the number of transfers, line speed, and stock addition system. The dryer section is approximately 80 feet in length with at least three transfers including the wet end transfers. These two factors combined translate into finding a way to impart more green strength into the unbonded material.

Another challenge in large scale manufacturing is the ability of the material to withstand the transfer from one belt to another before bonding. A paper machine applies a tensile force upon the sheet and the sheet is pulled through the process. This is due to the small differences in speed from one belt to another. It is believed that increasing fiber length will allow for more fiber entanglement and yield the necessary green strength to make the transfers into the dryer section and fully bond upon drying. The drawback to longer fiber length is the negative impact on dispersion. The fibers will provide more entanglement in the un-bonded mat, so will there be more entanglement in the stock tank inhibiting an even dispersion in the tank. These two factors must be balanced when selecting the appropriate fiber length.

The closed water loop of a traditional full scale paper machine is also of importance for the large scale manufacture of polymeric microfibrous material. As the water is recycled around the wet end, the accumulation of wet end additives can cause an imbalance in sheet formation characteristics. For this reason, wet end chemistry is as much an art in balance as it is a science of adding the necessary surface charges to a suspension. This is important because the accumulation of wet end chemicals could disrupt formation and even affect the absorption qualities of the final material. Although the wet end additives are long chain polymers which do not readily occlude active sites on the activated carbon, a large concentration of these additives will begin to align on the surface of the activated carbon and begin to cover active sties reducing capacity.

COMPARISON OF CURRENT AND NEXT GENERATION HVAC FILTRATION STRUCTURES

IV.1 HVAC Filtration Performance Introduction

The next generation of residential HVAC filter media must provide a high level of protection while adhering to strict performance specifications. The two specifications of greatest concern are pressure drop and gas life. Pressure drop is of concern because the resistance to air flow can be directly related to particulate filtration, the service life of the HVAC unit, and energy consumption. A balance between filtration capability and ease of air permeability should be found for a suitable material to be considered. Gas life is important because the final filter should have enough capacity to last a reasonable amount of time in service. The other implication of gas life is a relationship with pressure drop. The more capacity a material has the more sorbent it will contain resulting in a greater pressure drop. In this case where pressure drop and capacity are intertwined, pressure drop will take precedence because of current HVAC unit design. Protection of the HVAC unit is still of greater concern and will not be superseded until new HVAC configurations or filtering solutions are available. For these reasons, a rigorous set of experimental methods was developed and performed to select the characteristics needed in the next generation residential filter

The test methods described further below quantify the material basis weight, and thickness. Thickness is important because it relates the ease with which the material will be able to be pleated into a final HVAC filter. Pressure drop testing was performed to ensure the materials meet the requirement of less than 0.2 inches of H_2O at a local face velocity of 75 centimeters per second. Also gas life testing was performed in an attempt to achieve the target of 25000 – 39000 minutes.

IV.2 Experimental Methods

Secondary to the specifications of pressure drop and gas life performance are the specifications for physical characteristics (basis weight and thickness). Thickness and basis weight are both straightforward measurement tests which can be done for each filtration structure available. Testing for pressure drop and gas life were developed for this application.

IV.2.1 Materials Tested

A survey of currently available products produced four commercial products which were chosen for further study and evaluation. BEC Technologies, Inc. produces a gas phase filtration line of products termed Gray Matter. D-Mark, Inc. produces a filtration structure containing activated carbon particles and polymer fibers formed into a thick mat known as OdorGuard. Lewcott Corporation produces a thick, black, polymeric non-woven filter material, labeled Lewcott.

Testing of current commercial products establishes a performance baseline for the next generation HVAC filter medium. A developmental material is introduced here as a prototype for future filter media. This developmental material, polymeric microfibrous material, is based upon

personal protective equipment research. Two variants (Heavy and Light) of polymeric microfibrous material version four were chosen for testing in comparison to the commercial materials.

IV.2.2 Test Methods

Filtration material characteristics of interest include basis weight, thickness, pressure drop, and gas life. These characteristics were quantified through a series of testing methods based upon currently available standards, adapted expired standards, and new test methods developed in the laboratory.

IV.2.2a Physical Characteristics

Measuring thickness of materials with high loft is challenging due to the compressibility of the materials. This amount of compressibility is important to account for and isolate in thickness measurement. A thickness test method was developed based upon TAPPI Standard T 411 om-97 (TAPPI, 2002). A thickness gauge of a known pressure foot face area (0.7854 square inches) was modified to accept weights of a known amount. Knowing the face area of the caliper and the force applied by the weight, the pressure on the sample (24 kiloPascals) was fixed and maintained uniform across all filtration structures. The surface area of the caliper was large enough so that the force applied to the sample did not distort the measurements by concentrating the load in a small area.

Total basis weight was measured by following TAPPI Standard T 410 om-02 concerning grammage (TAPPI, 2002). Grammage (or basis weight) is a measurement of mass per unit area (grams per square meter). This standard requires three pieces of equipment to ensure the

accuracy of the measurements. A weighing device accurate to 0.25% of the applied load was used to measure the samples. A cutting device was used to obtain precisely cut samples. The precision of the sample cutter must be such that 95 out of 100 samples cut are within 0.2% of the known area. A graduated rule was used to measure the dimension of the sample within an accuracy of 0.2%. According to the TAPPI standard, the samples taken can be of any size and shape but the total number of samples taken should total at least 500 square centimeters. Due to the testing apparatus, a round sample size of 2.25 inches in diameter was chosen to perform flat media testing. With such a sample size, it would have required at least 20 samples to achieve 500 square centimeters. For all of the samples available, this was not possible due to lack of material. For this reason, the number of samples taken was ten. For small sample lots, five was the maximum number of samples possible for testing; thus the data was averaged accordingly.

IV.2.2b Pressure Drop

The testing of these filtration structures began with uniform sample conditioning. Sample conditioning followed TAPPI standard T 402 om-88 (TAPPI, 2002). This standard dictates three atmospheres for preconditioning, conditioning, and testing. The atmosphere for conditioning was adopted for all sample conditioning. Samples were placed in a 23°C environment with 50% humidity for 12 hours. This was the minimum conditioning time but for some tests was greater depending on the initial condition of the sample. Samples were massed before and after the specified time period to note any differences. After conditioning, the samples were placed in the sample holder with flowing house air (82 centimeters per second for 15 minutes) to allow any final degassing. Testing was performed in the same ambient temperature and humidity as conditioning.

Pressure drop testing was performed on the sample first to provide adequate time for sample conditioning in the test apparatus. The samples were tested for pressure drop using metered house air and face velocities ranging from 0 centimeters per second to 162 centimeters per second. The pressure drop testing began with the lowest flow, rate recording pressure drop values until the highest flow rate was reached. The flow rate was then reduced and the pressure drop recorded again to ensure the correct face velocity and pressure drop reading. The pressure drop curve for the empty apparatus was measured and the resulting pressure drop was subtracted from the sample results.

IV.2.2c Gas Life

After pressure drop testing, the conditioned sample mass was measured again and replaced in the sample holder for breakthrough testing. Breakthrough testing was performed at a face velocity of 75 centimeters per second and a challenge concentration of approximately 5 ppm of n-hexane. Breakthrough testing began with the time the challenge chemical was introduced into the influent stream. The apparatus filling time for a face velocity of 75 centimeters per second is approximately one minute (assuming a plug flow profile). The testing is complete when the effluent stream measures a chemical concentration equal to the influent stream concentration. The challenge concentration was chosen because literature shows concentration of individual indoor contaminants recorded at levels below 1 ppm. Collective contaminant concentrations have also been recorded at levels below 1 ppm. Thus 5 ppm would be a conservative challenge concentration and was deemed an achievable concentration in the testing apparatus.

IV.2.3 Description of Apparatus

Thickness testing was done using a digital micrometer (Mitutoyo Absolute ID-S1012E) and precision machined weights. Samples were measured under four different pressures, but only the 44 kiloPascals result was reported as the material thickness. The samples used for this testing were the same used in pressure drop and gas life testing; a round sample size of 2.25 inches in diameter.

Figure IV.1: Pressure Drop and Breakthrough Testing Apparatus

Pressure drop and breakthrough testing were performed in the same apparatus; a five foot long, two inch, schedule 40 stainless steel pipe apparatus (Figure IV.1). A foot long, parallel threaded sample holder was connected onto the end of the main pipe section securing the sample in place. Constant pressure (50 psi) house air was metered through four Omega direct reading rotameters (model numbers FLDA3208C, FLDA3219G, FLDA3407G, FLDA4333S) and divided to provide flow through two Ace Glass 250 mL gas washing bottles (Product number 7166-12) in series, filled with the desired chemical contaminant. Hexane was chosen because it

is an acceptable simulant for other VOCs reported in literature due to the molecule size and affinity for absorption onto carbon.

Figure IV.2: Constant Temperature Water Bath

A Blue M Magni-Whirl constant temperature, stirred water bath maintained the gas washing bottles and their contents isothermal during breakthrough testing. Maintaining the hexane isothermal is important to keep the challenge concentration constant. The contaminated air stream can be diverted to an exhaust hood while pressure drop testing is performed or joined with the pure air stream for breakthrough testing. Pressure drop across the sample was measured through a barbed fitting inserted into the main pipe section 5.5 inches before the sample face.

An Omega differential pressure cell (with digital output) was connected to the barbed fitting to record pressure drop measurements (Product Number PX154-010DI).

Figure IV.3: Sample Holder Section

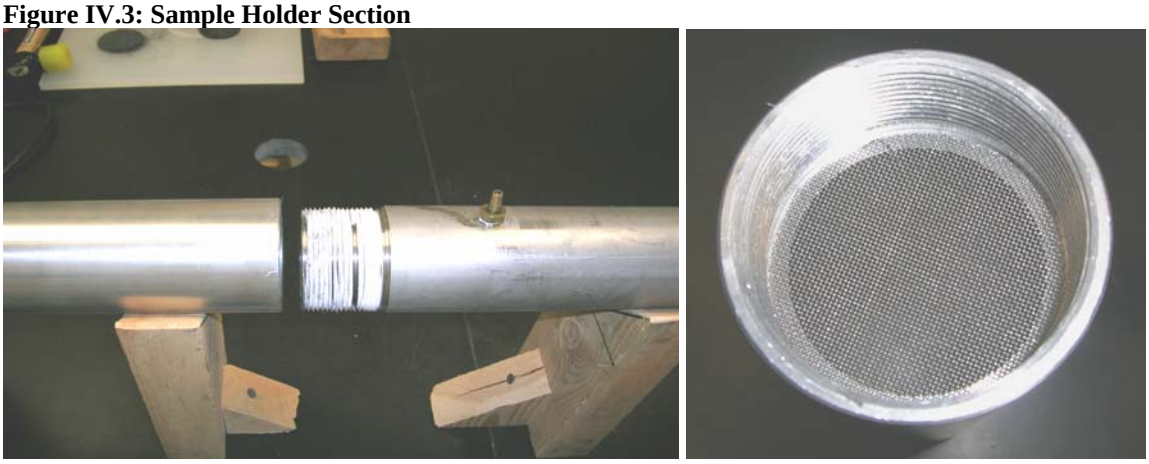

The sample holder was secured to the main pipe section via parallel threads. This securing method was necessary for testing of samples with varying thicknesses. The samples were supported using a stainless steel mesh screen (No. 20 ASTM Mesh). There was a one-eighth inch support mantle around the sample to allow for support and edge sealing. The threads were wrapped with PTFE tape to prevent any leakage.

Figure IV.4: Multi-RAE Plus PID and Mini-RAE 2000 PID

The effluent stream was monitored using a photoionization detector (PID) placed at the center of the sample holder exit. Two similar RAE Systems detectors were used according to availability: a MiniRAE 2000 and a MultiRAE Plus (MiniRAE 2000 has 10.6 eV lamp and MultiRAE Plus was equipped with ammonia, carbon monoxide, and VOC sensors with a 10.6 eV lamp). The monitors were calibrated according to manufacturer specifications before testing each sample lot with RAE Systems provided calibration gas. These specific monitors are sensitive down to 0.1 ppm of n-hexane concentration. Gas life testing data was recorded into the RAE detectors and regression was done using Microsoft Excel. Gray Matter V 1.8 and Lewcott were both measured with a sample point recorded every 10 seconds. OdorGuard 15 and OdorGuard 45 were both measured with a sample point recorded every 2 seconds. This data recording regime was increased from 2 seconds to 10 seconds for 5 of the 10 OdorGuard 15 samples tested. This was done for two reasons: the detector has limited data capacity; the data shown in previous tests would not be affected by a longer time span between data points. Four of the five PMM-V4 Light samples were tested with a 2 second interval between data points. The last sample was tested with a 10 second interval between data points because of the limited data capacity due to the long gas life of the samples tested. Since the PMM-V4 Light samples exhibited such a long gas life, the data point time interval for all 5 PMM-V4 Heavy samples was set at 5 seconds to obtain good resolution throughout the test and accommodate the data capacity of the detector.

IV.3 Results

Although each test yielded an important result in determining the best candidate for the next generation HVAC filter, the results should be reviewed to understand the overall material

performance. This performance is not only dependent upon gas life or pressure drop, but also physical characteristics which would make the filter material suitable in typical processing situations.

IV.3.1 Physical Characteristics

From the thickness and basis weight results, it can be seen that all of the structures have a wide range of basis weights and thicknesses (Table IV.1). OdorGuard 45 has the greatest basis weight and Gray Matter V 1.8 is on the opposite end of the spectrum (this trend is the same for thickness). This wide variation of thickness and basis weight of each filtration structure is indicative of their non-woven manufacturing methods. These manufacturing methods allow for the continuous production of the filtration structure with a typical basis weight variation of ± 10-15%. OdorGuard 45, Gray Matter V 1.8, and Lewcott all have a deviation in basis weight less than ± 10%; which is the typical range for basis weight deviation in wet laid materials but on the low end of deviation for non-woven structures. This could be attributed to rigorous quality control or an improved non-woven process. OdorGuard 15 has a basis weight deviation of approximately ± 13%. This amount of deviation is typical of materials produced with a spunbonding or melt blowing process.

Table IV.1: Thickness and Basis Weight Results of Selected Filtration Structures

Sample Name	Average Thickness* (mm)	Average Sample Basis Weight (g/m^2)	Standard Deviation ($\pm$ g/m^2)
OdorGuard 15 [1]	2.94	347.38	46.04
OdorGuard 45 [2]	6.58	703.03	34.36
Gray Matter V 1.8 [1]	1.31	64.24	2.34
Lewcott [2]	2.45	392.80	25.50
PMM-V4 Light	1.02	207.39	12.46
PMM-V4 Heavy	2.11	380.32	4.96

* – Denotes one sample tested; testing pressure was 44 kPa

The thickness results for both PMM-V4 variants are consistent with their difference in basis weight. The rule of thumb for wet laid materials concerning basis weight deviation is a maximum of ± 10% with a desired ± 5% deviation. The basis weight deviation result for PMM-V4 Light is ± 6%; within the maximum basis weight deviation range. The deviation result for PMM-V4 Heavy is ± 1.3%; within the desired basis weight deviation range. The other factor is that these materials have approximately the same basis weight as Lewcott and OdorGuard 15, but with the thickness of Gray Matter. The true effect of this difference between filtration structures will be noticed in the pressure drop performance testing described below.

The main objective of thickness determination was to qualitatively identify if a filtration structure would be suitable in a two inch deep, pleated HVAC filter. The optimum filtration structure should be able to be pleated into a two inch deep HVAC filter easily through automated equipment. Due to the thickness and basis weight, OdorGuard 45 would not be a good candidate for a pleated HVAC filter. OdorGuard 15 and Lewcott are at the high end of desired thickness and basis weight limit, but would be acceptable as a filtration structure because of their low thickness. The thickness and basis weight of PMM-V4 Light and Heavy make both versions candidates for the next generation HVAC filter. Physical observation shows that both samples are robust, flexible, and would process through pleating and filter assembly. This is an added benefit that is a result of the wet-laid process; manufacturing a robust yet flexible non-woven material.

IV.3.2 Pressure Drop Performance

The pressure drop results from three of the commercial samples are contained in Figure IV.5. The fourth pressure drop curve (the result of OdorGuard 15) is shown in Figure IV.6. The

results are separated to clearly show the statistical deviation and the results for each filtration structure. Figure IV.7 contains the results for the polymeric microfibrous material samples.

Figure IV.5: Pressure Drop Curves for Selected Filtration Structures

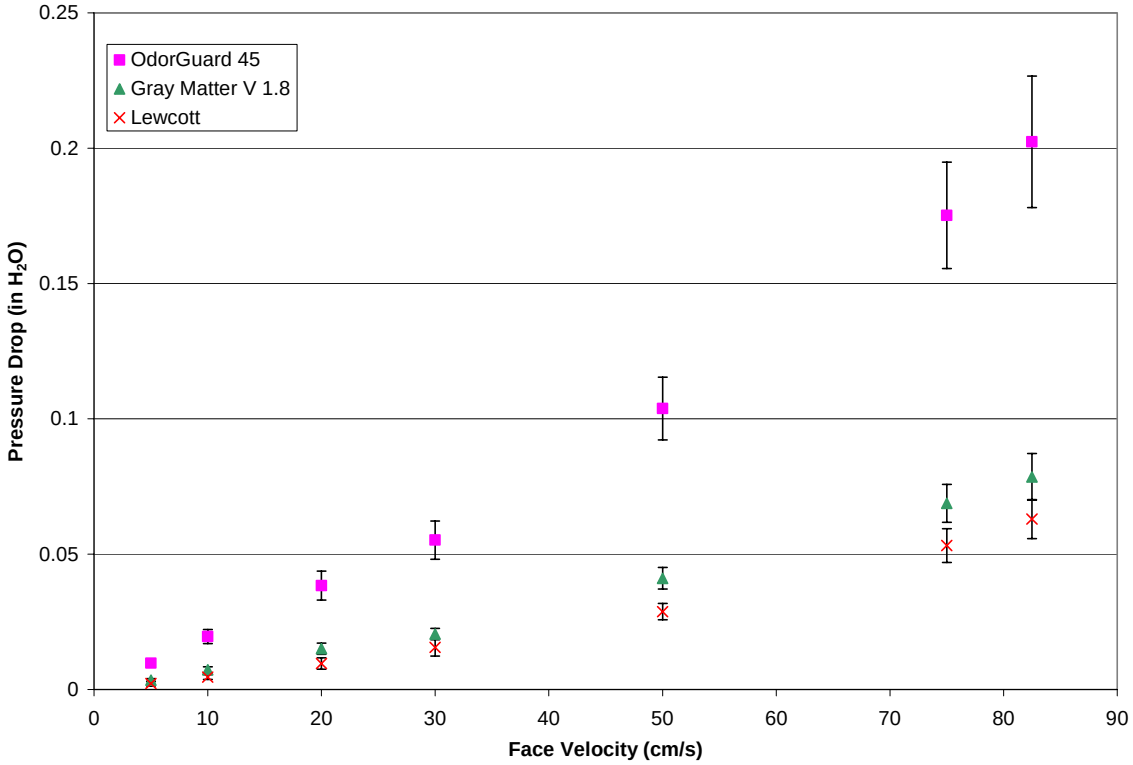

[1] – Gray Matter V 1.8 had ten samples tested
[2] – OdorGuard 45 and Lewcott each had five samples tested

The first result of note in Figure IV.5 is that all of three filtration structures pass the requirements for a 2 inch deep HVAC filter (<0.2 inches H_2O at 75 centimeters per second). The deviation in each of the filtration structures is also of interest. Both Lewcott and Gray Matter V 1.8 show little statistical variation between samples. OdorGuard 45 shows large statistical variation. This wide deviation in pressure drop is attributed to the basis weight deviation of the filtration structure. Although the basis weight deviation result of OdorGuard 45 is not large (below ± 10%), the visual inspection shows a large variation in the filtration structure with respect to

dispersion of carbon particles. Another factor contributing to the low deviation value for OdorGuard 45 is the lack of material for testing where available (only five samples). Both Gray Matter V 1.8 and OdorGuard 15 swaths yielded ten samples, leading to a more accurate standard deviation. Another contribution to the wide standard deviation is the construction of OdorGuard 45. OdorGuard 45 is a composite made by layering 3 sheets of OdorGuard 15 (the pressure drop curve for OdorGuard 15 is shown in Figure IV.6). The OdorGuard 15 results are isolated to show the large deviation in comparison to the other filtration structures.

Figure IV.6: Pressure Drop Curve for OdorGuard 15 (ten samples tested)

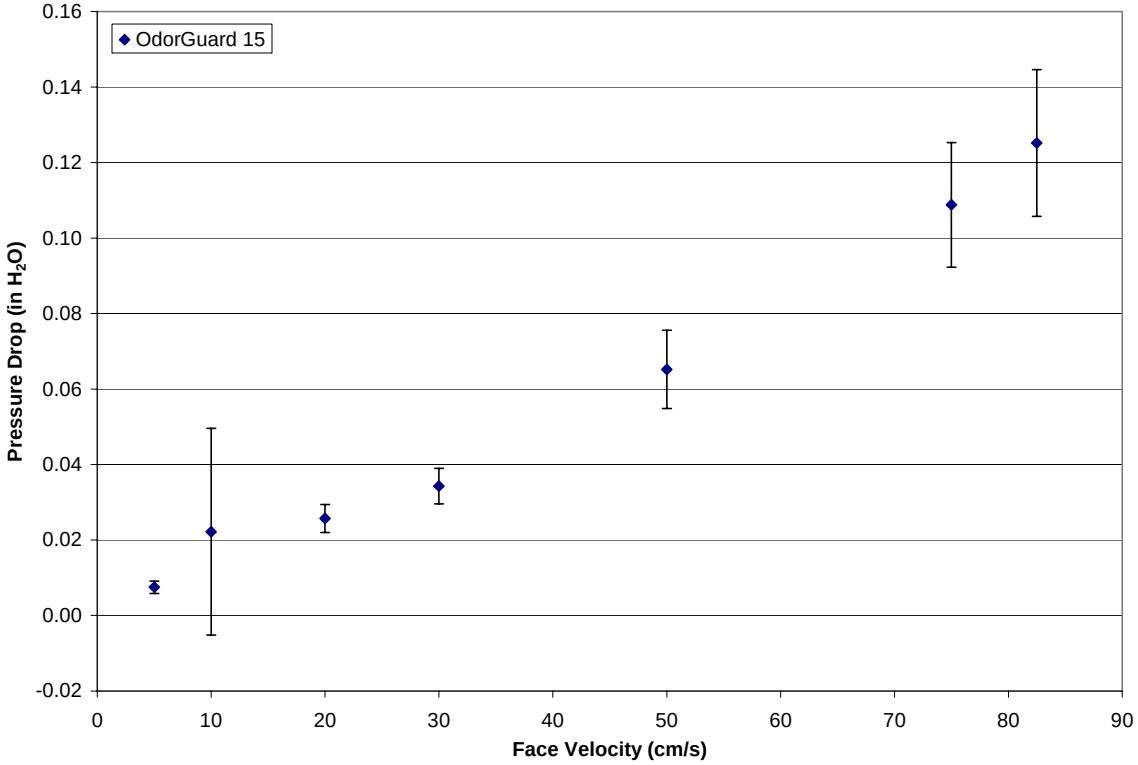

Figure IV.6 shows the large amount of deviation in the pressure drop results for OdorGuard 15. The data points of note are the pressure drops measured at 10 centimeters per second, 50 centimeters per second, 75 centimeters per second, and 82 centimeters per second. The average

pressure drop recorded for the face velocity of 10 centimeters per second is 0.022 inches H_2O. This pressure drop has a standard deviation of ± 0.027 inches H_2O (approximately 123%). The pressure drop points at 50 centimeters per second, 75 centimeters per second, and 82 centimeters per second all have approximately 15% deviation per data point. The large amount of deviation for the 10 centimeters per second pressure drop does not have a clear explanation. This deviation could be due to a combination of experimental/equipment error (i.e. inconsistency of sample placement and sample holder adjustment) and the amount of basis weight deviation in the samples. From the basis weight measurements, it can be seen that OdorGuard 15 has a basis weight variation of approximately ± 13%. Visual inspection of the samples revealed an uneven dispersion of carbon particles through out the filtration structure. The pressure drop deviation at the higher face velocities is indicative of the basis weight deviation for the filtration structure. The result of importance is that all four filtration structures recorded an acceptable pressure drop for a two inch deep HVAC filter.

Figure IV.7: Pressure Drop Curves for Polymeric Microfibrous Materals (five samples tested)

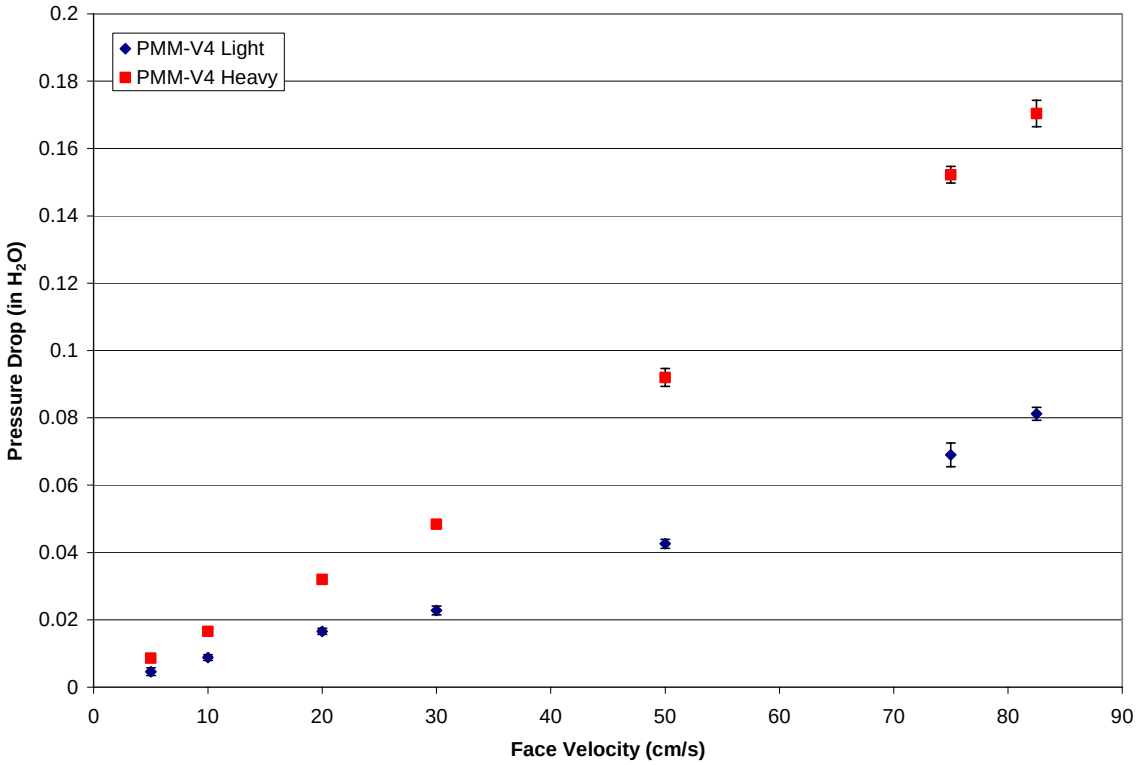

Both variants of polymeric microfibrous materials pass the pressure drop specification. The PMM-V4 Heavy variant has the higher pressure drop curve due to a higher basis weight (and sorbent content). This curve is similar to the pressure drop curve of OdorGuard 45, but with less deviation. The pressure drop curve of PMM-V4 Light is similar to the pressure drop curve of Gray Matter V 1.8. An important aspect of the results is the lack of deviation in the data points. This is a reflection of the lack of deviation in basis weight. There is very little variation in both of the versions which is a positive attribute for material produced at full scale.

The shape of the curves is also of importance to understand the physical phenomena contributing to the pressure drop of each filter material. At low face velocities, the pressure drop of the material was dominated by the resistance of flow through the fiber matrix. This flow resistance yielded a linear pressure drop curve. At high face velocities, the boundary layer

around each fiber was reduced and a second resistance contributed to the pressure drop. This resistance was the inertial loss of the flow as it comes into contact with the individual fibers within the matrix. The contribution of inertial losses was not linear, but exponential. Upon inspection, all of the pressure drop curves show this phenomenon. All of the filtration structures exhibited linearity in the face velocity range of 0 – 50 centimeters per second. In the face velocity range of 50 – 100 centimeters per second, the samples began to exhibit an increased slope which is indicative of inertial losses. The important part of the inertial loss contribution is that it was minimal in the materials and face velocity ranges studied.

IV.3.3 Gas Life Performance

Although the gas life results contained in Table IV.2 may seem vastly different, it is important to normalize these results and compare them on an even basis. This basis is apparent absorption capacity and single pass removal efficiency.

Table IV.2: Gas Life Results for Selected Filtration Structures

Sample Name	Average Gas Life (minutes)	Standard Deviation (± min)
OdorGuard 15 [1]	19.58	1.23
OdorGuard 45 [2]	43.57	4.01
Gray Matter V 1.8 [1]	4.90	0.31
Lewcott [2]	6.27	2.02
PMM-V4 Light [2]	45.13	5.30
PMM-V4 Heavy [2]	62.58	8.99

[1] – Denotes ten samples tested
[2] – Denotes five samples tested

It is important to note the variation in the sample results. Both OdorGuard15 and Gray Matter V 1.8 had approximately 6% deviation in the gas life results and OdorGuard 45 had approximately 9% deviation. Lewcott had the highest amount of deviation with 32% deviation in gas life. These results do not agree with the results from the basis weight testing. OdorGuard 15 had the highest basis weight deviation (13%) and Lewcott had a lower basis weight deviation (6%). This alludes to another factor impacting the gas life other than basis weight deviation. Another possibility is the amount of sorbent occlusion caused by the filtration structure manufacturing method. In the case of Lewcott, the material is made by either meltblowing or spunbonding fibers into a non-woven mat while trapping sorbent particles into the matrix as it is formed. As this is done, the sorbent particles are entrapped in the fiber matrix but are also adhered to the molten fibers. These contact points maybe random, large, and numerous enough that active sites are occluded and not available for chemical absorption.

Both variants of polymeric microfibrous material exhibit long gas life results when compared to the commercial filtration structures previously tested. PMM-V4 Light had a variability of approximately 12% while PMM-V4 Heavy had a variability of approximately 14%. From these results it would seem that the polymeric microfibrous material samples were the highest performing materials when compared to the commercial structures. Gas life can not be used as an accurate measure of performance because it does not account for the totality of the filtration structure. Although some structures may have exhibited a long gas life, the overall performance of the structure is important to consider when determining the best performing filtration structure.

IV.4 Chemical Contaminant Removal Performance

Gas life results alone do not show which filtration structure is the optimum selection for the next generation HVAC filter. A normalized comparison accounting for the apparent capacity for each filtration structure and the capacity usage efficiency should be utilized to compare the filtration structures.

IV.4.1 Organic Vapor Capacity

Organic vapor capacity is defined as the amount of capacity available in the filter media for VOC absorption. This can be calculated in two ways. The first is to know the amount of sorbent in the filtration structure, obtain the amount of capacity for the challenge chemical, and then determine the capacity in grams of challenge chemical. The second method is to obtain a breakthrough plot and integrate the area under the plot to calculate apparent absorption capacity. The second method was preferred because of the difficulty in accurately determining the type or measures the amount of sorbent in the commercial structures of matter.

From the breakthrough data obtained, this was calculated through the integration of the area under the curve using a numerical integration method. The area under the breakthrough curve is defined as the area from the beginning of the breakthrough test until the effluent concentration is the same as the influent concentration. This area is then subtracted from the total area possible (the product of gas life and challenge concentration).

Equation IV.1: Apparent Adsorption Capacity

$$Ca = C_0 t_{total} - \alpha$$

Apparent absorption capacity, or Ca in units of ppm-minutes, is shown in Equation IV.1 where C_0 is the challenge concentration in ppm, t_{total} is the time required for complete breakthrough in minutes, and α is the integrated area under the breakthrough curve in ppm-minutes. This numerical integration used the Mid-Ordinate Rule (right approximation) to obtain the area under the curve (obtained from the PID data). The results are shown in Table IV.3 with the standard deviation.

Table IV.3: Capacity Results for Tested Filtration Structures

Sample Name	Average Capacity (ppm-min)	Standard Deviation (± ppm-min)
OdorGuard 15 [1]	22.24	7.28
OdorGuard 45 [2]	89.91	23.83
Gray Matter V 1.8 [1]	3.04	0.93
Lewcott [2]	9.20	2.92
PMM-V4 Light [2]	95.32	18.72
PMM-V4 Heavy [2]	181.90	15.45

[1] – Denotes ten samples tested
[2] – Denotes five samples tested

Table IV.3 shows significant variability for each sample. This deviation was due in part to basis weight variability and in part to the variability of the hexane generator. Although the gas washing bottles and contents were isothermal, a low flow rate was required to achieve a 5 ppm concentration. The apparatus used was effective in achieving this target, but a more accurate apparatus needs to be developed in order to maintain this target accurately over a long period of time. This should be done with a high pressure gas cylinder containing a premixed combination and pressure regulators used to achieve the desired flow rate.

The shape of the breakthrough curve can indicate filtration behavior and filtration efficiency. To truly understand this phenomenon, it is necessary to understand the gas mask filtration application. In this application testing, influent is flowing at a lower rate (9.8 centimeters per second), contains more chemical contaminant (3000 miligrams per cubic meter), and the breakthrough limit is defined as the time elapsed before the lowest detectable limit (0.10 ppm) of chemical contaminant is recorded. Gas mask filtration is dependent upon long gas life and high chemical capacity to provide contaminant free air to the person wearing the gas mask.

The packed bed is the traditional technology used in gas masks and is characterized by a plug-flow distribution. This causes the first portion of the packed bed to be fully saturated, the middle portion to be partially saturated, and the end portion to be almost unused at time of breakthrough. The packed bed gas life curve is a long (elapsed time between breakthrough and the effluent concentration equaling the challenge concentration), smooth, sigmoidal curve indicative of the inefficient use of the sorbent within the packed bed. This behavior will be used as the baseline for single pass removal efficiency comparison. The tested filtration structures were analyzed for similar behavior using the breakthrough curves.

Figure IV.8: 3-Point Moving Average Breakthrough Curves for all Gray Matter V1.8 Samples Tested

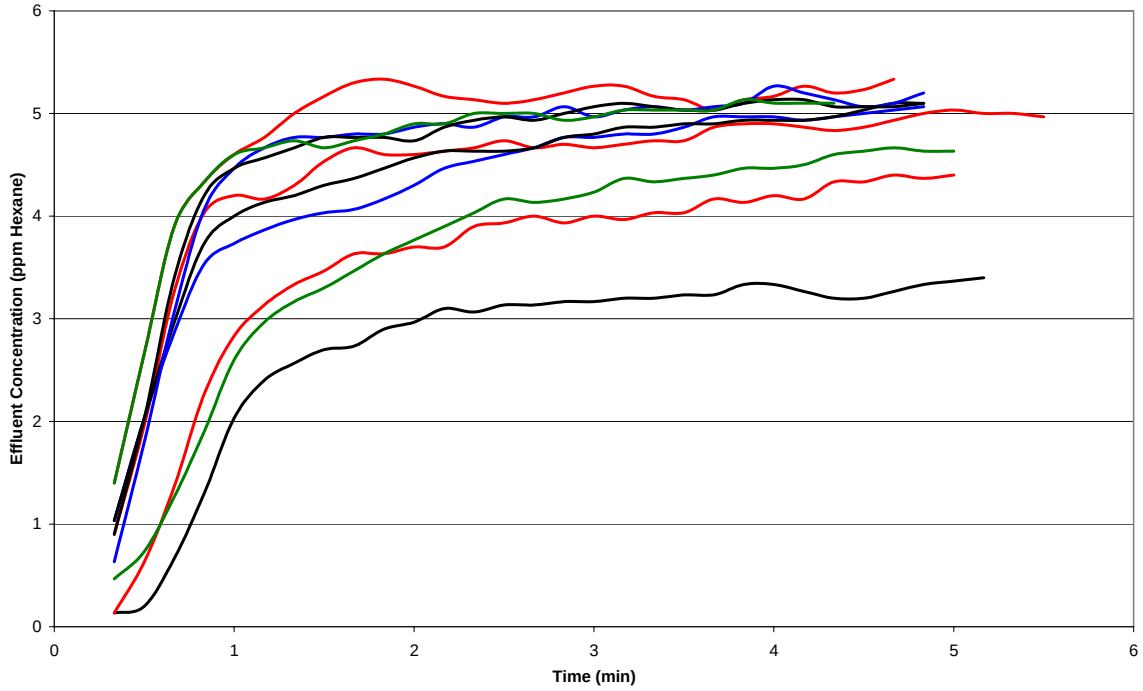

From Figure IV.8, it can be seen that Gray Matter V 1.8 exhibited very little chemical contaminant capacity in this testing scenario. Complete breakthrough took place within one to two minutes. This is indicative of a filtration structure with no capacity for hydrocarbons. The time elapsed between the introduction of challenge contaminant and breakthrough time was due to apparatus filling and the amount of time required for the challenge contaminant to pass through the filtration structure. This means that Gray Matter V 1.8 exhibited very little absorption capacity for n-hexane. Another phenomenon of note is the similarity of the breakthrough curves. Ignoring the variability in the challenge concentration, the curves were similar indicating little variability in the material.

Figure IV.9: 3-Point Moving Average Breakthrough Curves for all Lewcott Samples Tested

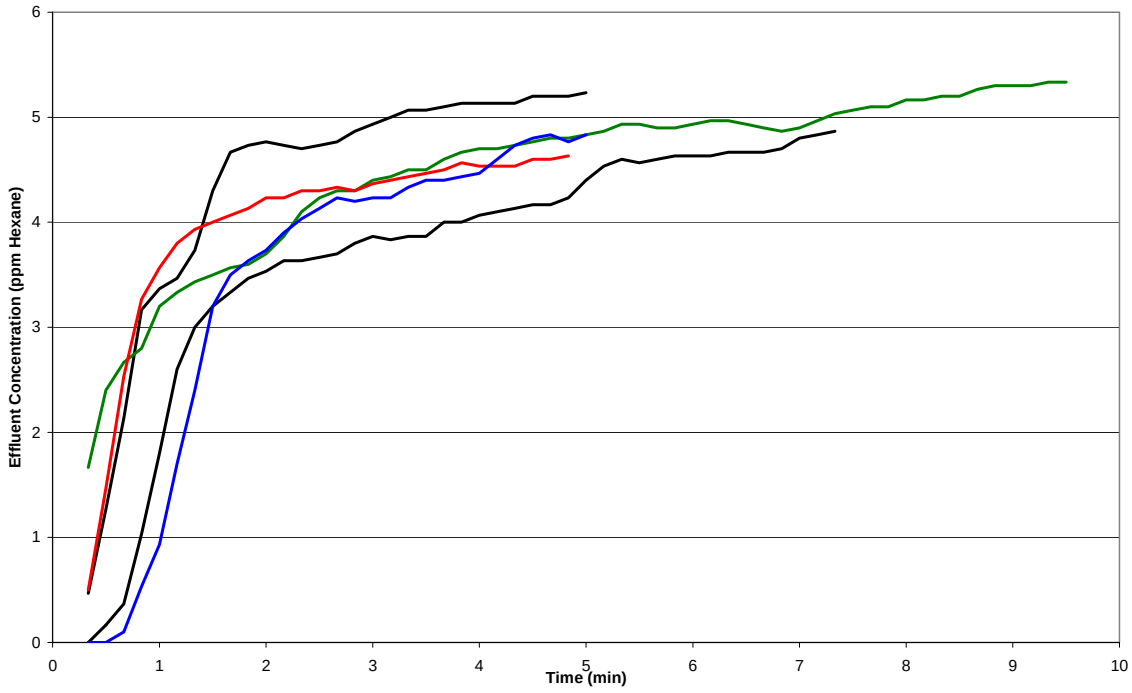

As with the Gray Matter V 1.8 results, the Lewcott results were similar in shape (Figure IV.9). In contrast, the gas life results were quite varied; ranging from 5 minutes to less than 10 minutes. This variability in gas life is attributed in part to the variability in the distribution of the absorbent particles. Another factor leading to variability is the randomness of occlusion around the sorbent particles (due to manufacturing method).

The breakthrough results show a sharp increase in effluent concentration which then slowly approaches the challenge concentration. This type of behavior is indicative of absorption capacity which is not immediately available during the breakthrough test. As the chemical contaminant comes in contact with the sorbent, it adsorbs to available sites near the surface and then diffuses into the mesopores of the sorbent followed by micropores (assuming a traditional pore structure). If a portion of the surface is occluded (i.e. coated with a polymer), then more time is needed for the chemical contaminant to move through the pore structure of the sorbent to

fully saturate the sorbent. In this case, the stringent test does not allow for equilibrium and the filtration structure fails the test earlier than full saturation of sorbent.

Figure IV.10: 5-Point Moving Average Breakthrough Curves for all OdorGuard 15 Samples Tested

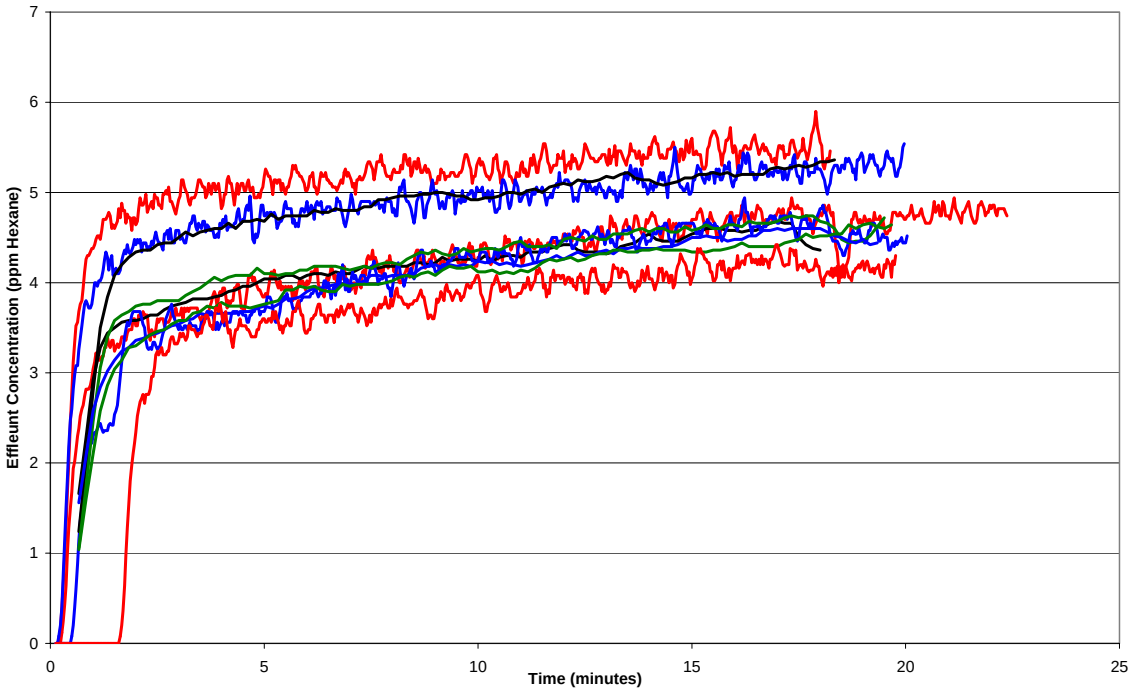

Similar to the previous commercial structures tested, the OdorGuard 15 samples closely mimicked the results for each sample (Figure IV.10). Similar to Lewcott, the samples showed a sharp increase in effluent concentration, but a long gradual increase until the breakthrough test was completed. This behavior lends to the idea that some of the adsorbent material is occluded and not readily available for absorption. In contrast to the Lewcott structure, this material mirrored the Gray Matter V 1.8 tests because all samples exhibited similar breakthrough times (characteristic of evenly distributed sorbent material).

Figure IV.11: 5-Point Moving Average Breakthrough Curves for all OdorGuard 45 Samples Tested

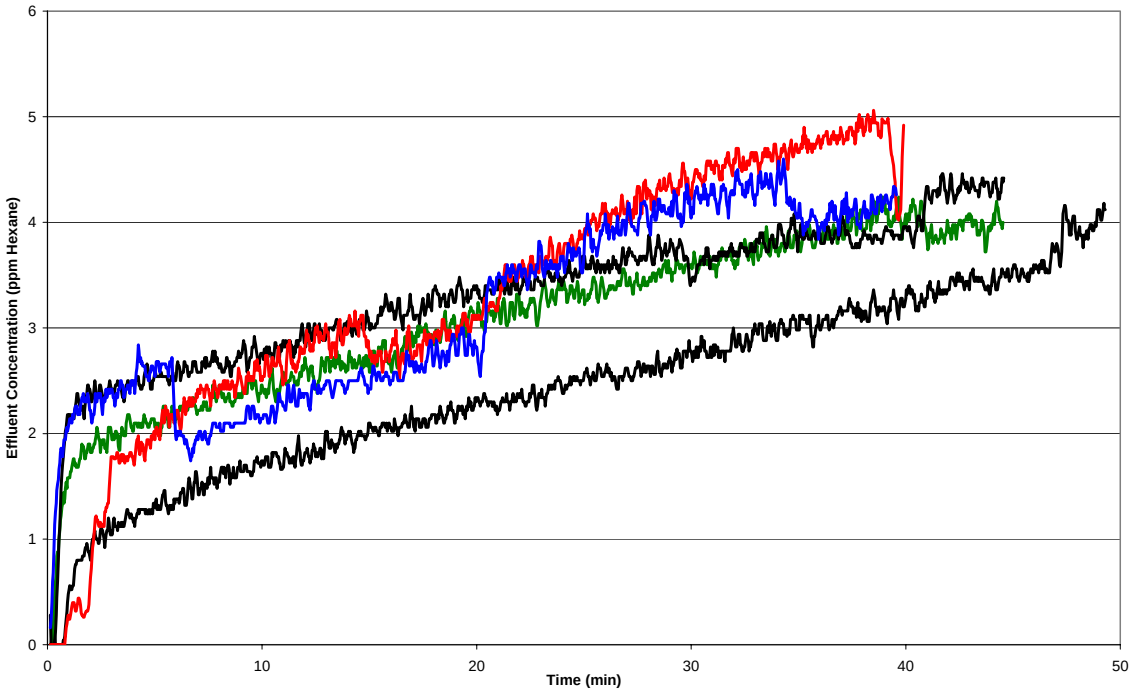

Figure IV.11 shows the results for OdorGuard 45. The first result of note is the similarity of gas life between the samples tested. Barring the variations in challenge concentrations, the OdorGuard 45 exhibited a uniform dispersion of sorbent material throughout the filtration structure. This material is a composite of 3 OdorGuard 15 layers. The gas life was comparable to a composite of layering OdorGuard 15, but not exactly three times the gas life. The increase in effluent concentration was less sharp than that observed with OdorGuard 15 and the gradual increase until the end of the breakthrough test requires more time. The method with which the layers are combined could explain this phenomenon. The layers of OdorGuard 15 were adhered using an adhesive layer (i.e. more fiber or adhesive). This not only led to an increase in basis weight without the addition of more absorption material, but also to occlusion of any sorbent material on the surface of the OdorGuard 15 layers, reducing apparent absorption capacity.

Figure IV.12: 5-Point Moving Average Breakthrough Curves for all PMM-V4 Light Samples Tested

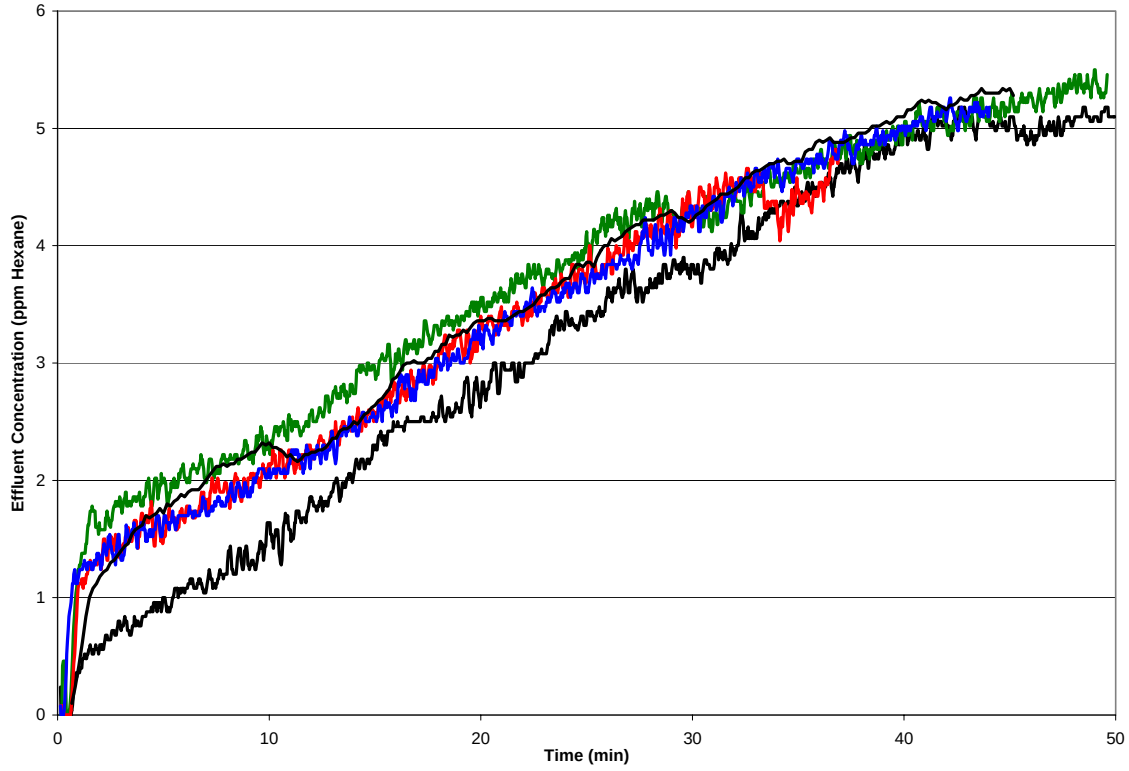

As with the OdorGuard 45 samples, the PMM-V4 Light breakthrough curves did not show a sharp increase in the effluent concentration at the onset of testing (Figure IV.12). The samples also showed similar breakthrough curves indicating little variability in sorbent particle distribution throughout the filtration structure. The trends of the breakthrough curves indicate that there was unused sorbent capacity at the end of breakthrough testing.

Figure IV.13: 5-Point Moving Average Breakthrough Curves for all PMM-V4 Heavy Samples Tested

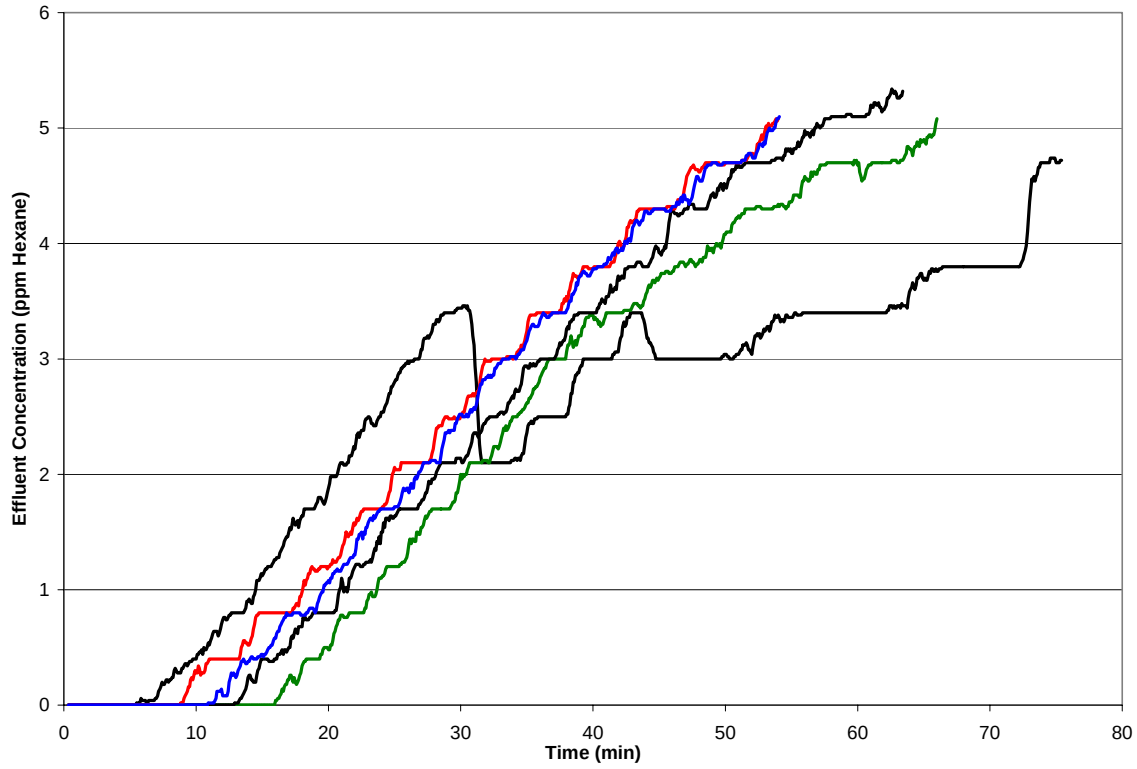

The first result of note is the lack of a sharp increase during the onset of the breakthrough test and the long gas life for PMM-V4 Heavy. The anomaly of this data set was the testing of Sample 5. Due to a malfunction in the hexane vapor generator, the challenge concentration increased from 5 ppm to 7 ppm during the onset of the breakthrough test. This was discovered during one of the routine inlet concentration checks performed during the test. The generator was then modified to provide a 5 ppm challenge concentration and the test continued. Barring this sample, the trends in the remaining breakthrough curves show close agreement between samples. The main result of note is the initial portion of the breakthrough test where there was no contaminant detected in the effluent stream. This is a marked performance improvement over the commercial filtration structures and PMM-V4 Light. The gas life improvement over all other

structures tested is also an improvement, but can only be truly understood through the determination of single pass removal efficiency.

IV.4.2 Single Pass Removal Efficiency

Single pass removal efficiency is defined as the amount of chemical contaminant removal performed by the filtration material compared to the amount of chemical contaminant flowed into the material through one pass. Single pass efficiency, or $\eta_{SinglePass}$, is shown in Equation IV.2 where Ca is apparent absorption capacity in ppm-minutes (Equation IV.1), t_{total} is time required for full breakthrough in minutes, and C_0 is the challenge concentration in ppm.

Equation IV.2: Single Pass Removal Efficiency

$$\eta_{SinglePass} = Ca \Big/ t_{total} C_0$$

Table IV.4 shows the results from the single pass removal efficiency calculation for each of the filtration structures. The high performing filtration structures appear to be the OdorGuard 45 and both PMM-V4 variants. It can be seen that only the PMM-V4 variants had a deviation of less than 10%. OdorGuard 15 and Gray Matter V 1.8 were the two lowest performing structures and exhibit the highest deviation. From these results, PMM-V4 Heavy was the best filtration structure according to single pass removal efficiency.

Table IV.4: Single Pass Removal Efficiency Results for Tested Filtration Structures

Sample Name	Average Single Pass Removal Efficiency (%)	Standard Deviation (± %)
OdorGuard 15 [1]	21.01%	6.54%
OdorGuard 45 [2]	40.06%	6.98%
Gray Matter V 1.8 [1]	12.97%	4.27%
Lewcott [2]	26.75%	4.09%
PMM-V4 Light [2]	38.62%	3.10%
PMM-V4 Heavy [2]	55.65%	3.03%

[1] – Denotes ten samples tested
[2] – Denotes five samples tested

When compared to Table IV.3, the results have removed any variability attributed to the testing apparatus by isolating the performance of the material. Thus the results only reflect the properties of the material tested, not the apparatus.

IV.5 Comparison of Novel Filtration Structures of Matter

The appropriate filtration structure for the next generation residential HVAC filter does not only possess outstanding performance in one area, but rather an optimum balance of several important factors. The overall performance and filtration structure properties are compared here to determine the optimum filtration structure.

Taking into account the physical parameters and the chemical contaminant removal performance of the filtration structures tested, PMM-V4 Heavy is the best candidate of the media tested for use in the next generation residential HVAC filter. This is because it possesses a structure which is robust enough for the filter manufacturing process (thickness and pressure drop) and exhibits superior performance (pressure drop and chemical contaminant removal).

Although the filtration structure does not possess enough chemical contaminant capacity to last for 90 days, the filtration structure is a promising start for future iterations.

The next generation filter should include the physical characteristics found in PMM-V4 Heavy, but should possess more gas life. Because of the low pressure drop recorded, this could be accomplished through the addition of more or a combination of sorbents. The structure and performance attributes of microfibrous material make this composite the most appropriate medium for the next generation HVAC filter. Table IV.5 shows the data and results for all of the filtration structures tested.

Table IV.5: Compilation of Testing Results for Novel HVAC Structures of Matter

Sample Name	Thickness*^ (mm)	Pressure Drop at 75 cm/s Face Velocity (in H_2O)	Average Sample Basis Weight (g/m^2)	Average Gas Life (minutes)	Average Capacity (ppm-min)	Average Single Pass Removal Efficiency (%)
OdorGuard 15 [1]	2.94	0.109	46.04	19.58	22.24	21.01%
OdorGuard 45 [2]	6.58	0.175	34.36	43.57	89.91	40.06%
Gray Matter V 1.8 [1]	1.31	0.069	2.34	4.90	3.04	12.97%
Lewcott [2]	2.45	0.053	25.50	6.27	9.20	26.75%
PMM-V4 Light [2]	1.02	0.069	207.39	45.13	95.32	38.62%
PMM-V4 Heavy [2]	2.11	0.152	380.32	62.58	181.90	55.65%

[1] – Denotes ten samples tested [2] – Denotes five samples tested
* – Denotes only one sample point ^ – Denotes a pressure of 44 kPa
Green color denotes lowest value in series and Red color denotes highest value in series

Table IV.5 shows that PMM-V4 Heavy is the best performing structure with respect to chemical contaminant removal while the best physical characteristics are divided between PMM-V4 Light, Lewcott, and Gray Matter V 1.8. Taking into account the physical parameters and the chemical contaminant removal performance of the filtration structures tested, PMM-V4 Heavy is the leading candidate for use in the next generation residential HVAC filter. This is because it possesses a structure which is robust enough for the filter manufacturing process (thickness and

pressure drop) and exhibits superior performance (pressure drop and chemical contaminant removal) as a novel filtration structure for the next generation residential HVAC filter. Although the filtration structure does not possess enough chemical contaminant capacity to last in a typical residential HVAC unit for 90 days, the filtration structure is a promising start for future iterations.

POLYMERIC MICROFIBROUS MATERIAL PARTICLE SIZE DISTRIBUTION OPTIMIZATION

V.1 Particle Size Distribution Introduction

Particle size distribution (PSD) is important to many performance factors of polymeric microfibrous material. PSD directly affects the physical characteristics, pressure drop, and gas life performance of polymeric microfibrous materials. The physical characteristics of concern are the dark/black appearance, particle shedding, and basis weight. As the particle size decreases and the bulk density of the particulate increases the color and basis weight of the final material are positively affected by this change. The pressure drop performance is also directly affected by changes in PSD. Pressure drop is the overall resistance to flow through the material. As particle size is decreased, the overall resistance is increased from a higher concentration of particles. This increased concentration not only blocks flow channels, but also causes inertial losses to become more pronounced at lower flow rates than typically expected. Gas life is the final component direct impacted by PSD. As particle size decreases and the amount of particulate entrapped in the material increases, gas life increases proportionally. Gas life is a measure of available capacity (taking into account occluded absorption sites). It is desired to entrap the most particulate as possible to achieve the highest gas life possible. This is in direct contradiction to the requirement for a low pressure drop (less particulate). Thus, the optimization of performance is found by defining the optimum PSD.

V.1.1 UL Testing Background

Underwriters Laboratory (UL) is one entity responsible for certification of household equipment for flammable safety in compliance with NFPA 90B (2008). This standard covers the combustibility for particulate filters in residential Heating-Ventilation and Air Conditioning (HVAC) systems. The combustibility of the filter is based upon the amount of smoke and possible fuel contribution generated when introduced to an open flame. There are two possible classes of filter classification referenced by this standard: Class One filters emit little to no smoke, and do not contribute fuel; Class Two filters emit a significant amount of smoke and/or burn easily when introduced to flame. Polymeric microfibrous material would fall into Class Two because of the activated carbon acting a source of possible fuel upon combustion.

The ANSI/UL 900 (2008) test is designed to determine the amount of smoke generation and fuel contribution of a clean filter during a 3 minute long test. During this test, the faces of the filter, the characteristics of the combustion products in the end section of the test duct, and the nature of any flame or sparks beyond the end of the duct are to be monitored and noted. The amount of smoke exiting the test apparatus is measured in an area density of obscuration. The smoke can not obscure more than nine square inches. The amount of sparks exiting the end of the test apparatus can not exceed 25 sparks for the duration of the test. The latter is of paramount concern for polymeric microfibrous material. When combusted in this type of environment, activated carbon particles appear as sparks upon exit of the test duct. The other test parameters are of less importance because polymeric microfibrous materials would readily pass the test based upon the characteristics of the polymer and particulate chosen. Both the activated carbon and the bicomponent polymer fibers are clean burning and do not produce smoke or propagate flame.

V.2 Particle Size Distribution Effect on Combustion

In order to truly understand ANSI/UL-900 performance, the relationship between PSD and combustion must be defined. PSD is one of many parameters that could be manipulated to pass the ANSI/UL-900 test. PSD is chosen for further study because it is the easiest of the polymeric microfibrous material parameters to be changed. To effectively optimize the PSD, the effect of combustion and the ANSI/UL-900 test must be investigated. This could be done in several different ways, but for this work a classical chemical engineering model will be employed along with a combustion test based upon the ANSI/UL-900 test.

V.2.1 Shrinking Core Model Introduction

The Shrinking Core Model (SCM) is a model traditionally used in chemical reaction engineering. This model was developed by Yagi and Kunii (Levenspiel, 2007). This model relates the consumption of a catalyst from the outer surface into the core during the course of a reaction. In the case of burning activated carbon particles, the reaction is proceeding from the outer surface into the core but the particle is reducing in size. This is a specialized variation of the SCM where the particle is of changing size during the course of the reaction. In this model, the reaction proceeds on the outer reactant material, creates an ash layer through which the gas phase reactant must pass, and then proceed on the deeper reactant material until the solid reactant consumed.

This model divides the reaction into three parts: the diffusion of Reactant A from the bulk fluid to the particle; the diffusion of Reactant A from the surface of the ash layer to the surface of Reactant B; and the resistance of the reaction of A with B. For the case of burning activated carbon, the resistance of the diffusion of Reactant A through the ash layer will be neglected.

This is because the particles are very small and are in the Stokes flow regime. In this regime, the small particle size reduces the Reynolds Number below unity and resulting in more influence from viscous forces rather than inertial forces. Thus, the resistance is a combination of the diffusion of Reactant A to the surface of Reactant B (film control) and the resistance of the reaction of A with B (reaction control). The resistance directly correlates to the time it takes for the reaction to proceed. This time is the important parameter for determining what particle size would be optimum to pass the ANSI/UL-900 test.

V.2.2 Shrinking Core Model: Activated Carbon Particles

The shrinking core model begins with the determination of conversion (Levenspiel, 2007). The reaction to be modeled is the conversion of carbon and oxygen into carbon dioxide (shown in Figure V.1).

Figure V.1: Carbon Combustion Reaction

$$C + O_2 \rightarrow CO_2$$

According to Levenspiel, the SCM (for particles in this range) can be separated into two control mechanisms to describe the combustion reaction. These mechanisms are based upon the controlling resistance in the overall combustion reaction; film diffusion control and reaction control. The reaction control mechanism is shown in Equation V.1 and the film diffusion control mechanism is shown in Equation V.2.

Equation V.1: Converison for Reaction Control Mechanism

$$t/\tau = 1 - (1 - X_B)^{1/3}$$

The control mechanism is a relationship between the elapsed reaction time (t), the time for complete conversion (τ), and conversion of carbon (X_B). The film diffusion control mechanism relates the same variables, but more weight is placed on the conversion of carbon in the reaction as opposed to the reaction control mechanism.

Equation V.2: Conversion for Film Diffusion Control Mechanism

$$t/\tau = 1-(1-X_B)^{2/3}$$

The residence time and conversion are both empirically derived variables, thus the time for complete conversion is theoretically derived from the physical characteristics of the particle undergoing combustion and the reaction parameters. The density of the particle (ρ_b) and initial radius (R_0) are the physical parameters of the particle used to calculate the time for complete conversion. The reaction coefficient for the solid particle (b), reaction rate constant (k´´), and the concentration of the diffusing reactant (C_{Ag}) are the reaction parameters of importance. Equations V.3 and V.4 show the time required for complete conversion for the reaction control and film diffusion control mechanisms.

Equation V.3: Time for Complete Conversion: Reaction Control Mechanism

$$\tau_{reaction} = \frac{\rho_B R_0}{bk'' C_{Ag}}$$

Equation V.4: Time for Complete Conversion: Film Diffusion Mechanism

$$\tau_{film} = \frac{\rho_B R_0^2}{2bC_{Ag}D_e}$$

The relationship between the physical nature of particles undergoing combustion and the time for conversion is directly proportional. The relationship of conversion time and the fluid system parameters (reaction constant, gas concentration, and diffusivity) is inversely proportional. These relationships indicate the smaller and/or more porous the particle, the less time it will take for complete conversion. Conversely, the lower the concentration of reactant A and/or the more resistance to diffusivity exists the longer conversion time based upon a film control mechanism.

Knowing the time required for complete conversion for each control mechanism, the time for complete conversion for the entire reaction is found by the summation of the two times (shown in Equation V.5).

Equation V.5: Total Time for Complete Conversion

$$\tau_{total} = \tau_{film} + \tau_{reaction}$$

Similarly, the total time for incomplete conversion is the addition of the elapsed reaction times for each of the control mechanisms (shown in Equation V.6). This relationship will be important to the combustion of material in the ANSI/UL-900 test. The result of note will be the number of sparks exiting the apparatus. These sparks, along with the loss of mass in the samples test, can be correlated to conversion.

Equation V.6: Total Time for Incomplete Conversion

$$t_{total} = t_{film} + t_{reaction}$$

The next step is to derive the reaction rate constants for both controlling mechanisms. Levenspiel (2007) presents the rate expression for the surface reaction control mechanism

proposed by Parker and Hottel. This reaction rate constant for a reaction control mechanism (shown in Equation V.7) is in the form of a modified Arrhenius equation.

Equation V.7: Reaction Control Rate Constant

$$k_s = 4.32x10^{11} T^{1/2} e^{-184000/RT}$$

This equation relates the reaction rate (k_S) to the product of the reaction temperature (T) and the exponential containing the reaction temperature and Universal Gas Constant (R with units of Joules/mole – °K). In this modified Arrhenius form, the pre-exponential factor is accompanied by the square-root of the reaction temperature. This shows an increased dependence on the reaction temperature with respect to the un-modified Arrhenius equation which only accounts for reaction temperature in the exponential term.

The film diffusion control mechanism reaction rate is derived from the flow characteristics of the particle in a flowing fluid. Levenspiel (2007) gives the reaction rate expression derived by Froessling which relates the reaction rate (k_g) to the dimensionless groups of the Schmidt Number (Sc) and the Reynolds Number (Re). The Schmidt Number is the ratio of momentum and mass diffusion ($\mu / \rho D_e$) and the Reynolds Number is the ratio of inertial and viscous forces ($\rho v d_p / \mu$). The film diffusion reaction rate expression is shown in Equation V.8.

Equation V.8: Film Diffusion Reaction Rate Constant

$$k_g = \left[2 + 0.6 \left(\frac{\mu}{\rho D_e} \right)^{1/3} \left(\frac{d_p v \rho}{\mu} \right)^{1/2} \right] \left(\frac{D_e}{d_p y} \right)$$

This reaction rate expression illustrates the importance of the fluid flow characteristics on the reaction rate through the inclusion of both the Reynolds and Schmidt Numbers. The film diffusion control reaction rate constant for small, porous particles would be much less than the surface reaction control rate constant. The large pre-exponential factor and high reaction temperature result in a large surface reaction controlled rate constant. The small, porous particles and low viscosity of the air at the elevated reaction temperature result in a lower film diffusion control rate constant (i.e. lower Reynolds and Schmidt Numbers). With the two separate reaction rates, the overall rate constant at any time during the reaction can be found from Equation V.9.

Equation V.9: Instantaneous Reaction Rate Constant

$$1/k'' = 1/k_s + 1/k_g$$

All of the parameters for calculating the reaction rate constants are system dependent (empirical), except the effective diffusivity (theoretical).

The effective diffusivity is found by separating the path of diffusion into two resistances: the diffusion of reactant A (O_2) from the bulk to the surface of reactant B (carbon particle surface), and the diffusion of reactant A into the pores of reactant B. The diffusion of reactant A from the bulk flow to the surface of reactant B can be described by many molecular interaction models. For this case, Fuller's Equation of Diffusion (Equation V.10) was selected as the binary diffusion model because of its accuracy with non-polar gases (Reid et al., 1987). The limiting factor with the Fuller equation is the reduction of accuracy at elevated temperatures.

Equation V.10: Fuller's Equation for Binary Bulk Diffusion

$$D_{AB} = \frac{0.00143T^{1.75}}{PM_{AB}^{1/2}\left(\Sigma_{VA}^{1/3} + \Sigma_{VB}^{1/3}\right)^2}$$

Fuller's equation relates the system temperature and pressure with the molecular mass of the reactants, where M_{AB} is the combined molecular mass of reactants A and B, shown in Equation V.11. Fuller also includes the parameters of diffusion volume. These constants are molecule specific and derived for a specific temperature range.

Equation V.11: Combined Molecular Mass

$$M_{AB} = 2\left(1/M_A + 1/M_B\right)^{-1}$$

Once reactant A has moved from the bulk flow to the boundary layer of solid reactant B, the following resistance is diffusion into the pore structure of reactant B. Diffusion of reactant A from the surface of reactant B into the pores is described by Knudsen diffusion, shown in Figure V.12 (Smith, 1970). This diffusion term can also be separated into diffusion resistances from the macropores and the micropores. This is done through the parameter "a", which is the pore radius.

Equation V.12: Knudsen Diffusion

$$D_k = a\left(9.70x10^3\right)\left(\frac{T}{M_A}\right)^{1/2}$$

Both diffusion resistances (bulk and Knudsen) are combined into the effective diffusivity to determine the overall resistance. The effective diffusivity (shown in Equation V.13) is the relationship between the average macropore and micropore diffusion, along with the porosity of reactant B. Equationss V.14 and V.15 show the average macropore and micropore diffusion expressions.

Equation V.13: Effective Diffusion

$$D_e = \overline{D_M}\varepsilon_M^2 + \frac{\overline{D_\mu}\varepsilon_\mu^2(1+3\varepsilon_M)}{1-\varepsilon_M}$$

Effective diffusivity accounts for the diffusion resistance in both the macropore and micropore structure. The porosity factors (ε_M and ε_μ) are the percentage of the void volume which contains either macropores or micropores. For the case of activated carbon particles, the pore structure is dominated by micropores. Literature shows that similar coconut shell derived carbons contain approximately 50% pore volume with 85% of that pore volume composed of micropores and 2% existing as macropores (Chiang et al., 1998). In this case, the macropore part of the effective diffusivity becomes less influential than the micropore side of the equation. The average macropore diffusion ($\overline{D_M}$) and average micropore diffusion ($\overline{D_\mu}$) are shown in Equations V.14 and V.15, respectively.

Equation V.14: Average Macropore Diffusion

$$1/\overline{D_M} = 1/D_{AB} + 1/D_{KM}$$

Equation V.15: Average Micropore Diffusion

$$1/\overline{D_\mu} = 1/D_{AB} + 1/D_{K\mu}$$

The model as derived is designed for loose, small, porous particles in a flowing system. There have been no modifications to account for any external factors influencing the combustion of the said particles. This model will be used as a baseline and compared with empirical data to determine the accuracy of the prediction on combustion with respect to the combustion test. It is desired to use this prediction to help optimize future versions of polymeric microfibrous material which will achieve the gas life, pressure drop, and combustion results desired.

V.3 Particle Combustion Testing

Combustion testing was performed according to a testing protocol based upon the ANSI/UL-900 standard. Testing was done on a variety of samples with loose activated carbon, impregnated activated carbon, and polymeric microfibrous material.

Figure V.2: Combustion Testing Apparatus

V.3.1 Combustion Testing Apparatus Background

The combustion testing protocol specifically defines a testing apparatus to be used for the certification of HVAC filters. This apparatus is designed to provide 4000 BTU per minute to the sample for three minutes. The apparatus is also designed to supply an ignition source in front of the test filter with eight feet of duct beyond the end of the test filter. The specifics of the test apparatus are important to the outcome of the combustion test and to the parameters of PSD modeling. The ignition source is eighteen inches in front of the leading filter face. The test filter is held in a section which can expand to hold several different filter depths. The particular

apparatus used is able to hold filters of twenty inches wide by twenty inches high. The ignition source is two flames produced from an unmixed natural gas flow with a flow rate low enough to produce a combined 4000 BTU per minute. The apparatus also includes a specific flow rate of air during testing. The testing protocol dictates a flow rate of 220 feet per minute measured at the exit of the test duct.

Figure V.3: Combustion Testing Apparatus with Sheet and Loose Particle Testing Peripherals

The apparatus flow rate is important because it dictates the characteristics of the burn pattern on the sample. As stated, the flow rate must be measured at the exit of the duct with the

sample in place. This measurement accounts for various filter types and the resultant pressure drop from the different filter types. As higher pressure drop materials are placed in the apparatus for testing, the burn patterns on the filters are more compact. This is a result of the increased flow rate at the points of ignition due to the reduced pressure drop through the combustion points as opposed to the filter material. The implications for small samples, or even particles, mean that placement is important as well as repeatability of placement.

Figure V.4: Combustion Testing Apparatus: Sheet Sample Setup

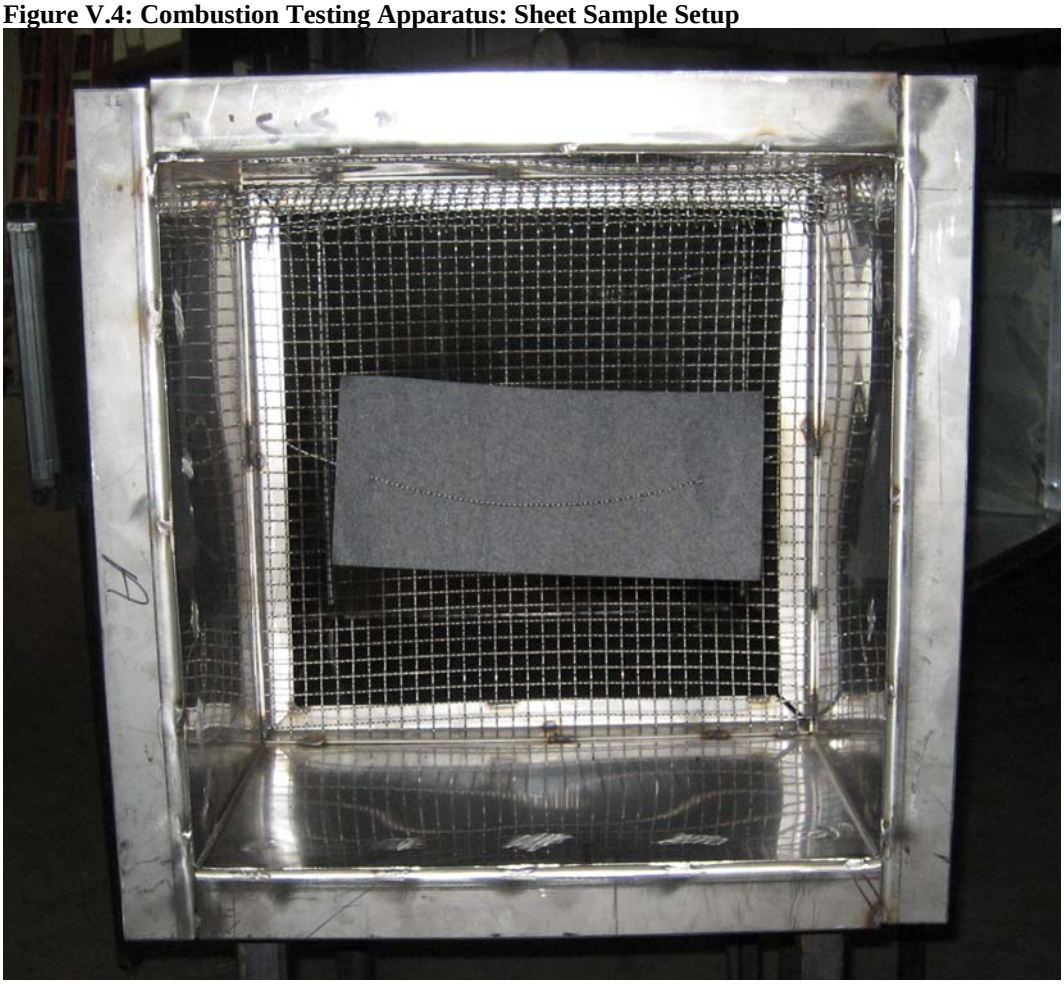

V.3.2 Combustion Apparatus and Experimental Methods

The combustion apparatus was modified to accept one square foot test samples of polymeric microfibrous material and air injected loose particle samples. For the sheet samples, a large mesh metal screen (316 Stainless Steel 2x2 mesh size) was added to anchor the sample in place. For the loose particle testing, a Venturi pump was used to inject the particles into the apparatus at the same point as the sheet tests. Baring these modifications, the apparatus was as similar to the specified test as possible. With an average face velocity of 220 feet per minute, the residence time of a particle from point of introduction to the exit of the duct is 2.18 seconds. The face velocity is an average of the face velocity measured in nine areas of the duct exit. During the measuring of the velocity, it was noted that the apparatus had an uneven distribution of flow. Flow was measured highest in the middle third of both the length and width. The exception to this phenomenon is the bottom third exhibiting higher flow rates than the top third. Flow distribution devices were placed in front of the air fan to help even the flow across the duct, but it did not completely even out the flow distribution.

One limiting factor of the sample mechanisms was residual sample deposited in the combustion section (section before the sample holder section) of the apparatus. As the Venturi pump introduced sample into the combustion chamber, the required flow rate to pump the carbon overcame the duct flow rate with a portion of the sample and deposited loose carbon in the combustion section. For flat sheet samples, the supporting screen also contained residual sample due to the ignition source combusting a portion of the sample and then being redirected away to an area of less resistance.

It was desired to test loose activated carbon particles in several particle size ranges and compare their combustion rates with that of polymeric microfibrous entrapped activated carbon

in the same ranges. The control sample is composed of neat activated carbon from Pica USA sieved between a 50 and 60 ASTM-E11 mesh sieves. Loose particle samples range from 40 to 50 mesh, 60 to 80 mesh, 80 to 100 mesh, and less than 100 mesh. The size ranges were further analyzed using a particle size analyzer (Malvern Mastersizer 2000) to determine the particle size distribution for each size range. The PSD curves in Figure V.5 were generated from the particle size analyzer data. The plot shows significant overlap between the mesh size ranges indicating mechanical separation (sieve separation) is not an accurate way to separate activated carbon particles in this range.

Figure V.5: Particle Size Distribution Curves for Each Mesh Size Range

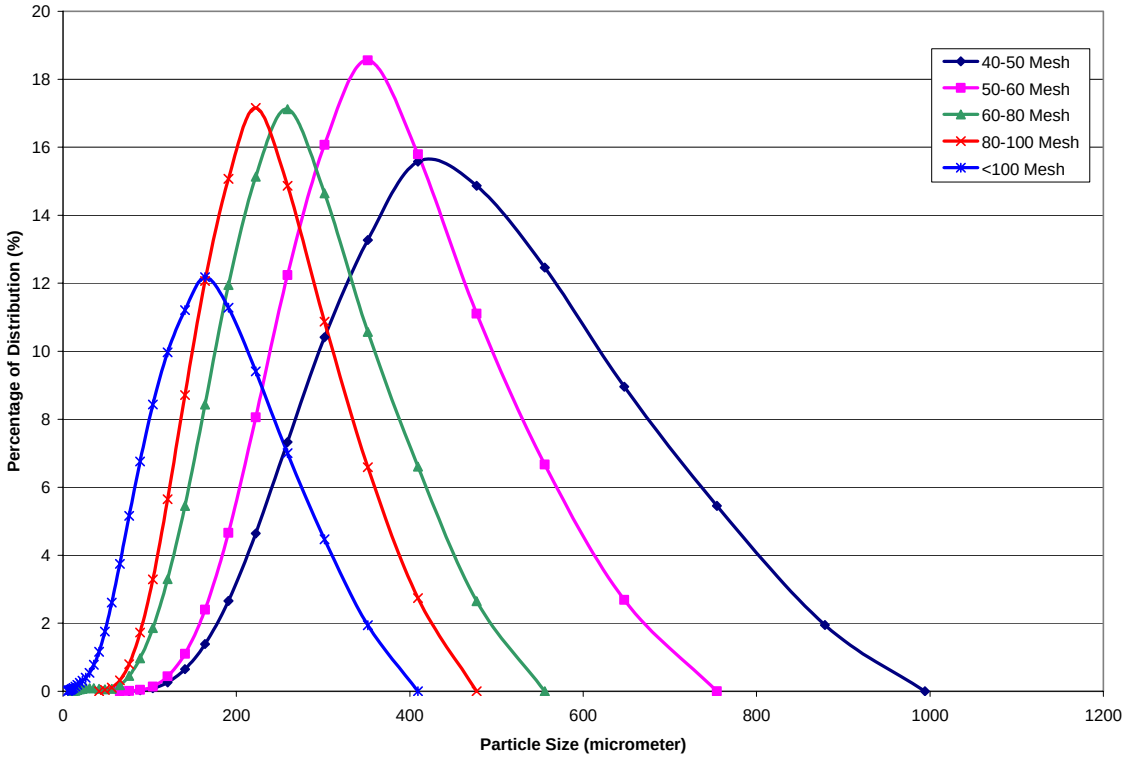

A portion of the sieved 300 – 250 micrometers (50 to 60 mesh size) activated carbon was taken and impregnated with Cruwik SYN, SuperFloc 4512, and water. A 1% aqueous solution (by weight) of Cruwik SYN and SuperFloc 4512 were mixed and 200 grams of 50 to 60 mesh activated carbon (per solution) was allowed to soak for 48 hours. Process water was used to create the 1% solutions and was also used to soak into the carbon for 48 hours to obtain samples with excess water in the pore structure. The amount of Cruwik SYN and SuperFloc 4512 impregnation was not determined, but the amount of excess water in the activated carbon was 40% (by weight).

Square foot sheets of polymeric microfibrous material were made using 300 – 250 micrometers (50 to 60 mesh size), 250 – 175 micrometers (60 to 80 mesh size), 175 – 150 micrometers (80 to 100 mesh size), less than 150 micrometers (100 mesh size). These sheets were made using an automated MK Systems square foot sheet mold. The samples are composed of approximately 23% (by weight) of polymer fiber (3 denier Invista T-105) and 77% (by weight) of activated carbon in each mesh size range. The sheets were made using only process water and no wet end additives to help formation. For this reason, sheets containing activated carbon in the 40 to 50 mesh range were not made. Without the additional formation aids, the 40 to 50 mesh sheets did not form correctly or exhibit any green strength. The lack of wet-end additives is also apparent in the formation and retention of each sheet made. Table V.1 shows the average retention for each particle mesh size range used to form sheets.

Table V.1: Average Carbon Retention for PMM Sheets

Activated Carbon Size (ASTM-E11 Mesh Number)	Average Carbon Retention (%)	Standard Deviation (± %)
50-60	70.10%	4.25%
60-80	60.73%	2.25%
80-100	49.58%	4.02%
<100	38.75%	4.07%

Table V.1 shows low retentions compared to conventional polymeric microfibrous materials (approximately 90%). The other trend of note is the reduction of retention as the particle size decreases. This is to be expected with the use of 3 denier fibers. Through the use of a larger denier fiber and a reduced amount of fiber, the amount and size of particles retained (without the use of wet-end additives) decreases dramatically because of the larger drainage channels formed in the wet laid mat. In terms of pressure drop, it is desired to use larger diameter fiber and use less of that fiber. Thus, the need for wet-end additives is required to ensure formation is optimum.

Testing was modified for each sample set tested. The amount of polymeric microfibrous material sample available for combustion was completely combusted within one minute. The loose particle testing did not have a set amount of time for complete combustion. This was due to manual addition of the carbon into the Venturi pump. Each sample set required a total mass of 200 grams divided into ten separate tests. It was desired to see the effect of addition rate on the combustion results. The rate of carbon addition was varied from thirty second to two minutes to observe this feed rate effect. Upon completion of the ten tests, the remaining sample left in the duct and beyond the exit of the duct was collected and massed.

V.4 Combustion Results

The results from the shrinking core model and the combustion tests will be compared to evaluate the accuracy of the model, define the effect of the wet lay process, and the effect of polymer bound carbon particles. It is desired to have an accurate model to use for optimization of future versions of polymeric microfibrous materials with respect to PSD of activated carbon.

V.4.1 Empirical Results

The results from loose particle testing are divided into the neat particles and the impregnated particles. The results for the polymeric microfibrous entrapped particles are also presented seperately. The loose, neat carbon particle test results are encapsulated in Table V.2. The results presented are the amount of sample combusted (in percentage and number of particles) and the amount exiting the test duct as visible sparks (in number and percentage of sample combusted).

Table V.2: Combustion Results for Loose, Neat Particles

Particle Size Range	Percent of Sample Combusted	Number of Sparks	Number of Particles Combusted	Percentage of Combusted Particles as Sparks
40-50	10.97%	25487	4494945	0.567%
50-60	17.80%	22583	11109279	0.203%
60-80	27.47%	6054	221243298	0.00274%
80-100	35.02%	534	105268693	0.000507%
<100	53.45%	39	4544489962	0.000000858%

Table V.2 shows several clear trends. As the particle size decreases, the amount of sample combusted increases while the amount of sample exiting the apparatus as sparks decreases. This indicates that the reaction time for loose particles in the smaller particle size range is closer to the

theoretical residence time of the apparatus (2.18 seconds for laminar plug flow) as compared to the particles in the 40 to 50 mesh size range.

The results of the impregnated carbon particles are shown in Table V.3. These samples were 50 to 60 mesh size particle impregnated with two common wet-end additives (used in traditional polymeric microfibrous material manufacturing) and with excess water (designated EW). The two wet-end additives are Cruwik SYN (designated CSYN) and SuperFloc 4512 (designated SF).

Table V.3: Combustion Results for Loose, Impregnated Particles

Particle Size Range	Percent of Sample Combusted	Number of Sparks	Number of Particles Combusted	Percentage of Combusted Particles as Sparks
50-60 CSYN	5.95%	51443	3460728	1.486%
50-60 SF	8.17%	50083	4465556	1.122%
50-60 EW	17.61%	5909	12189626	0.0485%

Table V.3 shows a significant difference in the results when compared to the neat 50 to 60 mesh particle results. For the wet-end additives, there is an order of magnitude decrease in the number of particle combusted. Of these combusted particles, there is a six-fold increase in the percentage of combusted sample exiting the duct as sparks. The sample impregnated with excess water shows an order of magnitude reduction in the number of sparks, but approximately the same amount of sample combusted. This shows that the impregnated samples may produce less combusted material, but that material will have more of a probability of exiting the test duct as sparks.

The polymer bound carbon particle results in Table V.4 show similar trends to those found in the loose, neat particle results in Table V.2. As the particle size is reduced, there is a

reduction in the amount of combusted material exiting the test duct as sparks. The other trend of note is the reduction of sample combusted. This is due to the limitation of the ignition source to completely combust sheets. The loose particle testing allowed the ignition source contact with the sample material. The sheet samples were secured into place and not able to completely combust through the duration of the test.

Table V.4: Combustion Results for Polymeric Microfibrous Entrapped Particles

Particle Size Range	Percent of Sample Combusted	Number of Sparks	Number of Particles Combusted	Percentage of Combusted Particles as Sparks
50-60 PMM	5.36%	3762	2346237	0.160%
60-80 PMM	9.68%	340	47348822	0.000718%
80-100 PMM	10.12%	124	15082539	0.000822%
<100 PMM	8.92%	53	293745537	0.0000180%

From the results presented, a few trends of note are readily apparent. As the PSD range decreases, the percentage of combusted material exiting the test duct decreases while the amount of combusted material increases. The use of wet-end additives decreases the amount of material combusted, but increases the amount of combusted material exiting the test duct as sparks. Entrapment of particles in polymeric microfibrous material decreases the amount of material combusted, but only because of the setup used in this apparatus (inability of the ignition source to combust the entire sheet). Baring this limitation, the trends are similar to the trends found in the neat, loose particle sample results.

V.4.2 Shrinking Core Model Results

The time required for complete conversion of the various particle size ranges is the baseline for the SCM as developed. This reaction time should mirror the resultant times from the

combustion testing of the loose, neat particles. The complete conversion time from the theoretical model are shown in Figure V.6.

Figure V.6: Time for Complete Conversion from the Shrinking Core Model

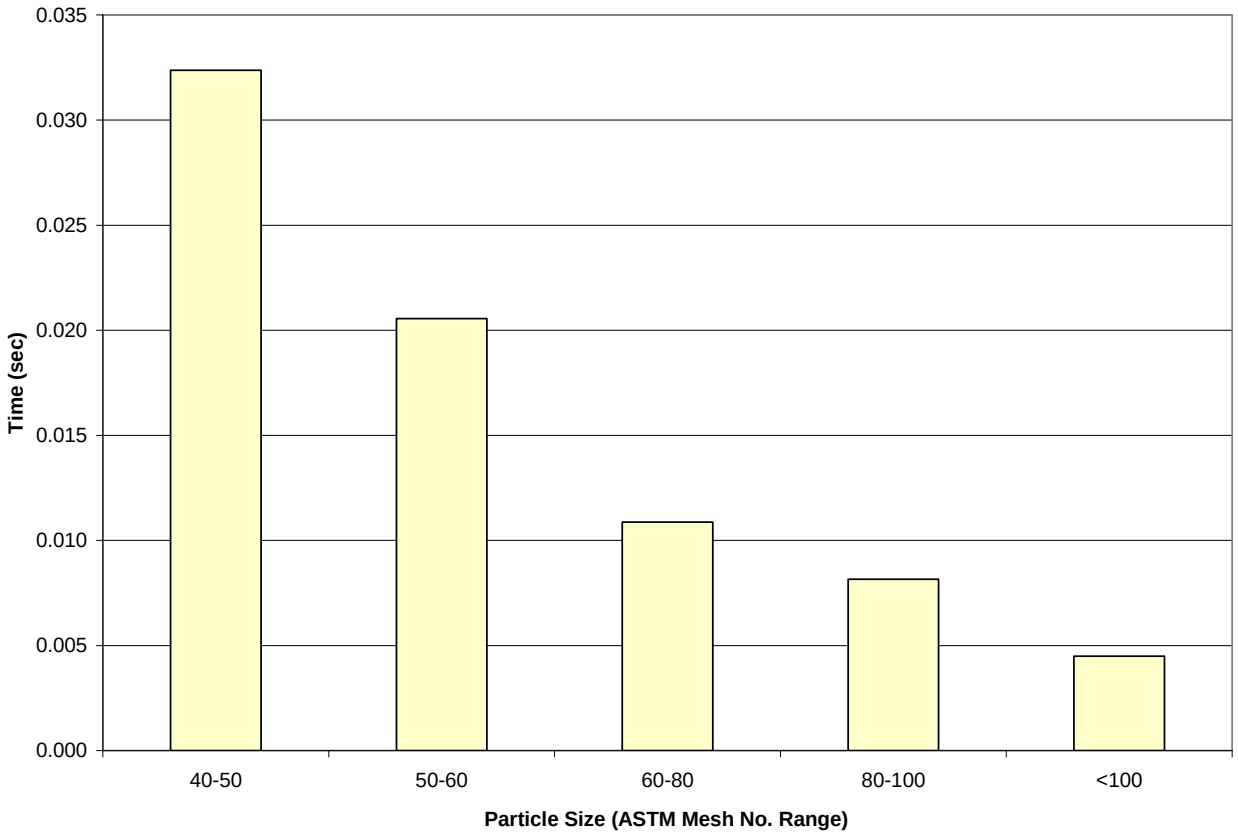

The time for complete conversion shown in Figure V.6 does mirror the results from the loose, neat particle combustion testing. Unfortunately, the results are not accurate when compared to the empirical data. The theoretical plug flow residence time for the apparatus is 2.18 seconds. According to the SCM, all of the particle size ranges should be fully combusted within 0.035 seconds. This means that none of the combusted samples should have exited the duct, much less exited as sparks. The SCM can also be used to determine reaction time elapsed from conversion data. Assuming that the amount of sample combusted is the only part of the sample that will

combust and the number of sparks exiting the test apparatus is the amount of unconverted sample, the resulting conversion is used in the SCM (Equations V.1 and V.2) to determine the elapsed reaction time. The results from the neat, loose particle and polymeric microfibrous material testing are shown in Figure V.7 (there were no samples of polymeric microfibrous material with 420 to 300 micrometer carbon tested).

Figure V.7: Incomplete Conversion Reaction Time Results for Neat Particles and PMM

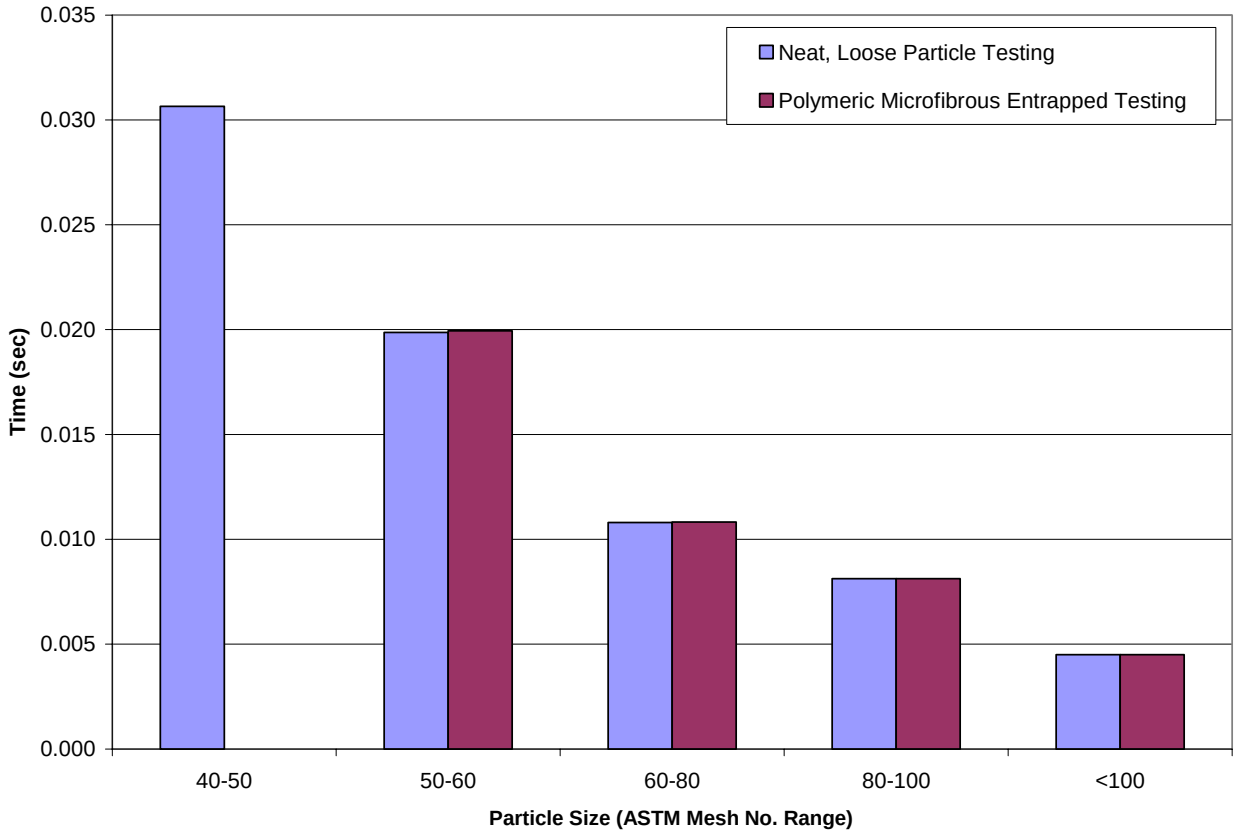

Figure V.7 shows lower reaction times when compared to the residence time of the test apparatus. The results mirror the SCM closely, but are significantly lower in the higher PSD size ranges and negligibly different in the lower PSD size ranges. The polymeric microfibrous material also exhibits this phenomenon.

The empirical data from the impregnated, loose particle testing is also used to determine the effect on conversion. These results are shown in Figure V.8 where CSYN is the sample impregnated with Cruwik SYN, SF is the sample impregnated with SuperFloc 4512, and EW is the sample containing excess water.

Figure V.8: Incomplete Conversion Reaction Time Results for Impregnated Particles

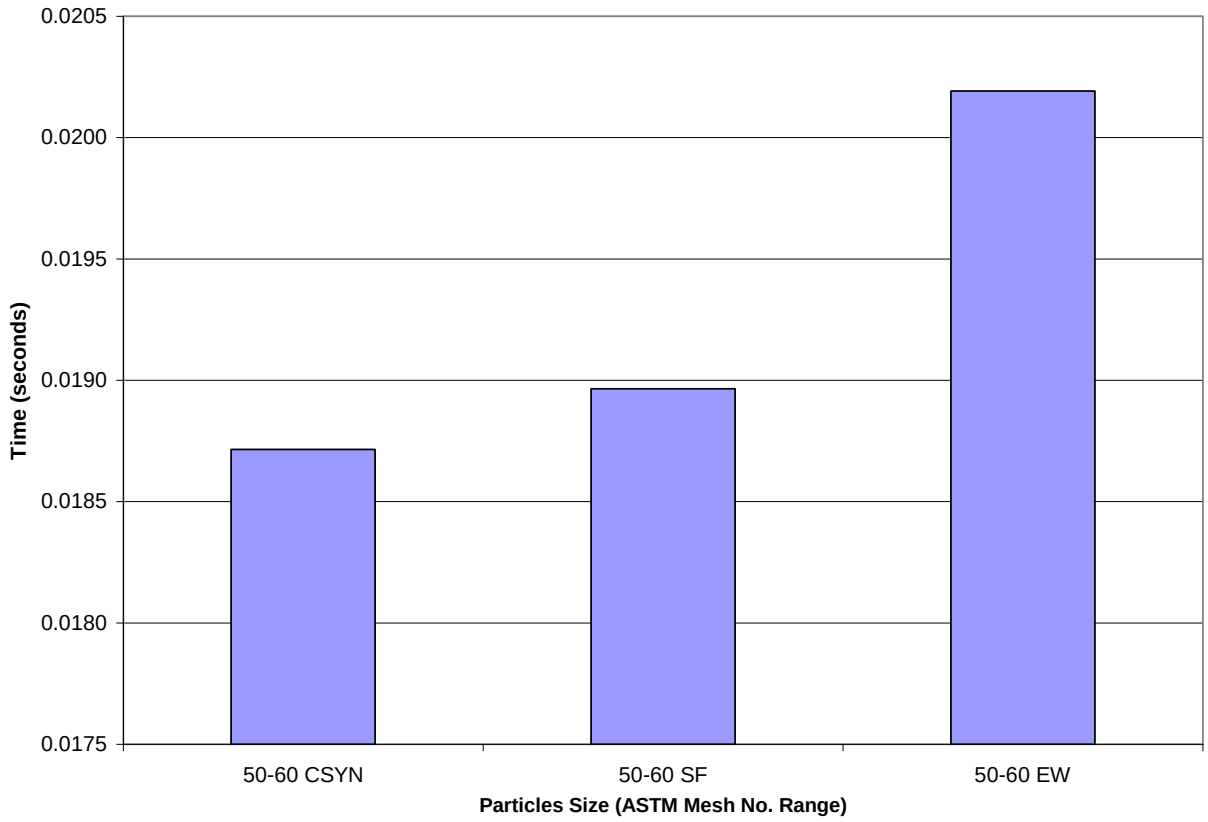

Figure V.8 mirrors the empirical results for the loose, impregnated particle rather closely. This perspective clearly shows how the wet-end additives hinder conversion when compared to the sample containing excess water. The impregnated samples exhibit one order of magnitude lower reaction time when compared to the control sample (300 to 250 micrometer, neat particles) indicating any impregnation of the activated carbon will reduce the conversion.

V.4.3 Discussion

Comparison of the model results and the empirical results show that there is a difference in what is predicted by the model and what was observed. It is known that the residence time of a particle in the test duct is 2.18 seconds. From the SCM, the time required for complete conversion of the largest particle is less than 0.035 seconds. This would dictate that no particles should exit the duct as sparks. There are two possible explanations for this discrepancy in reaction times: late ignition point and non-ideality. The system described in the SCM is an ideal system in which the particle is spherical and the pore structure is clear of all molecules. The bulk system is only a binary system of oxygen and carbon particles and the reaction is ignited by ambient energy (increased temperature). In the actual system, the particles are not spherical but rather irregular hexahedrons as shown in Figure V.9 (activated carbon entrapped in polymeric microfibrous material). The particles are not bone dry due to the capacity of activated carbon to readily absorb water from the atmosphere. The testing laboratory was naturally ventilated and the relative humidity of the environment was relatively high given the typical climate in South Alabama during July. The other source of non-ideality is the ignition source. The flame was fueled from an unmixed natural gas line; which produced carbon dioxide and carbon monoxide. Activated carbon has capacity to absorb both carbon monoxide and carbon dioxide and any other combustion products resultant from impurities in natural gas.

Figure V.9: Activated Carbon Entrapped in PMM (500x Magnification: Reference Line is 20 micrometers)

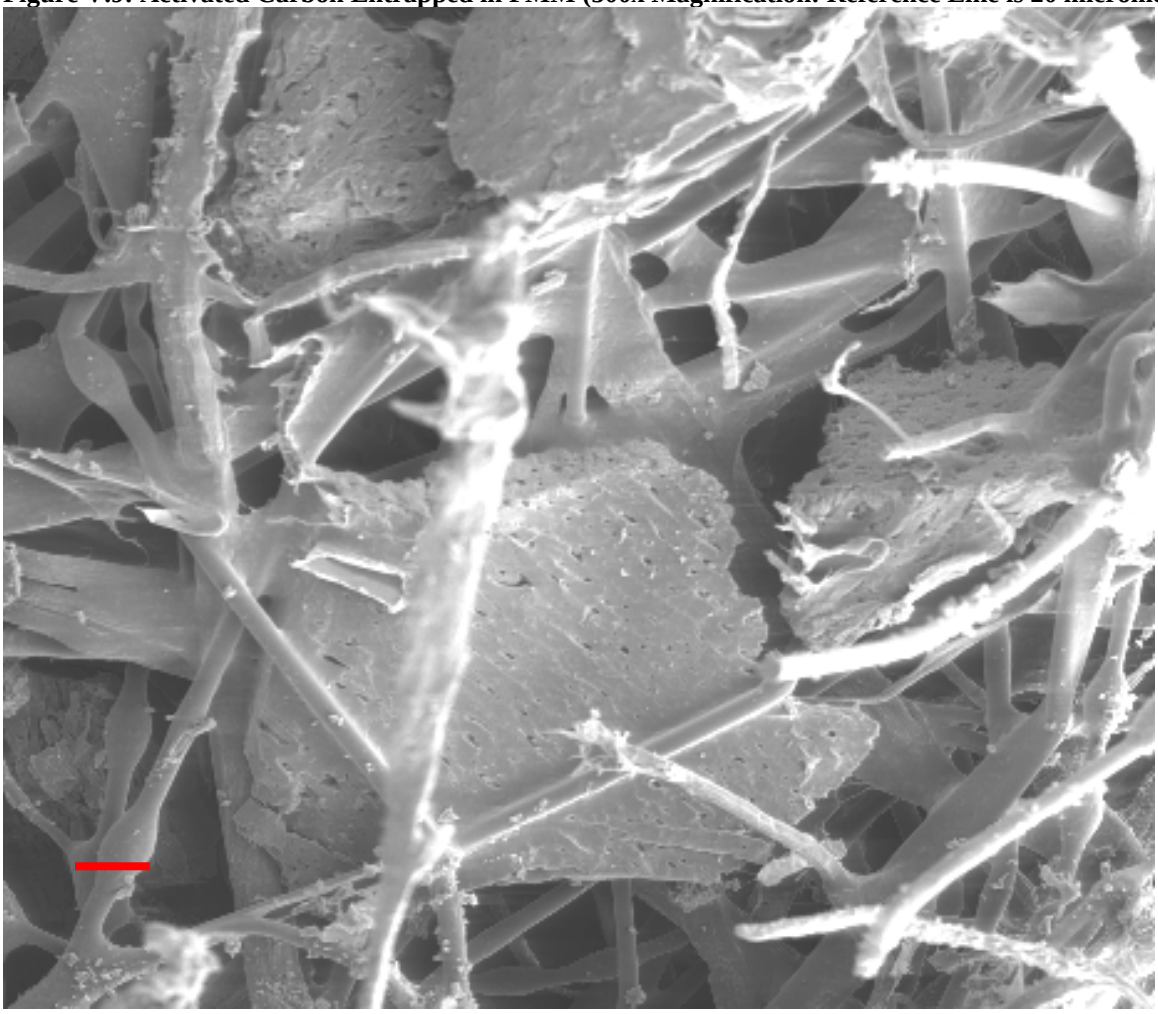

A later ignition point is the other contribution to the reaction time discrepancy between the SCM and empirical data. Although the samples were introduced into the apparatus eight feet from the exit of the test duct, the ignition source extended beyond that point. This extension length was not measurable in the apparatus at the time of experiment. The SCM also assumes that once the particle is introduced into the system, reaction proceeds until completion. For the system used in this study, it is believed that there is a time lag between the introduction of the particle and when the reaction begins. This time lag is enhanced from the system non-ideality as

well as the time required to reach the area of the ignition source yielding enough activation energy to begin the reaction.

From these results, it seems apparent that the optimum particle size would be smaller than 150 micrometers. This PSD yielded the least amount of sparks per amount combusted, as well as yielding the most amount combusted. From a gas life perspective, this particle size would also be advantageous because there is less diffusion resistance for the chemical contaminants to enter the micropore structure. The other area of performance impacted by this PSD is pressure drop. The effect of PSD on pressure drop must be understood before determining if particles less than 150 micrometers are the optimum size for future generations of polymeric microfibrous material.

V.5 Particle Size Distribution Effect on Pressure Drop

Although it has been shown that a smaller particle size is desired to fulfill the requirements for combustion testing, it is not the only parameter to dictate the final PSD. PSD directly affects the pressure drop and gas life of polymeric microfibrous material. As mentioned, the gas life would improve from the use of smaller particles because of less diffusional resistance into the micropore structure of the activated carbon. The effect on pressure drop is important to ensure future generations of polymeric microfibrous material are acceptable for current HVAC systems.

The effect of PSD on pressure drop for polymeric microfibrous material was investigated through several sample sheets. Figure V.10 illustrates the effect of varying particle and fiber weight percent on the pressure drop of polymeric microfibrous material. These samples were made using a TAPPI Standard six inch sheet mold (TAPPI, 2002). The samples were made with

polymer fiber ranging in basis weight from 109 to 164 grams per square meter and activated carbon ranging in basis weight from 330 to 822 grams per square meter. The samples were then processed as normal polymeric microfibrous material.

Figure V.10: PMM Pressure Drop for Various Fiber and Particulate Loadings

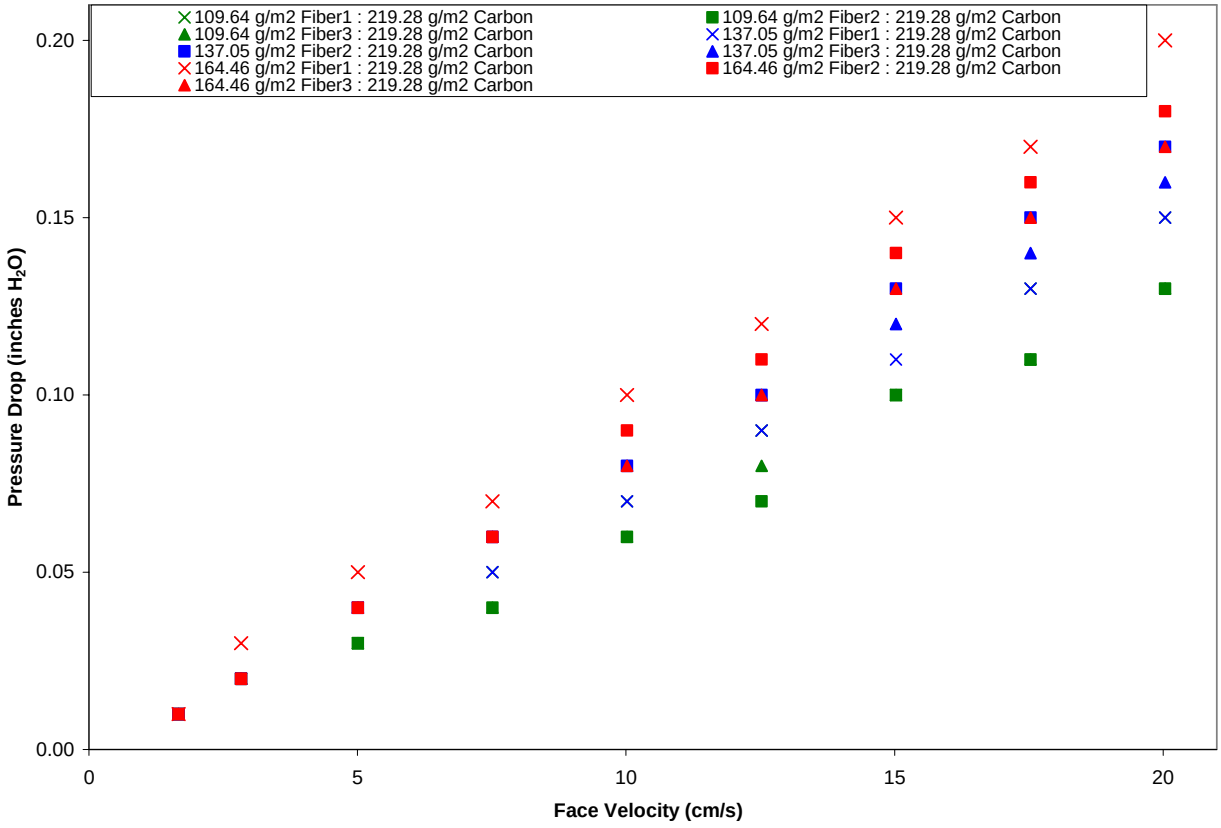

This figure shows that an increase in both particle and fiber loading will increase the pressure drop of the sample significantly. The higher loading of fiber has more impact on pressure drop when compared to the loading of particulate. The particulate does impart more pressure drop contribution at lower fiber loadings.

Another set of experiments were conducted to observe the effect of particulate loading and PSD on pressure drop. Figure V.11 contains the pressure drop results for various sheets of

polymeric microfibrous material. The sheets all contain approximately 200 grams per square meter of polymer fiber and 650 grams per square meter of activated carbon particles. The carbon was separated into four separate PSD ranges: 250 – 175 micrometers (60 to 80 mesh size), 175 – 150 micrometers (80 to 100 mesh size), 150 – 105 micrometers (100 to 140 mesh size), and 250 – 105 micrometers (60 to 140 mesh size). The samples also vary the fiber diameter and mix the fiber diameters available. The samples were compared with a base layer which contained only one fiber diameter at the same basis weight and activated carbon in the size range of 300 – 175 micrometers (50 to 80 mesh size).

Figure V.11: PMM Pressure Drop for Various Particulate Mesh Size Ranges

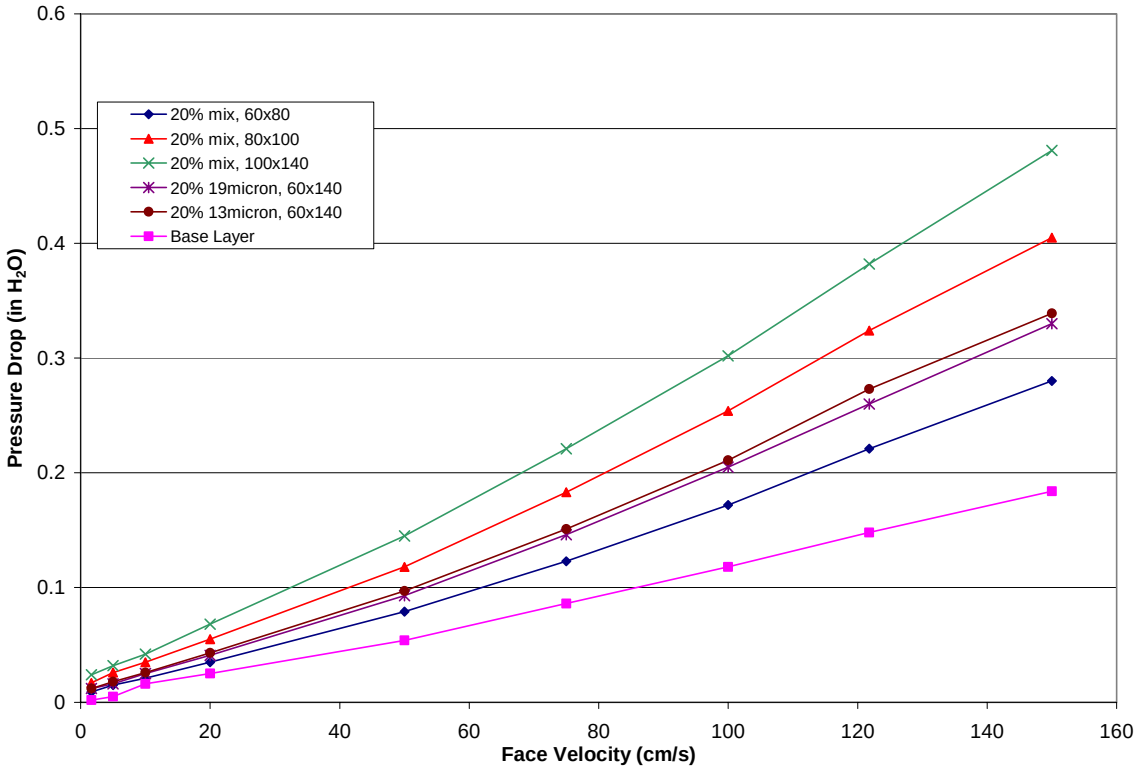

This figure shows that the reduction of particle size increases the resulting pressure drop of polymeric microfibrous material. This is because more retention of smaller particles decreases the permeability of the material. Permeability directly relates to pressure drop performance. Thus, the smaller particle size desired for combustion testing is not desired for pressure drop performance. Both tests are in direct contradiction to one another indicating an optimum particle size would not be immediately possible.

V.6 Summary

Selection of the optimum PSD is essential to the performance of polymeric microfibrous material. PSD directly influences pressure drop, gas life, and combustion testing of the final material. Combustion testing and modeling through the SCM shows a PSD range of less than 150 micrometers would be optimum for performance in the combustion test. Unfortunately, this PSD is too small for optimum pressure drop performance. Pressure drop testing shows that a PSD in the 300 to 250 micrometer range is optimum. Gas life does not immediately show dependence upon the PSD because the size ranges include particles of such a small size that saturation is almost instantaneous. The factor of PSD that does impact gas life is retention. Retention for smaller PSD ranges is decreased dramatically as compared to the larger size ranges. Wet-end additives can increase retention for all PSD ranges, but their use will directly impact combustion testing results.

The balance between pressure drop, gas life and combustion test performance can not be found only through PSD. The optimum will be found in the modification of particulate loading, fiber loading and diameter, and PSD. More works needs to be done to accurately determine the contribution of pressure drop of the individual components (fiber, particulate, and wet-end

additives). Once the pressure drop contribution is determined, the combustion effect of these components must also be determined. With these two effects defined, the gas life can then be considered (if possible) for the optimization of the final polymeric microfibrous material.

The SCM is a good base model to use when optimizing particle size distribution. It can provide an early screening tool during sorbent selection and particle size distribution determination. In the current state, the model lacks enough resolution and refinement to accurately model the system of particulates entrapped in polymeric microfibrous material. The first part of model refinement is in the data collection. The combustion testing protocol should have more reproducible and accurate analytical test methods. This includes accurately measuring particles before, during, and after combustion. The second area of refinement is found in the model and the assumptions taken. The non-ideality of the system must be taken into account to obtain suitable results from the SCM. The first part of this is in changing the assumptions to move the system from ideality to non-ideality (accounting for turbulent flow patterns and not laminar flow patterns). With these changes, the SCM can be a useful and accurate tool for sorbent screening and selection.

CONCLUSIONS AND FUTURE WORK

VI.1 IAQ and HVAC Summary

The data presented point to the imminent need for improved IAQ, especially in the residence where most people from adults to infants spend the majority of their day.

The 26% of Americans at an elevated pulmonary risk are the population segment of most concern, when taking into account that an average of 14.41 hours per day is spent indoors (at home or work). Although the time spent in transit (7% of the day) yields the highest instantaneous exposure level to chemical contaminants (mainly internal combustion engine exhaust), indoor air contaminant exposure would yield greater risks due to the time weighted average exposure being much greater. Another factor in the elevated risk from poor IAQ is the myriad of contaminants detected. These contaminants, found in both the residential and industrial settings, range from VOCs (formaldehyde, toluene, α-pinene, and benzene) to PAHs (naphthalene, pyrene, and phenanthrene) to particulate matter and heavy metal compounds. Such contaminants are known, or suspected, carcinogens, cytotoxins, or pulmonary irritants causing corporal reactions from mild coughs to fatal lung failure.

Although awareness and the ability to monitor IAQ are increasing, the drive for regulations is not moving at the same rate. The EPA has set guidelines and regulations for outdoor air with regards to point sources and large contamination contributors.

OSHA and NIOSH have set standards for industrial settings with regards to the most toxic chemicals. There are currently no federal regulations, standards, or guidelines for residential IAQ. The number of states calling for improved IAQ or proposing regulations is few with California and Washington at the forefront (CARB, 2005; WSDOH, 1999). Although these state regulations exist, they are not complete and do not cover a wide range of contaminants. The need for new standards and an engineered solution has never been greater due to this increase in contamination and awareness. Chemical contaminants are eluted from many sources including common cleaners, building materials, and furnishings. These contaminant sources show that improvement can not only come from a singular solution, but from the synergistic combination of using several different solutions. These solutions could be an increase in ventilation rates, low VOC building materials, and novel filtration mechanisms. The first step is to have standards and regulations to drive development of these solutions. Finally, the solutions should not only be effective, but also practical and economical for all people to use.

VI.2 Polymeric Microfibrous Material Future Work

The versions of Polymeric Microfibrous Material presented here are the first attempt to develop the next generation HVAC filter medium. More work concerning the optimization of the structure needs to be done in order to provide residents with all of the targets set forth in this dissertation. This includes optimization work with sorbent selection, particle size distribution, and large scale manufacturing.

VI.2.1 Particle Size Distribution Optimization

The difficult balance between pressure drop, capacity, and combustion testing has been identified. As of January, 2009, no regulations or industry standards exist with which to compare the performance of Polymeric Microfibrous Material. Thus, capacity can become a second tier objective with pressure drop and combustion testing remaining first tier objectives.

With this in mind, the optimization of particle size distribution should be done beginning with the observations made in this dissertation. Small particle sizes (less than 100 mesh number) are favorable for combustion testing, where large particle sizes (greater than 50 mesh number) are desired for low pressure drop. The effect of particle size distribution breadth should be studied to determine if a narrow distribution has a favorable performance compared to a broad distribution.

The effect of particle shape should also be investigated. The activated carbon from Pica USA is composed irregular hexahedral shapes. The difference between a more spherical particle and the Pica material would be of interest. According to classical fluid dynamics, the spherical shapes would induce less resistance (drag) and should yield a lower pressure drop.

VI.2.2 Sorbent Selection Optimization

The particle shape leads into work of sorbent selection. The Pica material is derived from coconut husks. The performance of a bituminous coal based activated carbon should also be studied for performance characteristics. Although activated carbon is a universal sorbent, other sorbents or carriers should also be investigated for use in the next generation HVAC filter medium.

The possible sorbents include impregnated version of activated carbon, impregnated inert supports, and combinations of the two. Possible impregnates include potassium permanganate, lithium hydroxide, and sodium bicarbonate. The activity of these compounds must be balanced with their cost and utilization efficiency in the final HVAC filter.

VI.2.3 Large Scale Manufacturing Challenges

To truly appreciate the benefit of a non-woven process such as the wet lay process, a material must be made in large volumes. The typical machine speeds at this scale will drive the overall cost of a product down. It is with this in mind that steps were taken to scale up the manufacture of polymeric microfibrous material from a hand sheet mold onto pilot and large scale machines.

For further development of the HVAC material, a larger and faster machine must be employed to make the material cost effective. A 108 inches wide inclined wire wet-lay line has been identified as the next step in this scale up study. Possible negative aspects of this machine include the number of transfers, line speed, and stock addition system. The dryer section is approximately 80 feet in length with at least three transfers including the wet end transfers. These two factors combined translate into finding a way to impart more green strength into the unbonded material.

Another challenge in large scale manufacturing is the ability of the material to withstand the transfer from one belt to another before bonding. A paper machine applies a tensile force upon the sheet and the sheet is pulled through the process. This is due to the small differences in speed from one belt to another. It is believed that increasing fiber length will allow for more fiber entanglement and yield the necessary green strength to make the transfers into the dryer

section and fully bond upon drying. The drawback to longer fiber length is the negative impact on dispersion. The fibers will provide more entanglement in the un-bonded mat, so will there be more entanglement in the stock tank inhibiting an even dispersion in the tank. These two factors must be balanced when selecting the appropriate fiber length.

The closed water loop of a traditional full scale paper machine is also of importance for the large scale manufacture of polymeric microfibrous material. As the water is recycled through the wet end, the accumulation of wet end additives can cause an imbalance in sheet formation characteristics. For this reason, wet end chemistry is as much an art in balance as it is a science of adding the necessary surface charges to a suspension. This is important because the accumulation of wet end chemicals could disrupt formation and even affect the absorption qualities of the final material. Although the wet end additives are long chain polymers which do not readily occlude active sites on the activated carbon, a large concentration of these additives will begin to align on the surface of the activated carbon and begin to cover active sties reducing capacity.

VI.3 Future HVAC Filter Design

The target for this dissertation was to develop a filtration medium for a two inch deep HVAC filter. Typical residential HVAC filters are only one inch deep. Further works needs to address the tailoring of Polymeric Microfibrous Material to satisfy the requirements for a typical one inch deep residential HVAC filter.

This work also led to the development of a testing protocol to screen potential filtration media. The testing protocol was successful in providing a tool to screen media. It was also successful in providing a way to determine the most important factors in a filtration medium.

The testing protocol will require further refinement, but it currently can provide valuable data in filter medium selection.

VI.3.1 Absorption Capacity Optimization

Along with the optimization of the particle size distribution, the capacity of the final medium must be balanced. Although this is a secondary goal, it is still important for the development of improved IAQ. A high performing medium is essential in catalyzing federal initiatives and regulations to improve IAQ. The capacity of the final material is also important for the improvement of residential IAQ. It is desired to provide chemical contaminant removal for a minimum of 30 days. This goal, although relegated to a second tier, is important.

VI.3.2 Physical Filter Specifications

The amount of material placed into a filter is a balance of performance and cost. For this reason, the optimization of the final HVAC filter should be taken into account and used in the design of Polymeric Microfibrous Material. The number of pleats, the depth of the pleats, the optimum height and width, and the type of support structure are all parameters to be considered for the next generation residential HVAC filter.

VI.4 Conclusions

The connection between poor IAQ and detrimental effect to human health is evident. The time spent indoors has increased to almost 100% of the day. Novel ways of improving IAQ are necessary along with new regulations and standards for IAQ. This work has shown that the improvement of IAQ is possible through simple HVAC filtration solutions.

Through the development of Polymeric Microfibrous Material, the first step has been taken towards the facile improvement of residential IAQ. This novel medium provides efficient sorbent usage and a favorable pressure drop regime. Through the utilization of low cost polymer fibers and wet-lay process, the end cost for a finished HVAC filter will be competitive with current commercial offerings. Through extensive testing including physical characteristic metrics, pressure drop testing, gas life testing, and combustion testing, Polymeric Microfibrous Material has been shown to be the optimum medium available as of January, 2009. This novel medium satisfies the desires of HVAC filter manufacturers by providing a low pressure drop, dark appearance, robust physical characteristics (no shedding of particles), and provides a measurable contaminant capacity.

The material developed did not satisfy all of the requirements set forth at the onset of this work. PMM is a good base technology to develop future generations of HVAC filter material. The first generation of PMM did not perform to the desired 5 ppm of challenge chemical for 13000 minutes. One possible reason for this failure is the standard. The standard was chosen based upon a worst case scenario from the literature. The actual challenge concentration could be on the order of 100 ppb and not 5 ppm. In this case, the current filtration medium would perform better but would require more optimization. To achieve this optimization, more work needs to be done but the base technology is a viable start.

REFERENCES

AAFA (2005), *Indoor Air Quality and Allergies*, Washington D.C, Asthma and Allergy Foundation of America

AARC (2002), *Cystic Fibrosis*, Irving TX, American Association for Respiratory Care

ALA (2005.1), *Asthma & Children Fact Sheet*, New York NY, American Lung Association

ALA (2005.2), *Asthma in Adults Fact Sheet*, New York NY, American Lung Association

ALA (2005.3), *Occupational Lung Disease Fact Sheet*, New York NY, American Lung Association

ALA (2006.1), *American Lung Association - State of the Air: 2006*, New York NY, American Lung Association

ALA (2006.2), *Chronic Obstructive Pulmonary Disease (COPD) Fact Sheet*, New York NY, American Lung Association

ASHRAE (1999) *Method of Testing General Ventilation Air-Cleaning Devices for Removal Efficiency by Particle Size*, Atlanta, GA, American Society of Heating, Refrigerating and Air-Conditioning Engineers (Standard 52.2-1999)

Bartekova, A., Huelman, P. H., Lungu, C. (2005) "The potential exposure of residents to emissions from building materials used in a new composite panel house". In: *Proceedings of AIHce 2005*, Anaheim, American Industrial Hygiene conference and expo.

BEC Technologies, *Gray Matter*, Inc., http://www.bec-tech.com/graymatter.asp, Colorado Springs, CO

Bird, R. B., Stewart, W. E., and Lightfoot E. N. (1960) *Transport Phenomena*, New York, John Wiley & Sons.

Boeglin, M. L., Wessels, D., Henshel, D. (2006) "An investigation of the relationship between air emissions of volatile organic compounds and the incidence of cancer in Indiana counties", *Environ. Res.*, 100, 242-254.

Bohart, G. S., and Adams, E. Q. (1920) "Some Aspects of the Behavior of Charcoal with Respect to Chlorine", *J. Am. Chem. Soc.*, 42, 523.

Bush, R. K., Portnoy, J. M., Saxon, A., Terr, A. I., Wood, R. A. (2006) "The medical effects of mold exposure", *J. Allergy Clin. Immunol.*, 117 (2), 326-333.

Cahela, D. R., and Tatarchuk, B. J. (2001) “Permeability of Sintered Microfibrous Composites for Heterogeneous Catalysis and Other Chemical Processing Opportunities”, *Catalysis Today*, 69, 33.

CARB (2005) *Report to the California Legislature: Indoor Air Pollution in California*, Shimer, D., Phillips, T. J., Jenkins, P. L., Sacramento CA, California Air Resources Board

CFF (2005), *Facts About CF*, Bethesda MD, Cystic Fibrosis Foundation

Chiang, Y., Chiang, P., Chang, E. (1998) “Comprehensive approach to determining the physical properties of granular activated carbons”, *Chemosphere*, 37 (2), 237-247.

Clariant Textile, Leather & Paper Chemicals, http://www.paper.clariant.com/, Charlotte, NC

Crucible Chemical Company, http://www.cruciblechemical.com/, Greenville, SC

CTE (2002), *Transit Factoids*, Washington D.C., Center for Transportation Excellence

Diez, U., Kroeßner, T., Rehwagen, M., Richter, M., Wetzig, H., Schulz, R., Borte, M., Metzner, G., Krumbiegel, P., Herbarth, O. (2000) „“Effects of indoor painting and smoking on airway symptoms in atopy risk children in the first year of life results of the LARS-study”, *Int. J. Hyg. Environ. Health*, 203, 23-28.

D-Mark Inc., *OdorGuard Carbon Pads*, http://www.dmarkinc.com, Chesterfield, MI

ES Fibervisions Inc., http://www.es-fibervisions.com/Default.aspx?AreaID=8, Athens, GA

EPA (1990) *Residential Air Cleaning Devices: A Summary of Available Information (#400/1-90-002)*, Washington D. C., United States Environmental Protection Agency.

EPA (1995), *The Inside Story: A Guide to Indoor Air Quality (#402-K-93-0007)*, Washington D. C., United States Environmental Protection Agency.

Farrow, S. C., Farrow, A. (1999) "Diarrhoea and nitrogen oxides", *Medical Hypotheses*, 53 (3), 224-231.

Fiber Innovation Technology Inc., http://www.fitfibers.com, Johnson City, TN

Garçon, G., Dagher, Z., Zerimech, F., Ledoux, F., Courcot, D., Aboukais, A., Puskaric, E, Shirali, P. (2006) "Dunkerque City air pollution particulate matter-induced cytotoxicity, oxidative stress and inflammation in human epithelial lung cells (L132) in culture", *Toxicol. in Vitro*, 20, 519-528.

Harris, D. K., Cahela, D. R., and Tatarchuk, B. J. (2001) "Wet Layup and Sintering of Metal-Containing Microfibrous Composites for Chemical Processing Opportunities," *Composites Part A: applied science and manufacturing*, 32, 1117.

HCUP (2003), *H-CUP 2003 National Statistics*, Rockville MD, Agency for Healthcare Research and Quality – Healthcare Cost and Utilization Project

Hodgson, A. T., Rudd, A. F., Beal, D., Chandra, S. (2000) "Volatile organic compound concentrations and emission rates in new manufactured and site-built houses", *Indoor Air*, 10 (3), 178-192.

Hodgson, M. J., Frohlinger, J., Permar, E., Tidewell, C., Traven, N. D., Olenchock, S. A., Karpf, M. (1991) "Symptoms and microenvironments measures in nonproblem buildings", *Occup. Med.*, 33 (4), 527-533.

Invista S.à r.l., http://www.invista.com, Wichita, KA

Jenkins, P. L., Phillips, T. J., Mulberg, E. J., Hui, S. P. (1992) "Activity patterns of Californians: Use of and proximity to indoor pollutant sources", *Atmos. Environ.*, 26A (12), 2141-2148.

Jo, W. J., Shon, J. Y. (2009) "The effect of environmental and structural factors on indoor air quality of apartments in Korea", *Build. Environ.*, 44, 1794-1802.

Jo, W. K., Yang, C. H. (2009) "Granular-activated carbon adsorption followed by annular-type photocatalytic system for control of indoor aromatic compounds", *Sep. Purif. Technol.*, 56, 438-442.

Koren, H. S. (1995) “Environmental Health Issues”, *Environ Health Perspectives Supplements*, 103 (S6), 235-242.

Laidler, K. J., Meiser, J. H. (1999) *Physical Chemistry, 2nd Edition*, New York, Houghton Mifflin.

Liccardi, G., Cazzola, M., D’Amato, M., D’Amato, G. (2000) “Pets and cockroaches: two increasing causes of respiratory allergy in indoor environments. Characteristics of airways sensitization and prevention strategies”, *Resp. Med.*, 94, 1109-1118.

Levenspiel, O. (2007) *Chemical Reaction Engineering 3rd Edition*, New York, NY, McGraw Hill

Lewcott Corporation, http://www.lewcott.com/solutions_commercial_filtration.htm, Millbury, MA

Marrion, C.J., Cahela, D. R., Ahn, S., and Tatarchuk, B. J. (1994) “Composite fiber structures for catalysts and electrodes”, *J Power Sources*, 47, 297.

Meffert, M. W. (1998) “Preparation and Characterization of Sintered Metal Microfiber-Based Composite Materials for Heterogeneous Catalyst Applications”, Ph.D. Thesis, Auburn University, AL.

Nazaroff, W. W., Weschler, C. J. (2004) “Cleaning products and air fresheners: exposure to primary and secondary air pollutants“, *Atmos. Environ.*, 38, 2841-2865.

Nilsson, A., Kihlström, E., Lagesson, V., Wessén, B., Szponar, B., Larsson, L., Tagesson, C. (2004) “Microorganisms and volatile organic compounds in airborne dust from damp residences”, *Indoor Air*, 14, 74-82.

NFPA (2006) *Standard for the Installation of Warm Air Heating and Air-Conditioning Systems*, Quincy, MA, National Fire Protection Agency, (Standard 90B)

NUG (2006), *Sustainability Report*, Alexandria VA, New Urbanism Group

Osawa, H., Hayashi, M. (2009) “Status of the indoor air chemical pollution in Japanese houses based on the nationwide field survey from 2000 to 2005”, *Build. Environ.*, 44, 1330-1336.

OSG (2005), *Surgeon General Releases National Health Advisory on Radon*, Washington D.C, U.S. Department of Health & Human Services – Office of the Surgeon General

Pankow, J. F., Luo, W., Bender, D. A., Isabelle, L. M., Hollingsworth, J. S., Chen, C., Asher, W. E., Zogorski, J. S. (2003) “Concentrations and co-occurrence correlations of 88 volatile organic compounds (VOCs) in the ambient air of 13 semi-rural to urban locations in the United States“, *Atmos. Environ.*, 37 (36), 5023-5046.

Partti-Pellinen, K., Marttilla, O., Ahonen, A., Suominen, O., Haahtela, T. (2000) “Penetration of nitrogen oxides and particles from outdoor into indoor air and removal of the pollutants through filtration of incoming air” Indoor Air, 10 126-132 (2000)

Phillips, M., Herrera, J., Krishnan, S., Zain, M., Greenberg, J., Cataneo, R. N. (1999) “Variation in volatile organic compounds in the breath of normal humans” Journal of Chromatography B, 729, 75-88.

Piechocki-Minguy, A., Plaisance, H., Schadkowski, C., Sagnier, I., Saison, J. Y., Galloo, J. C., Guillermo, R. (2006) “A case study of personal exposure to nitrogen dioxide using a new high sensitive diffusive sampler”, *Sci. Total Environ.*, 336 (1), 55-64.

Pouli, A. E., Hatzinikolaou, D. G., Piperi, C., Stavridou, A., Psallidopoulos, M. C., Stavrides, J. C. (2003) “The cytotoxic effect of volatile organic compounds of the gas phase of cigarette smoke on lung epithelial cells”, *Free Radic. Biol. Med.*, 34 (3), 345-355.

PSR (1997), *Asthma and the Role of Air Pollution*, Washington D.C., Physicians for Social Responsibility

Rehwagen, M., Schlink, U., Herbarth, O. (2003) “Seasonal cycle of VOCs in apartments“, *Indoor Air*, 13 (3), 283-291.

Reid, R. C., Prausnitz, J. M., Poling, R. E. (1987) *The Properties of Gases & Liquids 4th Edition*, New York, NY, McGraw Hill.

Riveros-Rosas, H., Pfeifer, G. D., Lynam, D. R., Pedroza, J. L., Julián-Sánchez, A., Canales, O., Garfias, J. (1997) "Personal exposure to elements in Mexico City air", *Sci. Total Environ.*, 198, 79-96.

SABHACC (2008) *Minimum Standards for Installation, Service and Repair of Heating and air Conditioning Systems by Certified Contractors*, Montgomery, AL, State of Alabama Board of Heating & Air Conditioning Contractors (Regulation 440-X-5)

SC (2003), *Transit in the United States Fact Sheet*, San Francisco CA, Sierra Club

Sexton, K., Hayward, S. B. (1987) "Source apportionment of indoor air pollution", *Atmos. Environ.*, 21 (2), 407-418.

Shinohara, N., Kai, Y., Mizukoshi, A., Fujii, M., Kumagai, K., Okuizumi, Y., Jona, M., Yanagisawa, Y. (2009) "On-site passive flux sampler measurement of emission rates of carbonyls and VOCs from multiple indoor sources", *Build. Environ.*, 44, 859-863

Shoemaker, R. C. (2006) "Mold illness after Katrina: The truth you haven't heard", *Filtration News*, 25 (3), 4-16.

Singer, B. C., Revzan, K. L., Hotchi, T., Hodgson, A. T., Brown, N. J. (2004) "Sorption of organic gases in a furnished room", *Atmos. Environ.*, 38, 2483-2494.

Smeets, M. A. M., Dalton, P. H., (2005) "Evaluating the human response to chemicals: odor, irritation and non-sensory factors", *Environ. Toxicol. Phar.*, 19, 581-588.

Smith, J. M. (1970) *Chemical Engineering Kinetics 2nd Edition*, New York, NY, McGraw Hill.

Smook, G. A. (2002) *Handbook for Pulp & Paper Technologists, 3rd Edition*, Vancouver, Angus Wilde Publications Inc.

Staessen, J. A., Nawrot, T., Hond, E. D., Thijs, L., Fagard, R., Hoppenbrouwers, K., Koppen, G., Nelen, V., Schoeters, G., Vanderschueren, D., Hecke, E. V., Verschaeve, L., Vlietinck, R., Roels, H. A. (2001) "Renal function, cytogenetic measurements, and sexual development in adolescents in relation to environmental pollutants: a feasibility study of biomarkers", *The Lancet*, 537, 1660-1669.

Sundell, J. (2004) "On the history of indoor air quality and health", *Indoor Air*, 14 (S7), 51-58.

Tatarchuk, B. J. (1992.1) *Method of optimizing composite preparation for electrical properties: maximum capacitance electrodes*, US Patent No. 5 096 663

Tatarchuk, B. J., Rose, M. F., Krishnagopalan, G. A. (1992.2) *Mixed fiber composite structures*, US Patent No. 5 102 745

Tatarchuk, B. J., Rose, M. F., Krishnagopalan, G. A., Zabasajja, J. N., Kohler, D. A. (1994) *Preparation of mixed fiber composite structures*, US Patent No. 5 304 330

Tatarchuk, B. J., Rose, M. F., Krishnagopalan, G. A., Zabasajja J.N., and Kohler, D. (1992.3) *Mixed fiber composite structures high surface area-high conductivity mixtures*, US Patent No. 5 080 963

TIAA (2005), *U.S. Travel Market Overview – Travel Volumes & Trends*, Washington D.C., Travel Industry Association of America

Tran, N. K., Steinberg, S. M., Johnson, B. J. (2000) "Volatile aromatic hydrocarbons and dicarboxylic acid concentrations in air at an urban site in the Southwestern US", *Atmos. Environ.*, 34, 1845-1852.

UL (2004) *Standard for Air Filter Units*, Camas, WA, Underwriters Laboratory Inc., (Standard UL-900 7th Edition)

USCB (2006), *U.S. and World Population Clocks – October, 2006*, Washington D.C., U.S. Census Bureau

USDOL (2004), *American Time Use Survey – 2004 Results Announced by BLS*, Washington D.C., U.S. Department of Labor – Bureau of Labor Statistics

Van Winkle, M. R., Scheff, P. A. (2001) "Volatile organic compounds, polycyclic aromatic hydrocarbons and elements in the air of ten urban homes", *Indoor Air*, 11, 49-64.

Wieslander, G., Norbäck, D., Björnsson, E., Janson, C., Bowman, G. (1996) "Asthma and the indoor environment: the significance of emission of formaldehyde and volatile organic compounds from newly painted indoor surfaces", *Int. Arch. Occ. Env. Hea*, 69, 115-124.

Wilke, O., Jann, O., Brödner, D. (2004) "VOC- and SVOC-emissions from adhesives, floor coverings and complete floor structures", *Indoor Air*, 14 (Suppl 8), 98-107.

Wong, S. K., Lai, L. W., Ho, D. C., Chau, K. W., Lam, C. L., Ng, C. H. (2009) "Sick Building syndrome and perceived indoor environmental quality: A survey of apartment buildings in Hong Kong", *Habitat Int.*, 33, 463-471.

WSDOH (1999), *Indoor Air Quality Primer*, Olympia WA, Washington State Department of Health – Office of Toxic Substances

Wyon, D. P. (2004) "The effects of indoor air quality on performance and productivity", *Indoor Air*, 14 (S7), 92-101.

Xu, X., Weisel, C. P. (2005) “Human respiratory uptake of chloroform and haloketones during showering”, Journal of Exposure Analysis and Environmental Epidemiology, 15, 6-16.

Yoon, Y. H. and Nelson, J. H. (1984) “Application of Gas Adsorption Kinetics I. A Theoretical Model for Respirator Cartridge Service Life”, *Am. Ind. Hyg. Assoc. J.*, 45 (8), 509.

Appendix A.1: PPE and CPE Filter Development

Controlled Environment Through Drying

The melding of through air drying and the sintering furnace is found in controlled environment through drying. This technique employs through air drying technology with the controlled environment of the sintering furnace. Instead of using the ambient environment for through air drying, nitrogen is supplied to prevent the degradation of the fibers. This provides the efficiency of through air drying with the quality of the sintering furnace. The process for sinter bonding the polymeric sheets is described in the following.

The one detracting facet of through air drying is the use of ambient environment. If fibers such as PET were used, the environment would be ideal for degradation of the fibers. This step is approximately 15 to 45 minutes per sheet; carried out in a furnace/oven with a controlled environment to tailor the composite to the desired application. The environment of drying/binding is important because it will also influence final sheet characteristics. If a mechanically robust sheet is desired, a high house air flow rate through the oven at the highest temperature possible (to still melt the sheath without melting the core) is necessary. If a softer, more compressible sheet is desired, a high inert gas flow rate through the oven at the lowest temperature possible is necessary. It is important to note that the drying/binding process is not

limited to a through-hot-air process. It can be any method that simultaneously dries the sheet and melts the sheath as to create the matrix. An infrared lamp and a heated press are examples of alternative drying/bonding methods. Once the composite has been dried and bound, it is ready for use. Further processing of the polymer composite can also be done at this point. For example, impregnation of chemicals into the pores of the entrapped particulate can now be done to further enhance performance.

Thin Polisher Media

It was requested that a reformulation of the media be developed to achieve a certain thickness of media while still providing a performance enhancement for Personal Protective Equipment (PPE). The standard polisher recipe yields sheets from 3.5 millimeter to 4.5 millimeter in thickness, depending on particulate loading. It was desired to produce a polisher media with a thickness of one millimeter to two millimeter. This media was to be used in two applications in particular: “pancake” filters and a new Joint Services General Purpose Mask (JSGPM). “Pancake” filters are an interchangeable filter and mask unit manufactured very thin with a large surface area. The JSGPM is a prototype mask being developed in conjunction with the Edgewood Chemical Biological Center (ECBC) for use across all branches of the armed services. One of the key features of both of these applications is a very thin bed. For this reason, both applications called for a thin polymer polisher. It was decided that the standard polisher ratio of particulate mass to total fiber mass (4:1) should be fixed to get the most capacity possible, as well as the polymer fiber to cellulose ratio (4:1) to reduce the amount of pressure drop while still having green strength from the cellulose. With these two parameters fixed, that left total sheet basis weight as the only variable. The next step was to vary the total sheet basis

weight from 900 grams per square meter (gsm) to 150 gsm. Having made several sheets along this range, the sheets were visually inspected and graded to yield the best recipe. Any reduction in the basis weight of fiber from the original polisher recipe resulted in a sheet with pin holes. To do five-log filtration, a sheet can not have pin holes or else the contaminant stream will channel through the pin holes and result in an early, if not instantaneous, breakthrough time. This is true for a polishing layer of microfibrous material by itself, but is not so important for the case of a composite bed where a layer of microfibrous material is placed behind a packed bed and acts a polisher to remove the effluent traces of contaminant from the packed bed. In the case of a composite bed, the thin polisher would need to be layered. When layers of a thin polymeric polisher are placed together, the pin holes in each layer do not overlap and the irregularities of each sheet are essentially averaged out by each additional layer. This then helped to fix the recipe for the thin polisher due to the fact that a certain amount of capacity had to be achieved by having several layers instead of just one. This also added flexibility to any future canister designs because each layer that is produced can have different particulates or impregnates for an array of chemical contaminants. The resulting material had an approximate total sheet basis weight of 175 gsm, 20% of the original polisher recipe. Individual component basis weights were approximately 140 gsm of particulate, 28 gsm of polymer fiber, and 7 gsm of cellulose fiber. This final recipe is characterized by a very disperse stock suspension, good formation, high retention (>80%), and green strength. The other modification to the standard polisher recipe made is in the particle size distribution of the particulate. Previously, a size distribution of 105 – 250 micrometer was used because it is a readily available product size used by Intramicron. To further reduce the pressure drop of a layer and to achieve a higher retention, a larger particle size distribution of 150 – 300 micrometer was used in the thin polisher recipe. At

this time, the thin polisher material is under testing and the evaluation of the material will be presented at a later date.

The trial work began by making hand sheets on a one square foot basis. These sheets were a combination of recipes decided upon during testing in the university laboratories and suggestions made by SENW during the trial. The reason for making a wide variety of sheets was due to the lack of equipment at the university. The capabilities include the easy transference of sheets as well as the appropriate bonding equipment. Combining the manufacturing capabilities of SENW and the testing capabilities of Auburn University and Intramicron allowed for an in depth testing of different recipes to achieve a more clear understanding of recipe modifications. Testing was done to evaluate cellulose loading, the difference in fiber diameter, and particulate loading. The parameters of cellulose and particulate loading were reevaluated because of the differences in formation and manufacturing techniques at SENW.

The results agreed with the testing and prediction done at the university; the use of cellulose and smaller diameter fibers was discontinued and the particulate loading remained 4:1 (by weight) compared to polymer fiber. Although the results agreed with the results from the university, the quality of sheet formation made for lower pressure drops than expected. This allowed for an increase in the sheet basis weight. Through this increase in basis weight, the secondary specification of aesthetics became a concern. At the desired face velocity of 121.8 centimeters per second, a material of approximately 150 gsm yielded 0.1 inches of H_2O of pressure drop. With the basis weight variability and lack of fine control of the machine in mind, this was chosen as the target basis weight. The problem with this material was a low particulate to fiber loading (3:1 by weight). Although the material appeared dark in nature and did not shed, it was desired to make the material appear darker. This translated into a higher particulate to

fiber loading of 4:1 (by weight). At this loading level without the addition of smaller diameter fibers, shedding of particulate became a problem.

There were two practical solutions to this problem: addition of more fiber and addition of wet end chemistry. The addition of more polymer fiber would decrease the darkness of the material and would bring the material to the pressure drop limit. The addition of a flocculant immediately became the preferred solution. The flocculant first used was a 1% cationic charged flocculant from Buckman Laboratories (5901) was used only to add a charge to the fiber and carbon particles. 100 milliliters of Buckman 5901 was added to a 450 gallon stock tank (less than 0.01% by volume). The addition of the flocculant helped to improve the formation, which was already improved from trial sheets made in the laboratory. The formation was improved by the equipment available as well as the addition of Milease-T as a fiber dispersant (30 milliliters of a 30% solution to 450 gallons). Through the addition of these two additives to the stock suspension, the formation and uniformity of the material on the SENW equipment was far superior to that made using the university equipment. The shedding of carbon particles was dramatically decreased using the flocculant, but it was not eliminated. The material produced met the pressure drop specifications for the one inch deep pleat filter. With this task accomplished, the filter manufacturer wanted to focus more attention on the two inch deep pleat filter. Although the material produced satisfied both specifications, the material was desired to be thicker and darker. Also, the machine was only running at 10 – 15 feet per minute; a speed much slower than desired.

Having a series of data points at various basis weights from the trials at SENW, a new prediction was made to determine the basis weight needed to satisfy the two inch deep pleat filter specifications (0.2 inches of H_2O at 74.8 centimeters per second). The approach taken in

determination of a material for the one inch deep pleat filter was mirrored using the data acquired and a basis weight of 250 gsm was determined to be the appropriate basis weight. At this time, it was desired to make the material on a larger basis and at a faster belt speed.

The scale up was straight forward in the matter of recipe development. The scale up problems came in bringing the machine online. At this point in time, the 63 inch machine had only been used to run ultra light basis weight material (10 – 50 gsm). This meant that the approximately 1000 gallon stock tanks, Air Operated Diaphragm (AOD) pumps, and white water recycle stream were either unused or untested under production conditions. The other change in the machine from the original setup was in the machine clothing. The belt had been changed from the original belt that clothed the machine due to failures from stress caused by rapid heating and cooling cycles. The new belt was a woven (simple weave) Teflon coated glass fiber fabric that is approximately 30 – 40% open. The belt was poorly seamed which caused any material produced to come in approximately 100 feet sections. The seam was a solid seam that did not allow for any drainage and caused in-continuities in the material.

The next problem to surface was in the white water recycle stream. The stream was pieced together from drainage grade PVC pipe. The entire system was constructed to be rigid with no dynamic points to flex or absorb shock. This became apparent on start up and shut down when the fan pump would surge and the entire line would move approximately a foot in either direction from center. This drastic movement caused a failure in a flange fitting near the head box and rupturing the flange and a few feet of the pipe. This problem was not immediately addressed and was replaced with the same type of materials and design. Future design options were provided to include a section of flexible hosing which would absorb the shock of the fan

pump start-up and to control the fan pump with a variable speed drive to ramp the pump up and down for start up and shut down.

The final problem is the overall set up of the machine. The head box is deckled incorrectly and stock is entrained under the deckle boards to the point that the entrained stock causes tears in the belt. The belt is approximately 100 ft in length and is driven by only one roller located at the exit of the heater section. The belt has approximately 90º of wrap on the drive roller and is in a section where the belt is undergoing rapid heating and cooling and hence expansion and contraction. Due to the small amount of wrap and the location of the drive roller, the belt slips frequently also causing in-continuities in the product.

Appendix A.2 Shrinking Core Model Generated Data

Input Variables

Variable	Value	Units	Symbol
Ambient Temperature	1175	Kelvin	Ta
ACP Surface Temperature	1723	Kelvin	Ts
Pressure	1.013	Bar	P
Macro Pore Radius	0.0000025	cm	a_M
Micro Pore Radius	0.0000001	cm	a_μ
Macro Pore Porosity	0.01	---	ε_M
Micro Pore Porosity	0.425	---	ε_μ
Molecular Weight of Air	28.97	g/mol	M_A
Molecular Weight of O_2	32	g/mol	$M_{A,B}$
Molecular Weight of ACP	12.01	g/mol	M_B
Diffusion Volume of Air	19.7	---	Σ_{VA}
Diffusion Volume of O_2	16.3	---	$\Sigma_{VA,B}$
Diffusion Volume of C	15.9	---	Σ_{VB}
Universal Gas Constant	8.314472	J/mol-K	R
Density of Carbon	0.5	g/cm^3	ρ_B
Concentration of O_2 in Air	6.95E-05	gmol/cm3	C_{Ag}
Universal Gas Constant	0.082057	L-atm/mol-K	R
Molar Volume of Air	0.0103716	mol/L	n/V
Mole Fraction of O_2	0.2095		X_B
Viscosity of O_2	5.239E-05	Pa-s	μ
Density of Air	0.0030034	kg/m^3	ρ_a
Velocity of Air	1.11252	m/s	v

Knudsen Diffusion

$$D_k = (9.70 \times 10^3)\, a\, (T/M_A)^{1/2}$$

Based upon O_2 and Ambient Temperature

Micro Pore Knudsen Diffusivity		
$D_{k\mu}$ =	0.005878	cm^2/s

Macro Pore Knudsen Diffusivity		
D_{kM} =	0.146945	cm^2/s

Fuller's Equation for Binary Bulk Diffusivity

$$D_{AB} = (0.00143\ T^{1.75}) / (P\ M_{AB}^{1/2} (\Sigma_{VA}^{1/3} + \Sigma_{VB}^{1/3})^2)$$

$$M_{AB} = 2\ (1/M_A + 1/M_B)^{-1}$$

M_{AB} for Air and O_2		
M_{AB} =	30.40971	g/mole

Diffusivity for Air and O_2 based on Ambient Temperature		
D_{AB} =	2.201621	cm^2/s

Effective Diffusivity

$$D_e = \underline{D_M}\ \varepsilon_M^2 + \underline{D_\mu}\ \varepsilon_\mu^2\ (1 + 3\varepsilon_M) / (1 - \varepsilon_M)$$

$$\underline{D_M}^{-1} = D_{AB}^{-1} + D_{KM}^{-1} \qquad \underline{D_\mu}^{-1} = D_{AB}^{-1} + D_{K\mu}^{-1}$$

$\underline{D_M}$ =	0.1377512		
		D_e =	0.0011154
$\underline{D_\mu}^{-1}$ =	0.0058622		

D_{AB} =	2.2016208

Particle Size Distributions

Mesh Size	Particle Size (micron)	Percentage in Size
40-50 Mesh	878.67	1.95%
	754.23	5.45%
	647.41	8.96%
	555.71	12.46%
	477.01	14.87%
	409.45	15.58%
	351.46	13.27%
	301.68	10.41%
	258.95	7.33%
	222.28	4.64%
	190.8	2.66%
	163.77	1.39%
	140.58	0.65%
	120.67	0.26%
	103.58	0.09%
	88.91	0.03%
50-60 Mesh	647.41	2.69%
	555.71	6.67%
	477.01	11.11%
	409.45	15.79%
	351.46	18.56%
	301.68	16.07%
	258.95	12.24%
	222.28	8.06%
	190.8	4.66%
	163.77	2.40%
	140.58	1.10%
	120.67	0.44%
	103.58	0.14%
	88.91	0.04%
	76.32	0.01%

Mesh Size	Particle Size (micron)	Percentage in Size
60-80 Mesh	477.01	2.65%
	409.45	6.61%
	351.46	10.57%
	301.68	14.65%
	258.95	17.12%
	222.28	15.14%
	190.8	11.95%
	163.77	8.43%
	140.58	5.45%
	120.67	3.30%
	103.58	1.86%
	88.91	0.97%
	76.32	0.45%
	65.51	0.18%
	56.23	0.07%
	48.27	0.06%
	41.43	0.07%
	35.56	0.09%
	30.53	0.09%
	26.2	0.09%
	22.49	0.07%
	19.31	0.06%
	16.57	0.04%
	14.22	0.02%
	12.21	0.01%
80-100 Mesh	409.45	2.74%
	351.46	6.59%
	301.68	10.87%
	258.95	14.87%
	222.28	17.16%
	190.8	15.07%
	163.77	12.07%
	140.58	8.71%
	120.67	5.65%
	103.58	3.29%
	88.91	1.73%
	76.32	0.80%
	65.51	0.32%
	56.23	0.11%
	48.27	0.04%

Mesh Size	Particle Size (micron)	Percentage in Size
<100 Mesh	351.46	1.94%
	301.68	4.47%
	258.95	7%
	222.28	9.41%
	190.8	11.28%
	163.77	12.18%
	140.58	11.21%
	120.67	9.97%
	103.58	8.43%
	88.91	6.76%
	76.32	5.16%
	65.51	3.75%
	56.23	2.61%
	48.27	1.76%
	41.43	1.16%
	35.56	0.78%
	30.53	0.54%
	26.2	0.40%
	22.49	0.31%
	19.31	0.25%
	16.57	0.19%
	14.22	0.14%
	12.21	0.10%
	10.48	0.07%
	9	0.05%
	7.72	0.03%
	6.63	0.03%

Reaction Rate Constants

$k_s = (4.32 \times 10^{11})\, T^{1/2}\, e^{-184000/RT}$ $\quad k_g = [\, 2 + 0.6\, (\mu / \rho\, D_e)^{1/3}\, (d_p\, v\, \rho / \mu)^{1/2}\,]\, (\, D_e / d_p\, y\,)$

$$\underline{k''}^{-1} = k_s^{-1} + k_g^{-1}$$

Surface Reaction Rate based on ACP Surface Temperature

$k_s =$ 47378273 cm/s

Size Cut	40-50	50-60	60-80	80-100	<100
Gas Phase Reaction Rate (Ambient Temperature)					
$k_g =$	687.83	847.29	1049.50	1170.52	1307.36 cm/s
	762.89	942.34	1170.52	1307.36	1462.33
	847.29	1049.50	1307.36	1462.33	1638.05
	942.34	1170.52	1462.33	1638.05	1837.52
	1049.50	1307.36	1638.05	1837.52	2064.30
	1170.52	1462.33	1837.52	2064.30	2322.53
	1307.36	1638.05	2064.30	2322.53	2616.67
	1462.33	1837.52	2322.53	2616.67	2952.35
	1638.05	2064.30	2616.67	2952.35	3335.79
	1837.52	2322.53	2952.35	3335.79	3774.28
	2064.30	2616.67	3335.79	3774.28	4276.13
	2322.53	2952.35	3774.28	4276.13	4851.37
	2616.67	3335.79	4276.13	4851.37	5511.26
	2952.35	3774.28	4851.37	5511.26	6268.30
	3335.79	4276.13	5511.26	6268.30	7139.15
	3774.28		6268.30		8140.59
			7139.15		9291.09
			8140.59		10620.13
			9291.09		12149.58
			10620.13		13910.70
			12149.58		15951.18
			13910.70		18307.02
			15951.18		21019.39
			18307.02		24163.08
			21019.39		27785.95
					32011.38
					36865.79

Total Reaction Rate

k" =	687.82	847.28	1049.48	1170.49	1307.33	cm/s
	762.88	942.32	1170.49	1307.33	1462.29	
	847.28	1049.48	1307.33	1462.29	1638.00	
	942.32	1170.49	1462.29	1638.00	1837.45	
	1049.48	1307.33	1638.00	1837.45	2064.21	
	1170.49	1462.29	1837.45	2064.21	2322.42	
	1307.33	1638.00	2064.21	2322.42	2616.53	
	1462.29	1837.45	2322.42	2616.53	2952.17	
	1638.00	2064.21	2616.53	2952.17	3335.56	
	1837.45	2322.42	2952.17	3335.56	3773.98	
	2064.21	2616.53	3335.56	3773.98	4275.75	
	2322.42	2952.17	3773.98	4275.75	4850.87	
	2616.53	3335.56	4275.75	4850.87	5510.62	
	2952.17	3773.98	4850.87	5510.62	6267.47	
	3335.56	4275.75	5510.62	6267.47	7138.07	
	3773.98		6267.47		8139.19	
			7138.07		9289.27	
			8139.19		10617.75	
			9289.27		12146.47	
			10617.75		13906.62	
			12146.47		15945.82	
			13906.62		18299.95	
			15945.82		21010.06	
			18299.95		24150.76	
			21010.06		27769.67	
					31989.77	
					36837.12	

Complete Conversion Reaction Times

$\tau_{reaction} = \rho_B R_0 / b \underline{k''} C^{Ag}$

Particle Size Distribution (mesh)	Particle Szie (microns)	Distribution (%)	$\tau_{reaction}$ (sec)
40-50	878.67	1.95%	0.01435366
	754.23	5.45%	0.01110859
	647.41	8.96%	0.00858547
	555.71	12.46%	0.00662612
	477.01	14.87%	0.00510699
	409.45	15.58%	0.00393046
	351.46	13.27%	0.00302066
	301.68	10.41%	0.00231805
	258.95	7.33%	0.00177628
	222.28	4.64%	0.00135923
	190.8	2.66%	0.00103856
	163.77	1.39%	0.00079233
	140.58	0.65%	0.00060368
	120.67	0.26%	0.00045927
	103.58	0.09%	0.00034891
	88.91	0.03%	0.00026470
50-60	647.41	2.69%	0.00858547
	555.71	6.67%	0.00662612
	477.01	11.11%	0.00510699
	409.45	15.79%	0.00393046
	351.46	18.56%	0.00302066
	301.68	16.07%	0.00231805
	258.95	12.24%	0.00177628
	222.28	8.06%	0.00135923
	190.8	4.66%	0.00103856
	163.77	2.40%	0.00079233
	140.58	1.10%	0.00060368
	120.67	0.44%	0.00045927
	103.58	0.14%	0.00034891
	88.91	0.04%	0.00026470
	76.32	0.01%	0.00020056

$\tau_{film} = \rho_B R_0^2 / 2b C_{Ag} D_e$

Particle Size Distribution (mesh)	Particle Szie (microns)	Distribution (%)	τ_{film} (sec)
40-50	878.67	1.95%	0.09850508
	754.23	5.45%	0.07257961
	647.41	8.96%	0.05347685
	555.71	12.46%	0.03940065
	477.01	14.87%	0.02903100
	409.45	15.58%	0.02138990
	351.46	13.27%	0.01576009
	301.68	10.41%	0.01161181
	258.95	7.33%	0.00855537
	222.28	4.64%	0.00630388
	190.8	2.66%	0.00464477
	163.77	1.39%	0.00342197
	140.58	0.65%	0.00252147
	120.67	0.26%	0.00185783
	103.58	0.09%	0.00136886
	88.91	0.03%	0.00100858
50-60	647.41	2.69%	0.05347685
	555.71	6.67%	0.03940065
	477.01	11.11%	0.02903100
	409.45	15.79%	0.02138990
	351.46	18.56%	0.01576009
	301.68	16.07%	0.01161181
	258.95	12.24%	0.00855537
	222.28	8.06%	0.00630388
	190.8	4.66%	0.00464477
	163.77	2.40%	0.00342197
	140.58	1.10%	0.00252147
	120.67	0.44%	0.00185783
	103.58	0.14%	0.00136886
	88.91	0.04%	0.00100858
	76.32	0.01%	0.00074316

$\tau_{reaction} = \rho_B R_0 / b \underline{k''} C^{Ag}$

Particle Size Distribution (mesh)	Particle Szie (microns)	Distribution (%)	$\tau_{reaction}$ (sec)
60-80	477.01	2.65%	0.00510699
	409.45	6.61%	0.00393046
	351.46	10.57%	0.00302066
	301.68	14.65%	0.00231805
	258.95	17.12%	0.00177628
	222.28	15.14%	0.00135923
	190.8	11.95%	0.00103856
	163.77	8.43%	0.00079233
	140.58	5.45%	0.00060368
	120.67	3.30%	0.00045927
	103.58	1.86%	0.00034891
	88.91	0.97%	0.00026470
	76.32	0.45%	0.00020056
	65.51	0.18%	0.00015174
	56.23	0.07%	0.00011465
	48.27	0.06%	0.00008654
	41.43	0.07%	0.00006521
	35.56	0.09%	0.00004909
	30.53	0.09%	0.00003693
	26.2	0.09%	0.00002773
	22.49	0.07%	0.00002080
	19.31	0.06%	0.00001560
	16.57	0.04%	0.00001168
	14.22	0.02%	0.00000873
	12.21	0.01%	0.00000653
80-100	409.45	2.74%	0.00393046
	351.46	6.59%	0.00302066
	301.68	10.87%	0.00231805
	258.95	14.87%	0.00177628
	222.28	17.16%	0.00135923
	190.8	15.07%	0.00103856
	163.77	12.07%	0.00079233
	140.58	8.71%	0.00060368
	120.67	5.65%	0.00045927
	103.58	3.29%	0.00034891
	88.91	1.73%	0.00026470
	76.32	0.80%	0.00020056
	65.51	0.32%	0.00015174
	56.23	0.11%	0.00011465
	48.27	0.04%	0.00008654

$\tau_{film} = \rho_B R_0^2 / 2b C_{Ag} D_e$

Particle Size Distribution (mesh)	Particle Szie (microns)	Distribution (%)	τ_{film} (sec)
60-80	477.01	2.65%	0.02903100
	409.45	6.61%	0.02138990
	351.46	10.57%	0.01576009
	301.68	14.65%	0.01161181
	258.95	17.12%	0.00855537
	222.28	15.14%	0.00630388
	190.8	11.95%	0.00464477
	163.77	8.43%	0.00342197
	140.58	5.45%	0.00252147
	120.67	3.30%	0.00185783
	103.58	1.86%	0.00136886
	88.91	0.97%	0.00100858
	76.32	0.45%	0.00074316
	65.51	0.18%	0.00054755
	56.23	0.07%	0.00040341
	48.27	0.06%	0.00029728
	41.43	0.07%	0.00021900
	35.56	0.09%	0.00016134
	30.53	0.09%	0.00011892
	26.2	0.09%	0.00008758
	22.49	0.07%	0.00006453
	19.31	0.06%	0.00004757
	16.57	0.04%	0.00003503
	14.22	0.02%	0.00002580
	12.21	0.01%	0.00001902
80-100	409.45	2.74%	0.02138990
	351.46	6.59%	0.01576009
	301.68	10.87%	0.01161181
	258.95	14.87%	0.00855537
	222.28	17.16%	0.00630388
	190.8	15.07%	0.00464477
	163.77	12.07%	0.00342197
	140.58	8.71%	0.00252147
	120.67	5.65%	0.00185783
	103.58	3.29%	0.00136886
	88.91	1.73%	0.00100858
	76.32	0.80%	0.00074316
	65.51	0.32%	0.00054755
	56.23	0.11%	0.00040341
	48.27	0.04%	0.00029728

$\tau_{reaction} = \rho_B R_0 / b \underline{k''} C^{Ag}$

Particle Size Distribution (mesh)	Particle Szie (microns)	Distribution (%)	$\tau_{reaction}$ (sec)
<100	351.46	1.94%	0.00302066
	301.68	4.47%	0.00231805
	258.95	7.00%	0.00177628
	222.28	9.41%	0.00135923
	190.8	11.28%	0.00103856
	163.77	12.18%	0.00079233
	140.58	11.21%	0.00060368
	120.67	9.97%	0.00045927
	103.58	8.43%	0.00034891
	88.91	6.76%	0.00026470
	76.32	5.16%	0.00020056
	65.51	3.75%	0.00015174
	56.23	2.61%	0.00011465
	48.27	1.76%	0.00008654
	41.43	1.16%	0.00006521
	35.56	0.78%	0.00004909
	30.53	0.54%	0.00003693
	26.2	0.40%	0.00002773
	22.49	0.31%	0.00002080
	19.31	0.25%	0.00001560
	16.57	0.19%	0.00001168
	14.22	0.14%	0.00000873
	12.21	0.10%	0.00000653
	10.48	0.07%	0.00000488
	9	0.05%	0.00000364
	7.72	0.03%	0.00000271
	6.63	0.03%	0.00000202

$\tau_{film} = \rho_B R_0^2 / 2b C_{Ag} D_e$

Particle Size Distribution (mesh)	Particle Szie (microns)	Distribution (%)	τ_{film} (sec)
<100	351.46	1.94%	0.01576009
	301.68	4.47%	0.01161181
	258.95	7.00%	0.00855537
	222.28	9.41%	0.00630388
	190.8	11.28%	0.00464477
	163.77	12.18%	0.00342197
	140.58	11.21%	0.00252147
	120.67	9.97%	0.00185783
	103.58	8.43%	0.00136886
	88.91	6.76%	0.00100858
	76.32	5.16%	0.00074316
	65.51	3.75%	0.00054755
	56.23	2.61%	0.00040341
	48.27	1.76%	0.00029728
	41.43	1.16%	0.00021900
	35.56	0.78%	0.00016134
	30.53	0.54%	0.00011892
	26.2	0.40%	0.00008758
	22.49	0.31%	0.00006453
	19.31	0.25%	0.00004757
	16.57	0.19%	0.00003503
	14.22	0.14%	0.00002580
	12.21	0.10%	0.00001902
	10.48	0.07%	0.00001401
	9	0.05%	0.00001033
	7.72	0.03%	0.00000760
	6.63	0.03%	0.00000561

Complete Conversion Reaction Time based upon Average Particle Size

$\tau_{reaction} = \rho_B R_0 / b \underline{k''} C^{Ag}$ $\tau_{film} = \rho_B R_0^2 / 2b C_{Ag} D_e$

Particle Size Distribution (mesh)	Particle Szie (microns)	$\tau_{reaction}$ (sec)	Particle Size Distribution (mesh)	Particle Szie (microns)	τ_{film} (sec)	τ_{total} (sec)
40-50	374.83	0.006123	40-50	374.83	0.017925	0.024049
50-60	312.40	0.004143	50-60	312.40	0.012452	0.016595
60-80	209.98	0.002248	60-80	209.98	0.005625	0.007873
80-100	189.78	0.001822	80-100	189.78	0.004595	0.006417
<100	109.83	0.000944	<100	109.83	0.001539	0.002483

Incomplete Conversion Reaction Times

Neat, Loose Particle Testing

Reaction Control Conversion				
Size Cut	Conversion	t / τ	τ (sec)	t (sec)
40-50	99.433%	0.822	0.00473	0.0038878
50-60	99.797%	0.873	0.00320	0.0027926
60-80	99.997%	0.970	0.00181	0.0017588
80-100	99.999%	0.983	0.00141	0.0013809
<100	100.000%	0.998	0.00081	0.0008094

Impregnated, Loose Particle Testing

Reaction Control Conversion				
Size Cut	Conversion	t / τ	τ (sec)	t (sec)
50-60 CSYN	98.51%	0.754	0.00320	0.0024115
50-60 SF	98.878%	0.776	0.00320	0.0024819
50-60 EW	99.952%	0.921	0.00320	0.0029465

Polymeric Microfibrous Entrapped Testing

Reaction Control Conversion				
Size Cut	Conversion	t / τ	τ (sec)	t (sec)
50-60	99.840%	0.883	0.00320	0.0028234
60-80	99.999%	0.981	0.00181	0.0017784
80-100	99.999%	0.980	0.00141	0.0013767
<100	100.000%	0.994	0.00081	0.0008065

Loose Particle Testing (complete conversion)

Reaction Control Conversion				
Size Cut	Conversion	t / τ	τ (sec)	t (sec)
40-50	100.00%	1	0.00473	0.0047315
50-60	100.00%	1	0.00320	0.0031977
60-80	100.00%	1	0.00181	0.0018134
80-100	100.00%	1	0.00141	0.0014051
<100	100.00%	1	0.00081	0.0008110

Neat, Loose Particle Testing

Film Control Conversion				
Size Cut	Conversion	t / τ	τ (sec)	t (sec)
40-50	99.43%	0.968	0.027640	0.026761
50-60	99.80%	0.984	0.017353	0.017074
60-80	100.00%	0.999	0.009052	0.009044
80-100	100.00%	1.000	0.006749	0.006747
<100	100.00%	1.000	0.003689	0.003689

Impregnated, Loose Particle Testing

Film Control Conversion				
Size Cut	Conversion	t / τ	τ (sec)	t (sec)
50-60 CSYN	98.51%	0.940	0.000000	0.000000
50-60 SF	98.88%	0.950	0.000000	0.000000
50-60 EW	99.95%	0.994	0.000000	0.000000

Polymeric Microfibrous Entrapped Testing

Film Control Conversion				
Size Cut	Conversion	t / τ	τ (sec)	t (sec)
50-60	99.84%	0.986	0.017353	0.017115
60-80	100.00%	1.000	0.009052	0.009049
80-100	100.00%	1.000	0.006749	0.006746
<100	100.00%	1.000	0.003689	0.003689

Loose Particle Testing (complete conversion)

Film Control Conversion				
Size Cut	Conversion	t / τ	τ (sec)	t (sec)
40-50	100.00%	1	0.027640	0.027640
50-60	100.00%	1	0.017353	0.017353
60-80	100.00%	1	0.009052	0.009052
80-100	100.00%	1	0.006749	0.006749
<100	100.00%	1	0.003689	0.003689

Neat, Loose Particle Testing

on Control Conv	Total
Size Cut	t (sec)
40-50	0.0306493
50-60	0.0198668
60-80	0.0108027
80-100	0.0081281
<100	0.0044983

Impregnated, Loose Particle Testing

on Control Conv	Total
Size Cut	t (sec)
50-60 CSYN	0.0024115
50-60 SF	0.0024819
50-60 EW	0.0029465

Polymeric Microfibrous Entrapped Testing

on Control Conv	Total
Size Cut	t (sec)
50-60	0.0199383
60-80	0.0108272
80-100	0.0081231
<100	0.0044953

Loose Particle Testing (complete conversion)

on Control Conv	Total
Size Cut	t (sec)
40-50	0.0323719
50-60	0.0205503
60-80	0.0108655
80-100	0.0081542
<100	0.0045000

Combustion Testing Results: Polymeric Microfibrous Sheets

Mesh Size Cut	50-60	ASTM Mesh No.	PMM	
ACP Introduced	140.20	grams	% Burned	5.36%
ACP Burned	7.52	grams	Sparks Observed	3762
Particles Burned	2346237		% Particles Out	0.160%

Mesh Size Cut	60-80	ASTM Mesh No.	PMM	
ACP Introduced	121.45	grams	% Burned	9.68%
ACP Burned	11.76	grams	Sparks Observed	340
Particles Burned	47348822		% Particles Out	0.00072%

Mesh Size Cut	80-100	ASTM Mesh No.	PMM	
ACP Introduced	99.16	grams	% Burned	10.12%
ACP Burned	10.04	grams	Sparks Observed	124
Particles Burned	15082539		% Particles Out	0.00082%

Mesh Size Cut	<100	ASTM Mesh No.	PMM	
ACP Introduced	77.50	grams	% Burned	8.92%
ACP Burned	6.91	grams	Sparks Observed	53
Particles Burned	293745537		% Particles Out	0.000018%

Combustion Testing Results: Loose, Neat Particles

Mesh Size Cut	40-50	ASTM Mesh No.				
Raw Material In	200	grams		Total Burned	21.93	grams
Material on Floor at Duct End	15.05	grams		% Burned	10.97%	
Material in 8ft End Duct Section	134.83	grams		Particles Burned	4494945	
Material in Front Duct Section	28.19	grams		Sparks Observed	25487	
				% Particles Out	0.567%	
Mesh Size Cut	50-60	ASTM Mesh No.				
Raw Material In	200	grams		Total Burned	35.6	grams
Material on Floor at Duct End	14.89	grams		% Burned	17.80%	
Material in 8ft End Duct Section	118.27	grams		Particles Burned	11109279	
Material in Front Duct Section	31.24	grams		Sparks Observed	22583	
				% Particles Out	0.203%	
Mesh Size Cut	60-80	ASTM Mesh No.				
Raw Material In	200	grams		Total Burned	54.94	grams
Material on Floor at Duct End	24.92	grams		% Burned	27.47%	
Material in 8ft End Duct Section	106.66	grams		Particles Burned	221243298	
Material in Front Duct Section	13.48	grams		Sparks Observed	6054	
				% Particles Out	0.00274%	
Mesh Size Cut	80-100	ASTM Mesh No.				
Raw Material In	200	grams		Total Burned	70.04	grams
Material on Floor at Duct End	27.4	grams		% Burned	35.02%	
Material in 8ft End Duct Section	88.25	grams		Particles Burned	105268692.9	
Material in Front Duct Section	14.31	grams		Sparks Observed	534	
				% Particles Out	0.000507%	
Mesh Size Cut	<100	ASTM Mesh No.				
Raw Material In	200	grams		Total Burned	106.89	grams
Material on Floor at Duct End	14.3	grams		% Burned	53.45%	
Material in 8ft End Duct Section	64.78	grams		Particles Burned	4544489962	
Material in Front Duct Section	14.03	grams		Sparks Observed	39	
				% Particles Out	0.00000086%	

Combustion Testing Results: Loose, Impregnated Particles

Mesh Size Cut	50-60	ASTM Mesh No.		Cruwik SYN		
Raw Material In	186.38	grams		Total Burned	11.09	grams
Material on Floor at Duct End	15.59	grams		% Burned	5.95%	
Material in 8ft End Duct Section	139.51	grams		Particles Burned	3460728	
Material in Front Duct Section	20.19	grams		Sparks Observed	51443	
				% Particles Out	1.486%	
Mesh Size Cut	50-60	ASTM Mesh No.		SuperFloc 4512		
Raw Material In	175.16	grams		Total Burned	14.31	grams
Material on Floor at Duct End	20.24	grams		% Burned	8.17%	
Material in 8ft End Duct Section	112.6	grams		Particles Burned	4465556	
Material in Front Duct Section	28.01	grams		Sparks Observed	50083	
				% Particles Out	1.122%	
Mesh Size Cut	50-60	ASTM Mesh No.		Excess Water		
Raw Material In	223.82	grams		Total Burned	39.062	grams
Material on Floor at Duct End	4.16	grams		% Burned	17.61%	
Material in 8ft End Duct Section	58.31	grams		Particles Burned	12189626	
Material in Front Duct Section	30.74	grams				
Material Trapped in Eductor	2.02	grams		Sparks Observed	5909	
Humidity %	40.00%			% Particles Out	0.0485%	

Particle Size Distribution Calculations:

Mesh Size	Particle Size (micron)	Percentage in Size	Volume of Sphere (m^3/particle)	Number of Particles in Sample	Particle Density (particles/ gram)
40-50 Mesh	994.14	0	5.14448E-10	0	204968
	878.67	1.95	3.55203E-10	183	
	754.23	5.45	2.24652E-10	809	
	647.41	8.96	1.42081E-10	2102	
	555.71	12.46	8.98552E-11	4622	
	477.01	14.87	5.68304E-11	8722	
	409.45	15.58	3.59419E-11	14449	
	351.46	13.27	2.27314E-11	19459	
	301.68	10.41	1.4376E-11	24137	
	258.95	7.33	9.09173E-12	26874	
	222.28	4.64	5.75042E-12	26897	
	190.8	2.66	3.63692E-12	24380	
	163.77	1.39	2.29986E-12	20146	
	140.58	0.65	1.45469E-12	14894	
	120.67	0.26	9.20019E-13	9420	
	103.58	0.09	5.81871E-13	5156	
	88.91	0.03	3.68002E-13	2717	
	76.32	0	2.32763E-13	0	
50-60 Mesh	754.23	0	2.24652E-10	0	312058
	647.41	2.69	1.42081E-10	631	
	555.71	6.67	8.98552E-11	2474	
	477.01	11.11	5.68304E-11	6516	
	409.45	15.79	3.59419E-11	14644	
	351.46	18.56	2.27314E-11	27216	
	301.68	16.07	1.4376E-11	37261	
	258.95	12.24	9.09173E-12	44876	
	222.28	8.06	5.75042E-12	46721	
	190.8	4.66	3.63692E-12	42710	
	163.77	2.4	2.29986E-12	34785	
	140.58	1.1	1.45469E-12	25206	
	120.67	0.44	9.20019E-13	15942	
	103.58	0.14	5.81871E-13	8020	
	88.91	0.04	3.68002E-13	3623	
	76.32	0.01	2.32763E-13	1432	
	65.51	0	1.47205E-13	0	

Mesh Size	Particle Size (micron)	Percentage in Size	Volume of Sphere (m^3/particle)	Number of Particles in Sample	Particle Density (particles/ gram)
60-80 Mesh	555.71	0	8.98552E-11	0	4026999
	477.01	2.65	5.68304E-11	1554	
	409.45	6.61	3.59419E-11	6130	
	351.46	10.57	2.27314E-11	15500	
	301.68	14.65	1.4376E-11	33969	
	258.95	17.12	9.09173E-12	62768	
	222.28	15.14	5.75042E-12	87762	
	190.8	11.95	3.63692E-12	109525	
	163.77	8.43	2.29986E-12	122181	
	140.58	5.45	1.45469E-12	124884	
	120.67	3.3	9.20019E-13	119563	
	103.58	1.86	5.81871E-13	106553	
	88.91	0.97	3.68002E-13	87862	
	76.32	0.45	2.32763E-13	64443	
	65.51	0.18	1.47205E-13	40760	
	56.23	0.07	9.309E-14	25065	
	48.27	0.06	5.88885E-14	33962	
	41.43	0.07	3.72343E-14	62666	
	35.56	0.09	2.35442E-14	127420	
	30.53	0.09	1.48998E-14	201346	
	26.2	0.09	9.41678E-15	318580	
	22.49	0.07	5.95617E-15	391751	
	19.31	0.06	3.77004E-15	530499	
	16.57	0.04	2.38213E-15	559722	
	14.22	0.02	1.50556E-15	442804	
	12.21	0.01	9.53116E-16	349730	
	10.48	0	6.02674E-16	0	

Mesh Size	Particle Size (micron)	Percentage in Size	Volume of Sphere (m^3/particle)	Number of Particles in Sample	Particle Density (particles/ gram)
80-100 Mesh	477.01	0	5.68304E-11	0	1502980
	409.45	2.74	3.59419E-11	2541	
	351.46	6.59	2.27314E-11	9664	
	301.68	10.87	1.4376E-11	25204	
	258.95	14.87	9.09173E-12	54518	
	222.28	17.16	5.75042E-12	99471	
	190.8	15.07	3.63692E-12	138121	
	163.77	12.07	2.29986E-12	174938	
	140.58	8.71	1.45469E-12	199585	
	120.67	5.65	9.20019E-13	204706	
	103.58	3.29	5.81871E-13	188473	
	88.91	1.73	3.68002E-13	156702	
	76.32	0.8	2.32763E-13	114566	
	65.51	0.32	1.47205E-13	72461	
	56.23	0.11	9.309E-14	39388	
	48.27	0.04	5.88885E-14	22642	
	41.43	0	3.72343E-14	0	
<100 Mesh	409.45	0	3.59419E-11	0	42515576
	351.46	1.94	2.27314E-11	2845	
	301.68	4.47	1.4376E-11	10364	
	258.95	7	9.09173E-12	25664	
	222.28	9.41	5.75042E-12	54547	
	190.8	11.28	3.63692E-12	103384	
	163.77	12.18	2.29986E-12	176532	
	140.58	11.21	1.45469E-12	256871	
	120.67	9.97	9.20019E-13	361225	
	103.58	8.43	5.81871E-13	482925	
	88.91	6.76	3.68002E-13	612315	
	76.32	5.16	2.32763E-13	738949	
	65.51	3.75	1.47205E-13	849158	
	56.23	2.61	9.309E-14	934580	
	48.27	1.76	5.88885E-14	996233	
	41.43	1.16	3.72343E-14	1038468	
	35.56	0.78	2.35442E-14	1104306	
	30.53	0.54	1.48998E-14	1208074	
	26.2	0.4	9.41678E-15	1415912	
	22.49	0.31	5.95617E-15	1734896	
	19.31	0.25	3.77004E-15	2210412	
	16.57	0.19	2.38213E-15	2658681	
	14.22	0.14	1.50556E-15	3099627	
	12.21	0.1	9.53116E-16	3497302	
	10.48	0.07	6.02674E-16	3871634	
	9	0.05	3.81704E-16	4366391	
	7.72	0.03	2.40908E-16	4150969	
	6.63	0.03	1.52595E-16	6553311	
	5.69	0	9.64574E-17	0	